

PLASMA STERILIZATION OF MICROORGANISMS

Doctoral Dissertation
Jožef Stefan International Postgraduate School
Ljubljana, Slovenia, May 2009

Supervisor: *A/Prof. Dr. Miran Mozetič*

Co-supervisor: *A/Prof. Dr. Uroš Cvelbar*

Evaluation Board:

Prof. Dr. Cristina Canal, University of Barcelona, Spain

A/Prof. Dr. Aleš Podgornik, Bia Separations and University of Ljubljana, Slovenia

A/Prof. Dr. Janez Kovač, Jozef Stefan Institute, Slovenia

Danijela Vujošević

PLASMA STERILIZATION OF MICROORGANISMS

Doctoral Dissertation

PLAZEMSKA STERILIZACIJA MIKRO ORGANIZMOV

Doktorska disertacija

Supervisor: A/Prof. Dr. Miran Mozetič

Co-Supervisor: A/Prof. Dr. Uroš Cvelbar

May 2009

MEDNARODNA PODIPLOMSKA ŠOLA JOŽEFA STEFANA
JOŽEF STEFAN INTERNATIONAL POSTGRADUATE SCHOOL
Ljubljana, Slovenia



Index

Abstract.....	VII
Povzetek.....	VIII
Abbreviations	IX
1 Introduction	1
1.1 Sterilization.....	1
1.2 Plasma and plasma technology	3
1.3 State of the art on low pressure plasma based sterilization.....	4
1.4 Commercial “plasma-based” sterilizers.....	6
1.5 Inactivation agents in low pressure oxygen or oxygen-containing plasma	7
1.5.1 Effect of the UV radiation.....	8
1.5.2 Effects of the reactive species.....	8
1.5.3 Effect of the charged particles	8
1.6 Kinetics of the bacterial inactivation process	9
1.7 Bacteria	9
1.7.1 Cell envelope structures.....	11
2 Aims and Hypothesis.....	13
3 Materials and Methods	15
3.1 Plasma and plasma experimental setup	15
3.1.1 Weakly ionized oxygen plasma	15
3.1.1.1 Double Langmuir probe	17
3.1.2 The plasma system with reactor.....	17
3.1.2.1 Low pressure oxygen plasma treatment	18
3.2 Sample preparation and analyses	20
3.2.1 Bacteria and processing	20
3.2.2 Plate count technique	20
3.2.2.1 Cultivation of bacteria – CFU measurements	20
3.2.2.2 Carriers.....	21
3.2.2.3 Preparation of carriers	21
3.2.3 Scanning Electron Microscopy (SEM)	21
3.2.4 Fluorescence Microscopy (FM).....	21
3.2.4.1 Fluorescent labelling of bacterial cells	22
3.2.5 Flow cytometry	22
3.2.5.1 Viability analysis and quantitative determination of live/dead bacteria by flow cytometry.....	24
4 Results.....	25
4.1 Plasma characteristics and activation of carriers.....	25
4.2 The influence of substrate material on bacteria sterilization in an oxygen plasma glow discharge	25
4.3 Analysis of oxygen plasma inactivation of bacteria by plate counting technique.....	27
4.3.1 Oxygen plasma inactivation of <i>Escherichia coli</i>	27

4.3.1.1 Influence of <i>Escherichia coli</i> concentration on plasma inactivation.....	28
4.3.2 Oxygen plasma inactivation of <i>Bacillus stearothermophilus</i>	28
4.3.2.1 Influence of pressure on <i>Bacillus stearothermophilus</i> inactivation	29
4.3.2.2 Influence of afterglow treatment on <i>Bacillus stearothermophilus</i> inactivation	30
4.3.3 Oxygen plasma inactivation of <i>Staphylococcus aureus</i>	30
4.3.3.1 Influence of <i>Staphylococcus aureus</i> concentration on plasma inactivation	31
4.3.3.2 Influence of pressure on <i>Staphylococcus aureus</i> inactivation.....	32
4.3.3.3 Influence of afterglow treatment on <i>Staphylococcus aureus</i> inactivation.....	32
4.4 Morphological changes caused by low-temperature oxygen plasma	33
4.5 Fluorescence viability analysis of bacterial cells using SYTO 9 - PI dual staining	38
4.6 Flow cytometric viability analysis	40
4.7 Quantitative viability analysis by flow cytometry	44
4.7.1 Analysis of <i>Escherichia coli</i> after plasma treatment	44
4.7.2 Analysis of <i>Bacillus stearothermophilus</i> after plasma treatment	46
4.7.3 Analysis of <i>Staphylococcus aureus</i> after plasma treatment.....	50
4.8 Optical emission spectroscopy during bacteria treatment	53
5 Discussion.....	56
5.1 The choice of plasma parameters	56
5.2 Preparation of bacteria and substrates	58
5.3 Effect of plasma treatment on bacteria inactivation.....	58
5.4 Inactivation of <i>Escherichia coli</i>	59
5.5 Inactivation of <i>Bacillus stearothermophilus</i>	62
5.6 Inactivation of <i>Staphylococcus aureus</i>	65
5.7 Optical emission spectroscopy of plasma inactivation process	68
6 Conclusions	71
7 Acknowledgements.....	73
8 References	75
Index of Figures	84
Index of Tables.....	88
Appendix - Bibliography	89

Abstract

The sterilization efficiency of oxygen plasma was studied. Plasma was created in pure oxygen with an inductively coupled radiofrequency discharge. The discharge power was estimated to about 180 W. Plasma parameters were measured with a double Langmuir probe and a catalytic probe. Plasma parameters depended on pressure in the discharge chamber. The density of charged particles exhibited a well pronounced maximum of $3.5 \times 10^{16} \text{ m}^{-3}$ at the pressure of 20 Pa. At lower pressure the density decreased rapidly with decreasing pressure, while at higher pressure it decreased slowly with increasing pressure. At 75 Pa it was about $7 \times 10^{15} \text{ m}^{-3}$. The density of neutral oxygen atoms was increasing monotonously with increasing pressure. At low pressure the increase was steep; while at pressure above 100 Pa the increase was almost negligible. Most experiments were performed at 75 Pa, where the oxygen atom density was $3.5 \times 10^{21} \text{ m}^{-3}$ and the dissociation fraction of oxygen molecules was the highest. Some experiments were also performed at 30 Pa and 150 Pa. Plasma was also characterized by optical emission spectroscopy to detect the evolution of reactive products from plasma interaction with bacteria.

Three different types of bacteria were used: *Escherichia coli*, *Bacillus stearothermophilus* and *Staphylococcus aureus*. Bacteria were typically deposited onto substrates in a monolayer. The sterilization effects were studied by scanning electron microscopy (SEM), fluorescence microscopy (FM), plate count technique (PCT), and fluorescence activated cell sorting (FACS). Samples were exposed to plasma for different periods up to several minutes. The treatment time was chosen for each type of bacteria according to the visual damage obtained at a preliminary investigation by SEM.

Bacteria were deposited onto well activated substrates made from different materials. Many materials were heated in plasma due to the heterogeneous surface recombination of oxygen atoms on the surface. In order to avoid the heating effects, the systematic experiments were performed using glass substrates which minimized the thermal effects.

Results obtained by fluorescence microscopy were not found to be conclusive, which was explained by the specifics of plasma sterilization. This effect was explained by the destruction of the bacterial DNA due to plasma action. The PCT and FACS techniques gave sound results in most cases. The PCT was used to determine the number of surviving bacteria and eventual sterility of the substrates, while the FACS allowed for quantitative determination of the total number of bacteria (live and dead) on the surface of substrates after plasma treatments.

The results of systematic measurements allowed for the calculation of the doses of plasma radicals needed for the destruction of a certain number of bacteria. The sterility of substrates contaminated with *Escherichia coli* and *Staphylococcus aureus* was obtained after receiving the dose of about $8 \times 10^{25} \text{ m}^{-2}$. Whereas the sterility of substrates contaminated with *Bacillus stearothermophilus* depended strongly on the bacteria form – vegetative or spores. We also established that when the number of bacteria was higher then a longer dose was required to obtain sterility.

The sterilization efficiency was found to be different for bacteria types, and depended primarily on the dose of neutral O atoms on the surface, as well as on the influx of charged species (positive O ions). In the case of *Staphylococcus aureus*, the efficiency of the process was achieved when we had a higher density of ions ($n_i = 3 \times 10^{16} \text{ m}^{-3}$) and a moderate density of neutral atoms ($n_o = 2 \times 10^{21} \text{ m}^{-3}$). Whereas for *Bacillus stearothermophilus*, the best efficiency was achieved by a balanced flux of positive ions and atoms on the surface at densities of $n_i = 1 \times 10^{16} \text{ m}^{-3}$ and $n_o = 3.5 \times 10^{21} \text{ m}^{-3}$. Therefore, the density of different plasma species and their influx to the surface gives different sterilization efficiencies depending on the bacteria type and their structure form. Moreover, charging bacteria by plasma provided synergetic effects and accelerated the bacteria inactivation process. Although the main reason for the destruction of cell wall was still chemical etching by reactive neutrals, atom by atom. This conclusion enabled us to upgrade the inactivation model presented by Moisan (Moisan et al., 2001), and proved Laroussi and Mendis' theory that charged particles play an important role in the plasma sterilization of bacteria.

Povzetek

Raziskovali smo sterilizacijske lastnosti plinske plazme. Plazmo smo ustvarili z visokofrekvenčno razelektrivjo v čistem kisiku pri moči okoli 180 W. Plazemske parametre smo merili z dvojno Langmuirjevo sondo in katalitično sondo. Plazemski parametri so bili odvisni od tlaka v razelektrivni posodi. Gostota nabitih delcev v plazmi je dosegla izrazit maksimum $3,5 \times 10^{16} \text{ m}^{-3}$ pri tlaku 20 Pa. Pri nižjem tlaku je gostota hitro padala z zniževanjem tlaka, pri višjem tlaku pa je padala počasi z naraščajočim tlakom. Pri tlaku 75 Pa je bila gostota nabitih delcev približno $7 \times 10^{15} \text{ m}^{-3}$. Gostota nevtralnih kisikovih atomov je monotono naraščala z naraščajočim tlakom v razelektrivni posodi. Pri nizkem tlaku je bilo naraščanje izrazito, pri tlaku preko 100 Pa pa domala zanemarljivo. Večino eksperimentov smo opravili pri tlaku 75 Pa, kjer je bila gostota nevtralnih kisikovih atomov $3,5 \times 10^{21} \text{ m}^{-3}$, stopnja disociiranosti kisikovih molekul pa največja. Nekatere eksperimente smo opravili tudi pri tlaku 30 in 150 Pa. Plazmo smo karakterizirali tudi z optično emisijsko spektroskopijo, s katero smo zaznali reakcijske produkte interakcije plazme z bakterijami.

Uporabili smo tri različne soje bakterij: *Escherichia coli*, *Bacillus stearothermophilus* in *Staphylococcus aureus*. Običajno smo bakterije nanесли na površino podlag v enoplastnem sloju. Sterilizacijske učinke kisikove plazme smo določali z vrstično elektronsko mikroskopijo, fluorescenčno mikroskopijo, tehniko štetja na hranilnih podlagah in fluorescenčno aktivirano sortiranje celic. Vzorce smo obdelovali pri različnih časih. Čase obdelave smo določali za vsak soj bakterij posebej glede na preliminarne rezultate, ki smo jih dobili z elektronsko mikroskopijo.

Bakterije smo nanесли na dobro aktivirane podlage iz različnih materialov. Za nekatere podlage smo ugotovili, da močno reagirajo s plazmo, kar povzroča neželjeno gretje podlag in s tem termične pojave. Da bi popolnoma izključili termične pojave, smo za sistematične raziskave uporabili zgolj steklene podlage, ki so interne za plazmo.

Rezultati, ki smo jih dobili s fluorescenčno mikroskopijo, so pokazali, da tovrstna tehnika ni primerna za analizo plazemsko obdelanih bakterij, saj plazma povzroči razpad bakterijskega DNA. Medtem, ko sta pretočna citometrija in štetje kolonij na hranljivih podlagah dali skladne rezultate. Tehnika štetja na hranilnih podlagah je omogočila ugotavljanje števila preživelih bakterij in sterilnosti podlag, medtem ko je fluorescenčno aktivirano sortiranje celic omogočilo kvantitativno določitev skupnega števila (preživelih in mrtvih) bakterij po plazemskih obdelavah.

Rezultati sistematičnih eksperimentov so omogočili izračun doze plazemskih radikalov, ki so potrebne za doseg sterilnosti podlag, na katere so bile nanešene različne bakterije. Sterilnost podlag z bakterijami *Escherichia coli* in *Staphylococcus aureus* je bila dosežena po prejeti dozi $8 \times 10^{25} \text{ m}^{-2}$. Za doseg sterilnosti podlag z bakterijami *Bacillus stearothermophilus* pa so rezultati jasno pokazali veliko odstopanje med vegetativno obliko in sporami. Ugotovili smo tudi, da potrebna doza radikalov za doseg sterilnosti nekoliko narašča z naraščajočo koncentracijo bakterij na podlagah.

Za različne soje bakterij smo odkrili različno obnašanje med izpostavo različnim plazemskim radikalom. Najpomembnejši faktor je prejeta doza nevtralnih atomov kisika, na drugem mestu pa je prejeta doza pozitivno nabitih kisikovih ionov. V primeru *Staphylococcus aureus* smo dosegli boljše sterilizacijske učinke pri povišani dozi kisikovih ionov, saj smo najboljše rezultate dosegli pri gostoti ionov $3 \times 10^{16} \text{ m}^{-3}$ in gostoti nevtralnih kisikovih atomov $2 \times 10^{21} \text{ m}^{-3}$, torej daleč od maksimalne stopnje disociiranosti. Za bakterije *Bacillus stearothermophilus* smo dobili najboljši sterilizacijski učinek plazme pri gostoti ionov $1 \times 10^{16} \text{ m}^{-3}$ in gostoti nevtralnih kisikovih atomov $3,5 \times 10^{21} \text{ m}^{-3}$. Opazili smo tudi, da k učinkovitosti sterilizacije prispeva tudi električni naboji, ki je posledica stika bakterij s plinsko plazmo. Kljub tem učinkom je glavni mehanizem sterilizacije jedkanje bakterijskega materiala z nevtralnimi kisikovimi atomi. Naši izsledki nadgrajujejo model sterilizacije, ki ga je prvi predložil Moisan leta 2001, obenem pa potrjujejo hipotezo, ki sta jo predstavila Laroussi in Mendis o sinergijskih vplivih nabitih plazemskih delcev.

Abbreviations

ATCC	=	American Type Culture Collection
ATP	=	Adenosine Triphosphate
CCP	=	Capacitively Coupled Plasma
CFUs	=	Colony Forming Units
DC	=	Direct Current
D(value)	=	Decimal reduction time
DNA	=	Deoxyribonucleic acid
ECR	=	Electron Cyclotron Resonance
EtO	=	Ethylene oxide
FACS	=	Fluorescence-activated cell sorting
FSC	=	Forward Scatter
FL	=	Fluorescent Labelling
FM	=	Fluorescence microscopy
FOCP	=	Fibre Optic Catalytic Probe
ICP	=	Inductively Coupled Plasma
IF	=	Inactivation Factor
IR	=	Infrared
LPS	=	Lipopoly-saccharide
LTA	=	Lipoteichoic acid
MW	=	Microwave power
OES	=	Optical Emission Spectroscopy
PCT	=	Plate Count Technique
PI	=	Propidium Iodide
SAL	=	Sterility Assurance Level
SEM	=	Scanning Electron Microscopy
RF	=	Radiofrequency
RNA	=	Ribonucleic acid
ROS	=	Reactive Oxygen Species,
SSC	=	Side Scatter
UV	=	Ultraviolet
XPS	=	X-ray photoelectron spectroscopy

1 Introduction

1.1 Sterilization

Sterilization is the act or process, physical or chemical, which destroys or eliminates all forms of life, especially microorganisms. However it can not be always known with certainty whether all types of microorganisms have been killed due to the existence of some new species, or not having suitable media for culturing organisms. Furthermore, we can never prove the achievement of negative absolute with one hundred percent accuracy. Therefore by definition, sterilization is the process by which living organisms are removed or killed to the extent that they are no longer detectable in standard culture media in which they previously have been found to proliferate. According to this definition, both the process used to achieve sterility and the methods for testing for it are equally important (Bruch and Bruch, 1971).

Microorganisms of the same species may vary in their resistance to chemical and physical agents, and if even one of a billion organisms survives there is the possibility of rapid multiplication and contamination of the substance. Although the term sterile implies an absolute (a substance can not be partially sterile), in practice it becomes a matter of probability whether sterility has been achieved (Lawrence, 1968). Different operations require different degrees of certainty of sterility, as measured by the percentage reduction or number of logarithmic reduction times (D values) in initial count brought about by the treatment. D value or decimal reduction time is defined as the time required to inactivate 90 % of the cells present, or to reduce the microbial population to one-tenth its number; that is a one-logarithm reduction. The D value is expressed in the unit of time (Block, 2001).

The spectrum of inactivation kinetic rates among experimental and in-use microbial challenges is shown in Figure 1. The bioburden is less than a thousand and consists of vegetative bacteria that are killed much more rapidly than bacterial spores.

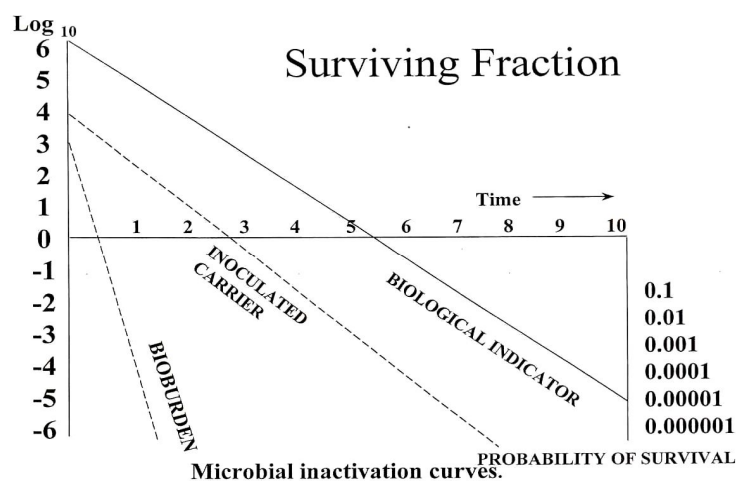


Figure 1: *Spectrum of inactivation kinetic rates.* Comparative resistance of bacterial spores used as biological indicators and the naturally occurring bioburden exposed to a sterilization process (Favero, 1998).

The concept of what sterile means has now become a matter of degree. There is a certain probability of

sterility for each unit of product being subjected to a sterilization process. This probability is commonly referred to as Sterility Assurance Level (SAL) of the product and is defined as the \log_{10} number probability of a nonsterile unit in that population, and a predictor of the efficiency of the process. The SAL of a sterilizing process is a degree of assurance with which the process renders a population of items sterile (Favero, 2001). Historically, the development of a sterilization cycle involves the determination of a sterility assurance level by using a specific biological indicator and constructing an inactivation curve and obtaining a D value. This approach is illustrated in Figure 2.

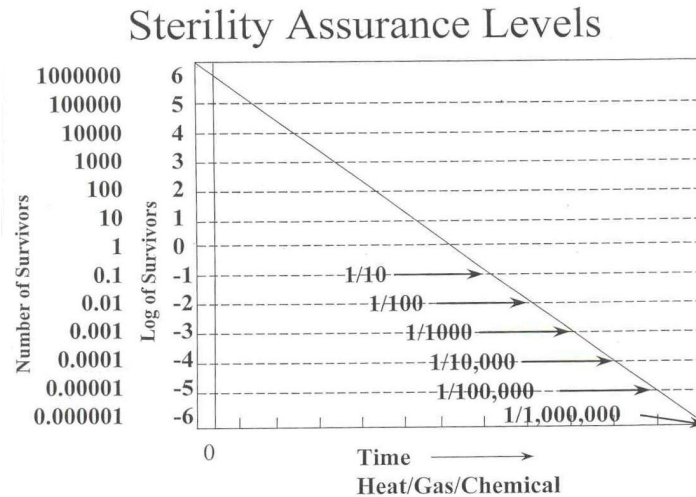


Figure 2: *Sterility assurance levels*. Determination of a sterility assurance level by using a specific biological indicator and constructing an inactivation curve (Favero, 1993).

A SAL of 6, for example, denotes a probability of not more than one viable microorganism in 1×10^6 sterilized items of the final product. If the probability of a survivor in a single unit is one in one million, the SAL number is denoted as 6 (ANSI/AAMI/ISO 11737-1, 1995).

Another parameter, which is of great importance for practical systems, is the inactivation factor (IF). The IF is the percentage kill of a microbial population by a particular treatment. The IF is generally determined for spores (highly resistant microorganisms) by taking the ratio of the initial count to the final extrapolated count. Since the IF depends on the initial count (before treatment, what is referred to as “the bioburden”), its value reveals the expected number of viable microorganisms after the treatment. Therefore, the IF of a treatment method directly reflects its sterilizing effectiveness, given a certain bioburden (Laroussi, 2002; Block, 1992).

Different approaches have been employed over the years to inactivate pathogenic microorganisms (Dorman, 1997). Sterilization by ionized gases (gaseous plasmas) is an alternative to conventional sterilization methods, which include dry heat (ovens), moist heat (boiling and autoclaving), filtration, radiation, and chemicals such as gaseous ethylene oxide (EtO) sterilization (Rutala, 1999; Goldman and Priutt, 1998; Shintani, 1995; Burgess and Reich, 1993; Moisan et al., 2002). Other less commonly used methods of sterilization have been developed. Among these are gaseous sterilants such as ozone, liquid sporicides like chlorine dioxide, glutaraldehyde, low-temperature steam formaldehyde, and vapour-phase hydrogen peroxide. However, these methods have a very narrow range of application (Ehrenberg et al., 1974; Taylor et al., 1969; Seballos et al., 1995).

Sterilization mechanisms of conventional methods rely on irreversible metabolic inactivation or on breakdown of vital structural components of the microorganisms. In cases where it is imperative not to damage the materials to be sterilized, conventional methods are either not suitable at all or offer very impractical and/or tedious and time consuming solutions. This situation led to the development of new techniques that are at least as effective as established ones, but with added superior characteristics such as short processing times, non-toxicity, and medium preservation. Among these new methods, gaseous plasma sterilization has been shown to present a great promise due to its efficacy at low temperature. Plasma

sterilization may be suitable for medical implants and devices that are sensitive to temperature, radiation and chemicals (Moisan et al., 2002; Helhel et al., 2005, Jacobs and Lin, 2001; Vujošević et al., 2004).

Due to a large number of heat- and moisture-sensitive devices in hospitals, especially in the diagnostic and minimally invasive surgery areas, there is a need for a rapid sterilization method of these devices that will enable reuse (Ernest, 1995). Ethylene oxide, as the conventional method for the sterilization of heat-sensitive devices, requires a long turn-around time due to the extended aeration times which are required to remove the toxic ethylene oxide from sterilized items. In addition, ethylene oxide has come under increased regulatory pressures worldwide because of its inherent toxicity, and its detrimental effect of the chlorofluorocarbons commonly used in the process on the earth's ozone layer (Holyoak et al., 1996; Samuel and Matthews, 1998).

Therefore we need a cheap, effective and non-toxic residual sterilization technique. Regarding this, plasma sterilization satisfies all requirements. Generally, low temperature plasmas have been shown to possess very effective germicidal characteristics. Their relatively simple and inexpensive design as well as their non-toxic nature gives them the potential to replace conventional sterilization methods in the near future (Laroussi and Leipold, 2004).

1.2 Plasma and plasma technology

Plasma is defined as fourth state of matter that is energetically distinguishable from solids, liquids and gases. It can be produced by the action of either very high temperatures or the presence of electric and/or magnetic fields, and it is normally composed of a cloud of ions, electrons, and neutral species such as atoms, molecules and other plasma radicals. It can also emit light, such as IR, visible and UV radiation. The temperature of the electrons is normally above 10,000 K; the kinetic temperature of the neutral particles and ions is strongly dependent on the type of plasma and can vary from room temperature to 10^7 K. Depending on the environment in which it exists (e.g. field strength, chamber configuration, interference), the exact composition of the plasma differs (Bell, 1974).

A well known example of plasma is the sun. Sometimes the flame of a candle is also considered plasma, but the concentration of ions is very low. Somewhat smaller specimens are encountered in every day life. Fire and lightning are natural plasma phenomena, while neon lamps and plasma TV displays are typical man-made plasmas. Plasmas can also be created on earth, in a laboratory; in most cases this is done inside a vacuum vessel at low pressure. These types of plasma are used for activating the surface of polymers, growing solar cells, and etching materials. One of the characteristic of plasma is also its chemical activity. Inside the plasma, radicals and other species are formed that are highly reactive (Hippler et al., 2001).

Plasma can be conveniently divided into two categories. The first category includes those plasmas that have temperatures over 5000 K, referred to as *high-temperature plasmas*. Although these plasma exist in nature (the sun or other stars), and can be created in high-pressure arcs or plasma jets. They are not of interest in the sterilization of medical devices because of the high temperatures involved. The plasmas used in a sterilization process are found in the second category. They are known as glow discharge or *low-temperature plasmas*. Low-temperature plasmas, such as those used in neon lights or sterilization processes, are created under reduced pressure conditions. These plasmas have average electron densities in the range of 10^{15} to 10^{17} m^{-3} . Low-pressure plasmas are of great value in fundamental research as well as plasma technology, but they have many serious drawbacks. These plasmas must be confined in massive vacuum reactors, their operation is costly, and the access for observation or sample treatment is limited (Hippler et al., 2001).

There is also a lack of thermal equilibrium in these plasmas between the electron temperature T_e and the gas kinetic temperature T_g . The ratio T_e/T_g is typically in the range of 10 to 100. For that reason, these plasmas have the unique property of having electrons with sufficient energy to disrupt molecular bonds, while the kinetic temperatures of the atoms and molecules in the plasma are near ambient conditions. It is this characteristic that makes the low-temperature plasma process well suitable for use in the sterilization of thermally sensitive materials.

Plasmas are normally referred to by gas or vapour from which they are formed. For example, if the plasma is generated from argon gas it would be known as argon plasma, or if it is generated from hydrogen peroxide vapour it would be known as hydrogen peroxide plasma. There are several different methods of generating low-temperature gas plasmas. The most common methods include direct current (DC), radiofrequency (RF), and microwave (MW) power applied to a gas. RF systems are the most common and provide more flexibility from a design standpoint. The RF discharges can be divided in inductively and capacitively coupled configurations (Boyd and Sanderson, 2003; Grill, 1994).

A very important segment of plasma technology is related to plasma sterilization. Plasma sterilization is still not a well explored process, but in recent years many authors have tried to demonstrate its effects and even explore its implementation in real case scenarios for the treatment of medical devices or implants. In these reports, different types of discharges (low pressure or atmospheric) and many gas chemistries were used. The gas itself has no biocidal effects prior to plasma formation in an electric discharge. The corresponding active species are present only when discharge is on, and disappear some milliseconds after the discharge has been turned off. The general conclusion is that then antibacterial plasma activity is due to the synergy of active plasma radicals and UV photons. Especially in the low pressure case, the role of (vacuum) UV photons is important. Since they are not re-absorbed in the gas phase, they can easily reach the bacteria and damage their DNA. Atmospheric plasmas bacterial inactivation is mainly due to the membrane damage as a result of plasma radical (reactive oxygen species, ROS) etching. It has been established that air and oxygen plasmas are more efficient than noble gas plasmas. Different types of bacteria (gram positive or negative), as well as spores were also reported to be sterilized via the plasma process. Typical D-values (treatment times that lead to deactivation of 90% of bacteria) range from minutes under low pressure conditions to seconds in atmospheric plasmas (Laroussi, 2002; Moisan et al., 2001; Laroussi, 2005, Lerouge et al., 2001; Fraser et al., 1976; Soloshenko et al., 2000).

1.3 State of the art on low pressure plasma based sterilization

Inactivation of microorganisms by plasma was first proposed in a patent by Menashi (Menashi, 1968). Menashi used a pulsed RF-driven corona discharge to create argon plasma at atmospheric pressure. He reported that 10^6 microbial spores could be inactivated in less than 1 s. It was thought that the biocidal action was due to intense heating of the spores. Further patents by Ashman and Menashi (Ashman and Menashi, 1972), as well as by Boucher and Bithell (Boucher, 1980; Bithell, 1982) showed that an electrical discharge in appropriate gases could lead to sterilization. In these patents the samples are inserted in a chamber, afterward evacuated with a fore pump to some 1–5 Pa, and subsequently filled with gas set at the required pressure, typically 5–300 Pa. Gas discharge is then achieved by applying an RF field (13.56 MHz) to the gas by means of a coil or parallel plates located on the outside of the dielectric chamber. Boucher reported that the sterilization efficacy increased with the RF power density absorbed in the discharge (Boucher, 1980). Most of these experiments used inert gases, such as argon or helium. However, Ashman and Menashi added halogens such as chlorine, bromine and iodine within the sterilization chamber to increase the efficiency of the process. Boucher seeded his carrier gas with aldehydes (Ashman and Menashi, 1972; Boucher, 1980). Instead of using rare gases as the carrier gas, Jacobs and Lin directly used hydrogen peroxide, a sterilant agent as an aqueous solution in a two-step process: first injection and contact of H_2O_2 with the objects to be sterilized and second application of an RF discharge ensures that no toxic residues remain on the sterilized items (Jacobs and Lin, 1987).

Ratner et al. showed that plasma sterilization can be achieved with many discharge gases (e.g. O_2 , N_2 , air, H_2 , halogens, N_2O , H_2O , H_2O_2 , CO_2 , SO_2 , SF_6 , aldehydes, organic acid) independently from the discharge type (Ratner et al., 1990). Recently, many studies have been done on the effects of low pressure plasma on biological matter in plasma-based systems. They were conducted for various gas mixtures. Examples are low-pressure oxygen plasma and O_2/N_2 plasmas created in RF and MW driven low pressure plasma discharges (Xu et al., 2007; Villeger et al., 2005; Villiger et al., 2004; Philip et al., 2002; Monna et al., 2002), or even more complex ternary mixtures with Ar (Kylian et al., 2009; Stapelmann et al., 2008).

The idea of employing low pressure plasmas for bacterial inactivation was introduced long ago (Fraser et al., 1976). It was primarily assumed that the key agent in plasma sterilization is the highly reactive unstable species-radicals. However, Soloshenko et al. (Soloshenko et al., 2000) also showed that the 160–220 nm UV radiation plays an important role in low-pressure plasma sterilization.

Khomich et al. (Khomich et al., 1997) reported sterilization with the glow DC discharge (direct exposure to plasma) at pressures in the range 6.5–26.5 Pa. The authors claimed that the charged particles (ions, electrons) of the DC plasma glow do not play an essential role in inactivating microorganisms if the ion energy doesn't exceed the few eV. In contrast, Lisovskiy et al. (Lisovskiy et al., 2000) showed that in capacitive (parallel plate) RF discharge, operated at RF voltages such that the ions reach energies between 100 and 200 eV, ion bombardment of the microorganisms plays a major role in their inactivation. Khomich et al. (Khomich et al., 1998) in a more recent experiment and then Soloshenko et al. (Soloshenko et al., 1999) claimed to have isolated the action of neutral particles on sterilization from that of UV radiation, concluding that the inactivation time by neutral particles only is merely twice longer in an oxygen discharge, and from five to six times longer in an air discharge. These authors believe that the sterilization of complex form objects (e.g. cavities) needs to rely on neutral particles because the action of UV photons is limited by shadowing. They further show (Soloshenko et al., 1999) that the most efficient sterilization precursor gas is O₂, which is followed in decreasing order by air, CO₂, H₂, argon and N₂. They observed that sterilization time was practically independent from gas pressure for all the above mentioned gases in the range investigated, but it decreased when increasing the discharge power. Their sterilization time was 3 minutes for an initial population of 10⁷ *Bacillus subtilis* spores in an oxygen discharge. Lerouge et al. (Lerouge et al., 2000a) used direct exposure of *Bacillus subtilis* endospores to a 2.45 GHz microwave discharge sustained in various gases (O₂, CO₂, O₂/Ar, O₂/H₂, O₂/H₂/Ar and O₂/CF₄) at the pressure of 10.5 Pa. To keep the gas temperature low, the discharge was applied in the form of 30 s pulses followed by 30 s pauses. Lerouge et al. (Lerouge et al., 2000b) have also examined the role of UV and VUV (vacuum ultraviolet) radiation on the killing of *Bacillus subtilis* endospores, showing the importance of the radiation wavelength in the inactivation process.

Lerouge (Lerouge et al., 2000a) investigated the sporicidal effects of microwave plasmas based on gas mixtures of O₂, CO₂, and CF₄. They found that the maximum sporicidal effects, corresponding to a decimal reduction time value (D value) of approximately 50 s, was obtained when the plasma was created in O₂ and CF₄ with the ratio of 88% and 12%, respectively. They argued that the prompt effect was due to the etching of the spore cell wall. The etch rate achieved by the O₂/CF₄ plasma is known to depend on the ratio of these two components, and the etch rate is very efficient in regards to power consumption when the plasma is excited by RF discharge (Wertheimer and Moisan, 1985). Lerouge et al. (Lerouge et al., 2000a) found that the sporicidal effect was higher at higher flow rates. However, in the current literature the influence of these parameters in the biocidal effects is sparsely described. Finally, different system designs with identical settings may result in different plasma processes (Wertheimer and Moisan, 1985; Gombotz and Hoffman, 1987).

Different groups performed experiments with oxygen plasmas as a means of bacterial inactivation. In one of the earlier works, oxygen in a flowing afterglow reactor at 30–130 Pa was identified (Fraser et al., 1976) to be inferior to helium and argon. This is probably due to owing a short lifetime of oxygen atoms in that design geometry. Microbial spores exposed to oxygen plasma exhibited greater etching resistance than organic polymers owing to higher complexity in their structural macromolecules, multilayer coating architecture, and sophisticated morphology (Lerouge et al., 2000a).

Hury et al. (Hury et al., 1998) observed that electron cyclotron resonance (ECR) discharge in CO₂, H₂O, or H₂O₂ exhibited a slightly higher destruction efficiency than oxygen plasma, but all oxygen-based plasmas were more efficient than pure argon plasma. They claimed that under their conditions, degradation of microorganisms was a result of chemical etching by oxygen-containing radicals. Survivability of spores depended on the density of population, so that isolated spores were less resistant than stacked or aggregated spores.

Sharma et al. (Sharma et al., 2004) conducted a series of biological decontamination experiments to assess the sterilization capability of RF oxygen plasmas. *Deinococcus radiodurans* and plasmid DNA were exposed to the oxygen plasma operating over a range of low pressures between 13 and 67 Pa, and powers between 100 and 330 W. It was found that the oxygen plasma sustained at higher power and lower pressure was more effective in causing microbial degradation.

Soloshenko et al. (Soloshenko et al., 2000) evaluated the experimental sterilization efficacy of the glow discharge in oxygen, air and nitrogen at pressure 10–33 Pa. They concluded that the complete inactivation of sporulated *Bacillus subtilis* on open surfaces was readily achieved by oxygen radiation in the far UV

region <220 nm, but radiation at longer wavelengths was not effective. They emphasized that sterilization of complex surfaces, where parts of the sample cannot be directly irradiated by the plasma, was realized by neutral oxygen atoms and excited molecules O_2^* .

Moreau et al. (Moreau et al., 2000) investigated procedures of spore inactivation in flowing afterglow plasma with microwave excitation at pressures between 130 and 930 Pa. They found that the inactivation process occurs in three steps interpreted as follows: fast killing of the exterior microorganisms on the surface of a microbial film, slow removal of the dead exterior microorganisms covering lower-lying organisms, and the fast destruction of residual spores. These researchers showed that plasma from an O_2/N_2 mixture provided faster sterilization than a 100% oxygen plasma. This effect was attributed to the bactericidal role of UV photons originating from NO molecules formed in the discharge. However, Moreau et al. (Moreau et al., 2000) and then Moisan et al. (Moisan et al., 2002) confirmed that oxygen atoms effectively participated in chemical reactions with bacteria to form volatile products such as CO_2 and H_2O . Removal of spores by plasma chemical etching takes a longer time than just inactivation of their genetic material by UV radiation, but etching is essential for complete sterilization. Sterilization time was inversely dependent on plasma density and fluxes of the indicated species O and O_2^* , while the fluxes increased linearly with input power but changed weakly with pressure under their conditions. The conclusion from the investigations was that the biological degradation efficacy of the plasma can be increased when plasma density is enhanced. The efficiency is supposed to be due to increased fluxes of neutral chemically reactive atoms and excited molecules, as well as more intense ultraviolet radiation in more energetic discharges. Therefore, the authors suggested that the application of plasma in an inductively coupled mode where the neutral radical density is high, as opposed to capacitively coupled regimes (Soloshenko et al., 2000).

Recently, Bol'shakov et al. published a detailed study of the effects of radiofrequency oxygen plasma at reduced pressure on bacteria. The study was carried out for two modes of operation, the inductively coupled mode and the capacitively coupled mode. The inductive mode was found to offer a better efficiency in destroying biological matter. This was due to higher electron and ion densities in this mode, which resulted in an enhancement of electron-impact process. High densities of atomic oxygen and perhaps O_2^* in synergy with UV photons induced chemical degradation of the biological materials followed by volatilization of the decomposition products (CO_2 , CO, N_2) (Bol'shakov et al., 2004).

Boucher (Boucher, 1980) referred to the possibility of creating plasma with either inductive or capacitive coupling techniques, but placed the main focus of his invention on aldehyde additives into agent gases like oxygen, argon, or nitrogen activated in RF or MW discharges. No systematic study was conducted on the distinction between sterilizing efficacies of plasmas sustained in the inductive and capacitive regimes.

A number of studies have been also specifically devoted to microbial inactivation during low-temperature atmospheric plasma exposure (Montie et al., 2000; Schutze et al., 1998; Kunhardt, 2000; Stark and Schoenbach, 1999; Duan et al., 2005; Herrmann, et al., 1999). Low-temperature atmospheric plasma is a new emerging technology with some advantages as well as disadvantages over low pressure plasma sterilization. The major advantage of lower pressure sterilization over atmospheric pressure plasmas is the typically safe removal of toxic residuals that are products of sterilization. In these cases, we need vacuum systems connected to discharge sources (e.g. MW, RF, DC, DBD, etc.). The vacuum systems pumps out toxic products through the system, recombines them, and later releases the waste as non-toxic residuals. Whereas in atmospheric pressure plasmas, one can be exposed directly to toxic residuals like CN molecules. The price for atmospheric plasma systems can be specifically lower than low pressure systems which involve expensive vacuum equipment. However, the atmospheric plasmas used for bacterial sterilization are beyond the scope of this thesis.

1.4 Commercial “plasma-based” sterilizers

The interest in plasma sterilizing systems was certainly enhanced by existing commercial devices bearing the name “plasma sterilizers”. These are hydrogen peroxide plasma-based sterilizer STERRAD[®] 100 (Johnson & Johnson Company) and peracetic acid plasma-based Plazlyte[®] sterilizer (AbTox) that use plasma only for disinfection of sterilizing agent, but not for sterilization itself (Krebs, 1998).

The STERRAD 100 Sterilizer represents the first sterilization product using low-temperature gas plasma to be successfully commercialized as a general-purpose sterilization system as a supporting unit. The sterilizer has a usable chamber volume of approximately 75 liters. The cycle time is approximately 75 minutes, and the process temperature does not exceed 50 °C. The STERRAD sterilization process comprises the following steps. The items to be sterilized are placed in the sterilization chamber, the chamber is closed, and vacuum is drawn. A 59% aqueous solution of hydrogen peroxide is injected and vaporized into the chamber to provide a minimum hydrogen peroxide concentration of 6.0 mg/l. After subsequent reduction pressure into the sterilization chamber, a low-temperature gas plasma is generated by applying 400 W of RF energy to create an electrical field, which in turn initiates the generation of the plasma. In the plasma, the hydrogen peroxide vapour is broken apart into reactive species that are capable of colliding/reacting with and killing microorganisms. The activated components ultimately recombine to form oxygen, water, and other non-toxic by-products. The combined use of hydrogen peroxide and plasma rapidly sterilizes most medical devices without leaving a toxic residue. At the completion of the process, the RF energy is turned off, the vacuum is released, and the chamber is returned to atmospheric pressure by the introduction of air filtered by high-efficiency particulate air (HEPA) filters (Vickery et al., 1999; Rutala et al., 1998).

AbTox's Plazlyte sterilizer was reported to use 0.5 mg/l of peracetic acid, formed by evaporating a solution of peracetic acid into the sterilization chamber, followed by exposure to a low-temperature plasma consisting of hydrogen, oxygen, and inert carrier gas argon. The alternating peracetic acid and plasma treatment would be repeated multiple times. The mode of action for the process was reported to be due to the oxidation by the peracetic acid or the active species present in the plasma phase (Jacobs and Lin, 2001).

In both systems, it is condensation of the chemical vapour phase on the surface of microorganisms that provides the sterilizing action. Plasma has no bactericidal action, but serves simply as a detoxifying agent by removing noxious residues and limiting the oxidation effect of the highly reactive chemical elements (hydrogen peroxide and peracetic acid based mixture, respectively) that are injected in the form of vapours as the sterilizing agent (Moisan et al., 2001). It is therefore suggested calling these systems "plasma-assisted" sterilization systems, keeping the designation plasma sterilizers for those where the inactivation of microorganisms stems from species produced by an electrical discharge; they are otherwise without any bacterial action (Laroussi, 2005).

In the second generation hydrogen peroxide gas plasma sterilizer, the STERRAD 100S system load tolerance was improved, which achieved faster kill in diffusion-restricted areas. It also has the advantage of being retrofittable to the original STERRAD 100 and of having faster cycle time (54 minutes). Whereas the STERRAD 100 provides a single sterilization phase, and consists of two consecutive, equal sterilization phases. The process parameters in each phase are identical (Yamamoto, 2001).

Later also smaller volume versions of sterilizer with 44 l of usable space (STERRAD 50) and larger volume with 150 l (STERRAD200) were developed (Jacobs and Lin, 2001). However the toxic agents in these devices are still preserved on surfaces and this makes STERRAD sterilizers not appropriated for a wide range of applications. Although a lot of effort was put in direct plasma sterilization, no sterilizers are available on the market.

1.5 Inactivation agents in low pressure oxygen or oxygen-containing plasma

Under plasma treatment of surfaces, bacterial cells can be inactivated by one of known factors or by a synergistic combination of these. These factors are UV radiation, reactive neutral species, and charged particles (electrons and ions). The extent of the influence of each factor depends on the plasma operating discharge parameters such as power and gas mixture and flow rate (Laroussi, 2004). However these discharge parameters can vary for the same system due to plasma characteristics. Therefore, we need to look at plasma parameters that are generated by discharge parameters.

1.5.1 Effect of the UV radiation

The inactivation of microorganisms as a result of UV radiation is almost entirely attributable to photobiochemical reactions that are induced within microorganisms. Therefore, these processes are not visible directly. Moreover, these reactions are constituent specific; the vast majority of change occurs in nucleic acids and proteins. UV affects the cell of bacteria by inducing the formation of thymine dimers in the DNA. This inhibits the bacteria's ability to replicate properly.

By comparing the killing kinetics of UV radiation from the low-pressure mercury lamp of atmospheric pressure cold plasma, Laroussi concluded that UV does not play a prominent inactivation role (Laroussi, 2004). Other researchers carried out various experiments that also supported the claim that UV plays only a minor role as a killing mechanism (Yamamoto et al., 2001; Kuzmichev et al., 2001). The reason for this is that UV is known to inactivate cells only if its wavelength is within the "germicidal range" (220 nm to 280 nm) and its dose is high enough. Therefore, if the created plasma discharge does not emit UV radiation in this range, then we don't expect any pronounced inactivation effect (Herrmann, 1999). Oxygen plasma has some weak emissions of UV lines in the range between 200 nm and 300 nm, but the role of this emission can be mostly disregarded in most of low pressure plasmas (Cvelbar et al., 2007). However, when we add oxygen gas with other gases, typically nitrogen the UV emission becomes more pronounced and plays important role in inactivation of bacteria (Xu et al., 2007; Villeger et al., 2005; Villiger et al., 2004; Philip et al., 2002; Monna et al., 2002).

1.5.2 Effects of the reactive species

The reactive species, generated in thermodynamically nonequilibrium gas discharge through electron-impact excitation and dissociation, play an important role in inactivation of bacteria. Several investigators experimentally showed that gas discharges containing oxygen have a strong germicidal effect, whereas the D-value decreases if a certain amount of oxygen is added. This is due to the presence of oxygen-based active species such as neutral atomic oxygen, the metastable singlet state of oxygen, and ozone (Kuzmichev et al., 2001; Herrmann et al., 1999; Richardson et al., 2000; Moreau et al., 2000; Villiger et al., 2005). Other radicals such as hydroxyl-radical OH have also been found to play a significant role in the inactivation process by chemically attacking the outer structures of bacterial cells (Laroussi, 2002). However, there are very little or no reports with the quantitative or cumulative effect of reactive species on bacterial cells, including the role of oxygen plasma neutral atoms. The major reason for reports absence is the shortage or complexity of detection methods for quantification of reactive species including neutral atoms.

1.5.3 Effect of the charged particles

The average energy, or kinetic temperature, of the electrons in a nonequilibrium-discharge is in the electron-volt range, and that of the ions is close to room temperature. At low pressures and with relatively low energies, bombardment of bacterial cells by charged particles is expected to play no role in the destruction of microorganisms. Because of this fact, most researchers in this field have neglected to investigate the role, if any, of the electrons and ions in the inactivation process of bacteria. However, Mendis et al. and Laroussi et al. suggested that charged particles might play a very significant role in the rupture of the outer membrane of bacterial cells. By using a dusty-plasma model, they showed that the electrostatic force caused by charge accumulation on the outer surface of the membrane could overcome the tensile strength of the membrane and cause its rupture (Mendis et al., 2000; Laroussi and Mendis, 2003).

1.6 Kinetics of the bacterial inactivation process

Inactivation kinetics studies reveal that bacteria inactivation by non-equilibrium low pressure plasmas is a complex process. Several factors can impact the killing process (Laroussi, 2003):

- the type of bacteria,
- the type of medium in/on which cells are seeded,
- the number of cell layers in the sample,
- the type of exposure,
- contribution of UV or lack thereof,
- operating gas mixture.

Three basic mechanisms are involved in the plasma inactivation of microorganisms:

- direct destruction by UV irradiation of the genetic material of microorganisms;
- erosion of the microorganisms atom by atom, through intrinsic photodesorption by UV irradiation to form volatile compounds combining atom intrinsic to the microorganisms;
- erosion of the microorganisms, atom by atom, through etching to form volatile compounds as a result of slow combustion using oxygen atoms or radicals emanating from the plasma (Moisan, 2001).

The concept of inactivation or destruction of a population of microorganisms is not an absolute one. As stated before, it is impossible to determine if and when all microorganisms in a treated sample are destroyed. It is also impossible to provide the ideal conditions that inactivate all micro-organisms. Some cells can always survive under otherwise lethal conditions. Therefore, experimental investigation of the kinetics of cell inactivation is paramount in providing a reliable temporal measure of microbial destruction (Block, 1992).

1.7 Bacteria

Bacteria are the oldest, the simplest, and the most numerous forms of life. There are thousands of kinds of bacteria. Most of them are harmless to humans. Although the vast majority of these bacteria are rendered harmless by the protective effects of the immune system and a few are beneficial, some are pathogenic bacteria and cause infectious diseases.

Bacteria are visible only with aid of microscope. The smallest bacteria are only 0.1 to 0.2 μm in diameter, whereas larger bacteria may be many microns in length. However, most species are approximately 1 μm in diameter. For example, *Escherichia coli*, an "average" sized bacterium with an average cell length of approximately 1 μm has a cell volume of 1 - 2 μm^3 . This corresponds to a wet mass of about 1 pg, assuming that the cell consists mostly of water. The dry mass of a single cell can be estimated as 20 % of the wet mass, amounting to 0.2 pg. About half of the dry mass of a bacterial cell consists of carbon, and also about half of it can be attributed to proteins. Small size is extremely important because it allows for a large surface area-to-volume ratio, which allows for rapid uptake and intracellular distribution of nutrients and excretion of wastes.

A bacterium's structure is quite simple (Figure 3). From the outside in, there is the capsule, the cell wall, and then the cell membrane. Inside is the cytoplasm, which holds the hereditary material, and at times the endospore. There are no intracellular organelles.

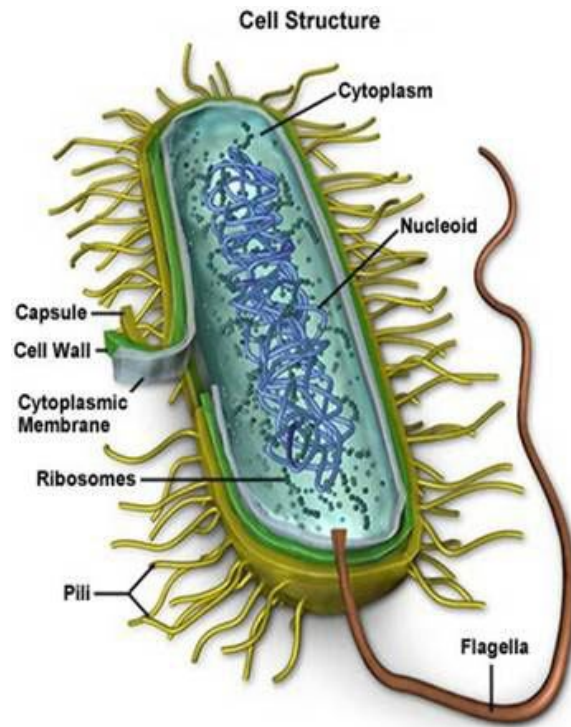


Figure 3: *Basic bacterial cell structure.* (<http://www.micro.magnet.fsu.edu/cells/bacteriacell.html>)

Cells from animals, plants, and fungi are eukaryotes (Greek for “true nucleus”), whereas bacteria and the blue-green algae belong to the prokaryotes (Greek for “primitive nucleus”). In addition to lacking a nucleus and other organelles, most bacteria contain a mesh-like peptidoglycan cell wall that surrounds the membranes to protect it against the environments. Bacteria can survive and in some cases grow in hostile environments in which the osmotic pressure outside the cell is so low that most eukaryotic cells would lyse in the following conditions: at extreme temperatures (both hot and cold), with dryness, and with very dilute and diverse energy sources. Bacteria have evolved the structures and functions to adapt to these conditions. Several of these distinctions provide the basis for antimicrobial action. In general, the interior organization of eukaryotic cells is more complex than that of prokaryotic cells. The eukaryotic cell is usually larger and contains membrane-encased organelles or compartments that serve various functions; the prokaryotic cell is noncompartmentalized.

Bacteria do not contain a membrane-bound nucleus. Their DNA consists of a single circular chromosome. This appears as a diffuse nucleoid or chromatin body (nuclear body), which are attached to a mesosome, a saclike structure in the cell membrane. Bacterial ribosomes are found free in the cytoplasm or attached to the cytoplasmic membrane.

Stained bacteria sometimes reveal the presence of granules in the cytoplasm (cytoplasmic granules). These granules are storage deposits and may consist of polysaccharides such as glycogen, lipids such as poly- β -hydroxybutyrate, or polyphosphates.

Pili are hollow, hair-like structures made of protein that allow bacteria to attach to other cells. A specialized pilus, the sex pilus, allows the transfer from one bacterial cell to another. Pili (sing., pilus) are also called fimbriae (sing., fimbria). The purpose of flagella (sing., flagellum) is motility. Flagella are long appendages which rotate by means of a “motor” located just under the cytoplasmic membrane. Bacteria may have one, a few or many flagella in different positions on the cell. Certain genera, such as *Bacillus* and *Clostridium*, produce *endospores* in response to harsh environmental conditions. Once the hazard is removed, the spore germinates to create a new population.

Bacteria can be distinguished from one another by their morphology (size, shape, and staining

characteristics) and by their metabolic, antigenic, and genetic characteristics. Although bacteria are difficult to differentiate by size, they do have different shapes. A spherical bacterium, such as *Staphylococcus*, is a coccus; a rod-shaped bacterium, such as *Escherichia coli*, is a bacillus or rod; and the snakelike treponeme is a spirillum. Bacteria generally form distinctive cell morphologies when examined by light microscopy and distinct colony morphologies when grown on Petri plates. These are often the first characteristics observed by a microbiologist to determine the identity of an unknown bacterial culture.

All bacteria have three major nutritional needs for growth:

- A source of carbon (for making cellular constituents);
- A source of nitrogen (for making proteins);
- A source of energy (ATP) (for carrying out cellular functions).

Bacteria replicate by binary fission, one cell dividing into two cells. The time required for one cell to divide into two cells is called the generation time or doubling time. The generation time of a bacterium in culture can be as little as 20 minutes for a fast-growing bacterium such as *Escherichia coli* or as long as 24 hours for a slow-growing bacterium such as *Mycobacterium tuberculosis* (Murray et al., 1999).

1.7.1 Cell envelope structures

The cell envelope consists of the membrane and structures surrounding the cytoplasm. In bacteria, these are the cell membrane and the cell wall. Some species also produce capsules and slime layers. The *cell membrane* is a lipoprotein membrane that surrounds the cytoplasm. It is made of phospholipids and proteins. The cell membrane is responsible for many of the function attributable to organelles in eukaryotes. The *cell wall* of prokaryotes is a rigid structure that maintains the shape of the cell. The two major types of cell walls are the gram-positive and gram-negative types (Figure 4). Gram-positive and gram-negative bacteria have similar internal but very different external structures.

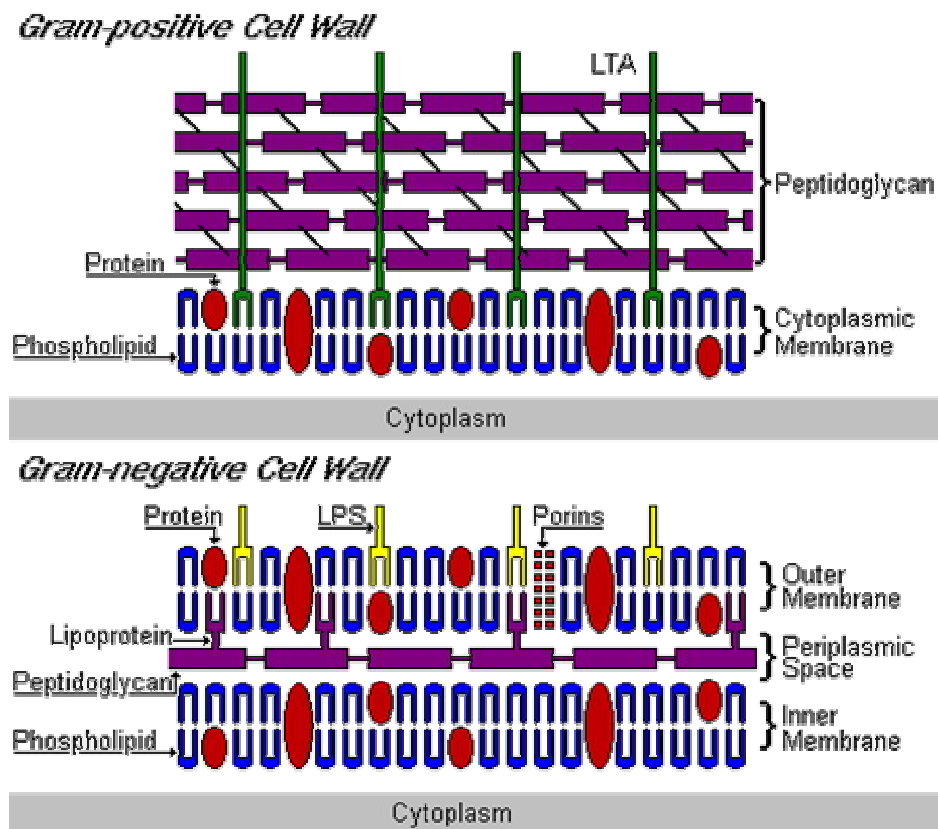


Figure 4: *Cell wall structure.* Gram positive and gram negative (bacteria) cell wall structure. (<http://www.cehs.siu.edu/fix/medmicro/genmicr.htm>)

The *gram-positive cell wall* is composed of a very thick protective peptidoglycan (murein) layer which surrounds the cytoplasmic membrane. The peptidoglycan is essential for the structure, replication, and for survival in the normally hostile conditions in which bacteria grow. The gram-positive cell wall may also include other components such as teichoic and lipoteichoic acids and complex polysaccharides.

Gram-negative cell walls are more complex than are gram-positive cell walls. The cell wall of gram-negative microorganisms is composed of two layers. The inner peptidoglycan layer is much thinner than in gram-positive cell walls. Outside the peptidoglycan layer is an additional *outer membrane* unique to gram-negative cell wall. The outer membrane contains proteins, phospholipids, and lipopolysaccharide. Between the outer membrane and the inner membrane, and encompassing the thin peptidoglycan layer, is an area referred to as periplasmic place. Within the periplasmic place is a gel like matrix containing nutrient-binding proteins and degradative and detoxifying enzymes.

Some bacteria (gram-positive or gram-negative) are closely surrounded by loose polysaccharide or protein layers called *capsules*. If the layer is strongly adhered to the cell wall, it is called a capsule; if not, it is called a slime layer. These layers provide resistance to phagocytosis and serve as antigenic determinants (Mahon, 2000).

2 Aims and Hypothesis

The aim of this thesis was to evaluate the inactivation efficiency of bacteria with precisely determined plasma parameters of low pressure oxygen plasma created by radiofrequency discharge at 27.12 MHz.

In order to achieve these aim:

- The reliable and accurate “real-time” monitoring of plasma sterilization was applied during the process.
- The surface analysis methods were used to evaluate morphological changes of bacteria prior and after plasma treatment.
- The analysis methods for evaluation of bacterial viability were applied.
- The analysis methods for the quantitative determination of live, dead and total number of bacterial cells were used.
- The influence of different plasma parameters (such as the electron density and the electron temperature, the potential difference between plasma and substrate, the density of neutral atoms, the density of plasma ions, the kinetic energy of the ions, etc) on plasma sterilization were studied since discharge parameters were found to be unreliable (e.g. the discharge power, the pressure, the type of discharge, etc). For this, plasma characterization techniques were used.

The hypothesis is that plasma sterilization efficiency is not determined by the treatment time or discharge parameters, but by the density and flux of neutral oxygen atoms, as well as charged plasma species to the contaminated surface, whereas presence of charged species, in our case positive oxygen ions, accelerates the inactivation process of bacteria.

3 Materials and Methods

3.1 Plasma and plasma experimental setup

3.1.1 Weakly ionized oxygen plasma

Cold, weakly ionized, highly dissociated oxygen plasma created in a low pressure radiofrequency or microwave gas discharges have been extensively used in various industrial and research applications such as surface activation and functionalization, plasma cleaning, selective plasma etching, sterilization, and cold ashing. (Canal et al., 2007; Canal et al., 2009; Cvelbar et al., 2005a; Grill et al., 1994; Hippler et al., 2001; Klanjek Gunde et al., 2005; Mozetič et al., 2004). The common characteristic of these applications is that they are based on a chemical modification of only the topmost atomic layers, while the bulk material is left fairly intact. This is due to neutral radical interactions with the surface, in particular with neutral atoms, the most abundant active species in weakly ionized plasmas. Neutral atoms are usually created by the dissociation of the source gas molecules. The radical neutrals do not carry an electric charge and therefore do not receive any additional energy from electromagnetic fields. Thus, their kinetic energy is comparable with the thermal kinetic energy of the precursor molecules. In thermally non-equilibrium plasmas produced by RF and microwave discharges, the neutral species usually find themselves at room temperature. The corresponding kinetic energy of the neutral species is thus about 0.03 eV, which is not enough to penetrate beneath the surface of the material being processed. Therefore, the effect of these species is mostly limited to the topmost atomic layer of the surface. At the same time, atoms are chemically much more reactive than the molecules of the source gas which makes the threshold temperatures for certain processes comparable to room temperature. Thus, reactive species lead to higher reaction rates compared to the cases when only precursor molecules of the source gas are involved (Ricard et al., 2004). In order to determine certain characteristics of atomic processes (reaction probabilities, etc.) it is practically important to be able to perform reliable measurements of the neutral atom density.

Densities of neutral atoms are hard to predict and can not be estimated from discharge parameters (such as the source gas pressure and temperature, the discharge voltage and current, the discharge volume, the materials facing plasma) alone. Whereas the discharge parameters are important factors in terms of atom production, atom losses in the plasma reactor which occur upon contact with solid surfaces (i.e. walls of the plasma reactor) and due to chemical processes in the reactor are equally important if not more so. (Cartry et al. 2000; Cartry et al., 2006). Losses on the surfaces of the plasma reactor are due to recombination (or association) which happens with the probability that depends not only on the material composition and structure, but also on the surface temperature. In some cases, the latter can change dramatically during the discharge operation. One can thus see that accurate determination of the atom density in the plasma reactor is crucial.

3.1.2. Measurements of plasma parameters

The discharge parameters (gas pressure, discharge power, flow rate, discharge frequency, etc.) alone are not enough to give enough ideas about the conditions inside reactors, where samples are treated and sterilized. Therefore we need to know the real conditions as the density of neutral species, density of charged species, and energies of ions/electrons, which are the plasma parameters. Typically, the neutral atom densities are measured by catalytic probes, the charged particles by Langmuir probes, whereas the qualitative information on plasma species is measured by Optical Emission Spectroscopy (OES).

3.1.2.1 Catalytic probes

Measurements of neutral atom densities are indispensable in a thorough plasma characterization process. Although in the past decades many spectroscopic methods of measuring atom densities have been developed, (Cvelbar, et. al., 2007, Dean, 2007; Drenik et al., 2005a; Drenik et al., 2006; Mozetič et al., 2003) less sophisticated yet robust and reliable catalytic probes are rapidly emerging (Šorli, 2000). A catalytic probe is a piece of solid material immersed into an atom-rich atmosphere. As the atoms recombine on its surface, the probe surface absorbs the energy (which is almost the same as the energy of dissociation) released at association, and as a result the probe temperature rises. By measuring the temperature of the probe material, it is possible to determine the neutral atom density. The main appeal of the catalytic probe is a straightforward interpretation of experimental data, which is not always the case for many other methods. Moreover, catalytic probe designs have benefited enormously from recent technological advances. Indeed, the Fibre Optic Catalytic Probe (FOCP) represents a substantial advance as compared with the original thermocouple-based probe configuration (Cvelbar et al., 2005b; Cvelbar et al., 2008; Mozetič et al., 2005). Unlike the original prototype, where a disc of catalytic material is attached to a thermocouple, the main part of the FOCP is a glass sphere (diameter typically around 0.4 mm) connected to an optical fibre. The catalyst material is in the form of a thin foil wrapped over the glass sphere. Although the manipulation of materials of such small dimensions is difficult and tedious, such a configuration appears to be more stable and resistant than other techniques of applying metal to the glass surface or using physical or chemical vapour deposition.

The absolute temperature of the probe material is determined with a photodetector. As the foil heats up due to atom recombination on its surface, it radiates heat which is then collected by the glass sphere and transmitted through the optical fibre to the photodetector. The main advantage of this design is that the signal is an optical one and therefore is not susceptible to electromagnetic interference, which is unavoidable in a typical radiofrequency discharge sustained in a plasma reactor. However, it should be noted that a catalytic probe cannot differentiate between the species and their different excited and ionized states. Therefore, it is particularly useful in environments where one of the plasma species is dominant, which is the case in weakly ionized plasmas created in pure diatomic gases.

3.1.2.2. Optical Emission Spectroscopy

Reliable and accurate plasma diagnostic techniques have been developed to provide real-time information in the presence of excited plasma species. Low pressure plasma emits visible radiation, so the examination of the nature of plasma glow enables the study of chemical and physical processes during the plasma treatment of materials. The method is called optical emission spectroscopy (OES). Optical emission spectroscopy is used for investigation of many plasma processes (Kanazawa, 1989). It can recognize the ions and radicals in the plasma by measuring the wavelengths and intensities of the emitted light quanta.

Optical emission spectroscopy is therefore a powerful tool of plasma diagnostics for detection of plasma species, but not for the quantification of their densities. The radiation intensity depends on the nature of the excited states. For instance, radiation from metastable states is usually not observed, while strongest emission is often observed from atomic transitions (Cvelbar et al., 2007; Krstulović et al., 2006).

Optical emission spectroscopy was performed with the HR2000CG-UV-NIR spectrometer (OceanOptics), which was set to a spectral resolution of 1 nm and a spectral range of 200–1100 nm. A quartz window is mounted perpendicularly to the discharge tube, and an optical fiber is fixed on the axis. The 600 μm diameter, solar resistant fiber collects radiation from the entire length of the discharge tube. Typically spectra were recorded with an integration time of 300 ms (Cvelbar et al., 2007; Krstulović et al., 2004).

The majority of experiments with optical emission spectroscopy were performed during the bacteria treatment to evaluate the possibility of real-time monitoring of the sterilization. Optical emission spectra were measured simultaneously as the sterilization of bacteria was in progress. For each pressure, the background was measured as well to prove that particular spectral features are really due to bacteria degradation, and not to any other effect (Vujošević et al., 2007).

3.1.1.1 Double Langmuir probe

The measurements of electron temperature and oxygen ion density were performed with a double Langmuir probe (Dorman, 1997). The standard double probe was immersed into plasma and the $I = I(U)$ characteristics were drawn at various pressures.

An electrode is biased relative to a second electrode, rather than to the vessel when using the double Langmuir probe. The theory is similar to that of a single probe, except that the current is limited to the ion saturation current for both positive and negative voltages. One advantage of the double probe is that neither electrode is ever very far above floating, so the theoretical uncertainties at large electron currents are avoided. Another advantage is that there is no reference to the vessel, so it is to some extent immune to the disturbances in radiofrequency plasma. On the other hand, it shares the limitations of a single probe concerning complicated electronics and poor time resolution. In addition, the second electrode not only complicates the system, but it makes it susceptible to disturbance by gradients in the plasma. The detailed description of these standard double Langmuir probe measurements is beyond the scope of this thesis, and was previously done by Mozetič (Mozetič, 1992).

3.1.2 The plasma system with reactor

The experimental setup used for bacterial inactivation studies is shown in Figure 5.

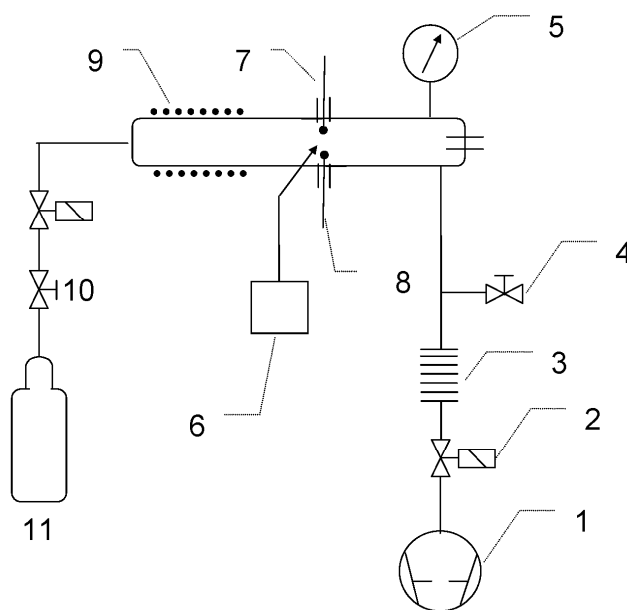


Figure 5: *Schematic of the experimental system.* 1 - rotary pump, 2 - valve, 3 – trap with molecular sieves, 4 – air valve, 5 - vacuum gauge, 6 – optical emission spectroscopy / IR temperature measurements, 7 - catalytic probe, 8 – Langmuir probe, 9 - discharge chamber with RF coil, 10 - leak valves, 11 - oxygen flask.

The discharge vessel was a cylindrical tube with diameter of 40 mm and the length of 600 mm. The tube was made of a borosilicate glass (Schott 8250) with the recombination coefficient for oxygen atoms at the room temperature of 1.9×10^{-4} . At both ends it was joined to kovar rings, which were welded to standard KF 40 flanges. The glass-to-metal joint was bakeable up to 400°C. On one side, the tube was connected to the vacuum system. The system was pumped with a two-stage oil rotary pump with the pumping speed of 4.4 l s^{-1} and the ultimate pressure of 0.1 Pa. All connections between the pump and the discharge vessel were made of components with the conductance of approximately two orders of magnitude higher than the pumping speed of the pump, so that the effective pumping speed in the discharge vessel was nearly as high as that of the pump. The pressure in the system was measured with a Pirani gauge. Prior to experiments, the

gauge was calibrated for oxygen with a precise baratron. A recombinator for O atoms was placed in front of the gauge in order to prevent its degradation during plasma experiments. The base pressure in the system was about 6 Pa. The discharge vessel was placed in a coil connected to a RF generator. The frequency of the generator was 27.12 MHz and the output power approximately 180 W to 200 W.

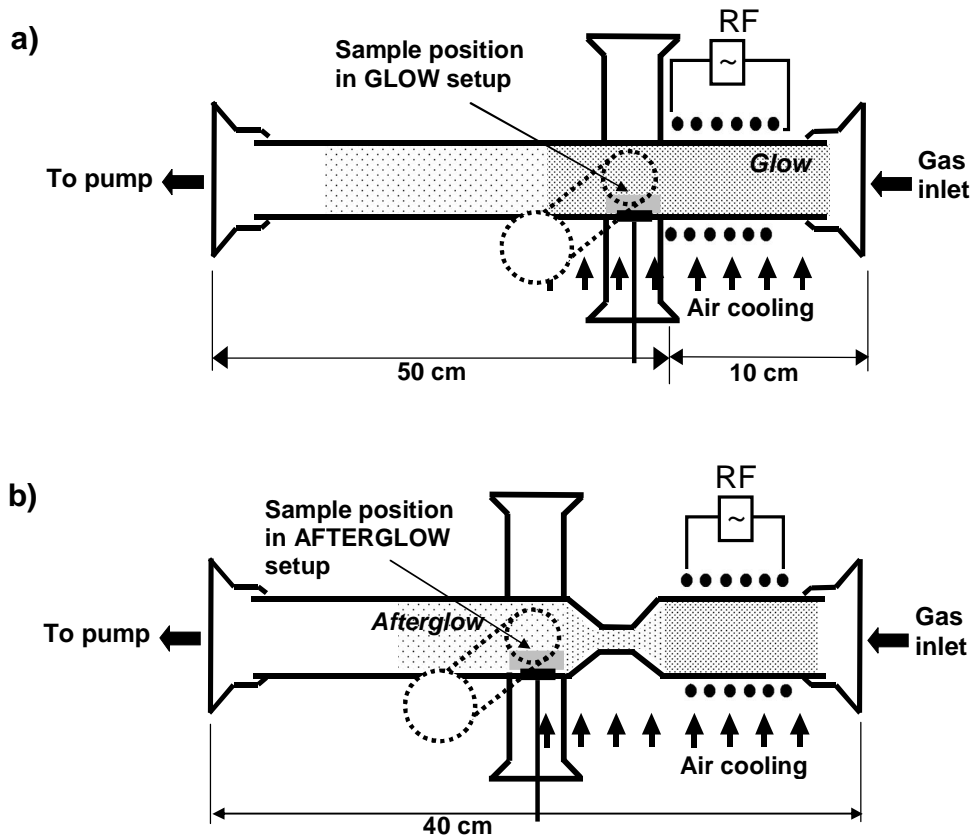


Figure 6: *Schematic of plasma reactors.* The schematic of plasma reactor vessels: a) glow setup and b) afterglow setup.

Two configurations of the plasma reactor were used. They are schematically presented in Figure 6. One side of each of the reactors was connected to the pump, and the other side to a gas inlet system. Commercially available oxygen was leaked to the system through a leak valve. Both discharge vessels were forced air-cooled. The main difference between the plasma reactors presented in Figure 6b is in the narrow tube that may be inserted between the discharge and the afterglow sections. The narrow tube serves as an excellent recombinator of charged particles. Ions that are created in the discharge region recombine on the walls of the narrow tube so the atmosphere in the afterglow is virtually free from charged particles, including electrons (Cvelbar et al., 2006b). In the configuration without the narrow tube, the boundary between discharge and afterglow is not at all sharp, so there is a gradual decrease of the charged particle density along the tube. The narrow tube also represents a perturbation in the gas flow: there is a small but finite gradient of pressure along the narrow tube, so the drift velocity of gas in the afterglow chamber with the narrow tube is much larger than in the absence of the tube. Probes for measurements as well as OES and IR measurements were performed through supporting glass side arms. Whereas the pressure measurements with vacuum gauge are performed just after kovar rings in the direction of the gas flow towards the pump.

3.1.2.1 Low pressure oxygen plasma treatment

The samples inserted into the glow discharge region were on a floating potential to prevent any additional acceleration of ions and thus heating of the sample surface. The plasma density and the electron temperature were estimated with a simple double Langmuir probe mounted in the centre of the discharge chamber prior to sterilization experiments. The electron temperature slowly decreases with increasing pressure: at 20 Pa, it is about 5 eV, while at 100 Pa, it is about 3 eV. The plasma density depended largely

on pressure and is plotted in Figure 7.

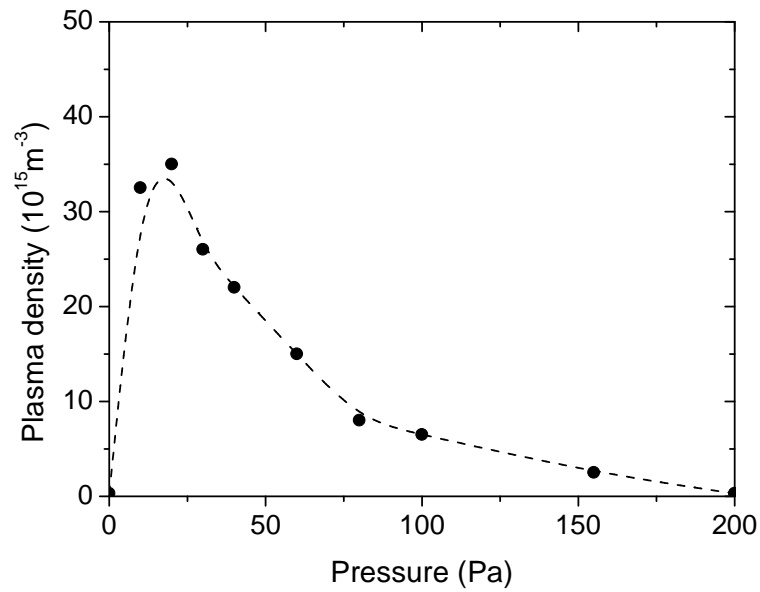


Figure 7: *Plasma density*. Plasma density or density of charged species versus pressure in the pressure range from 1 Pa to 200 Pa. (Mozetič, 1992; Vujošević et al. 2006)

The density of neutral oxygen atoms was also measured prior to sterilization experiments with a catalytic probe in the reactor side arms. The O-atom density versus pressure is plotted in Figure 8.

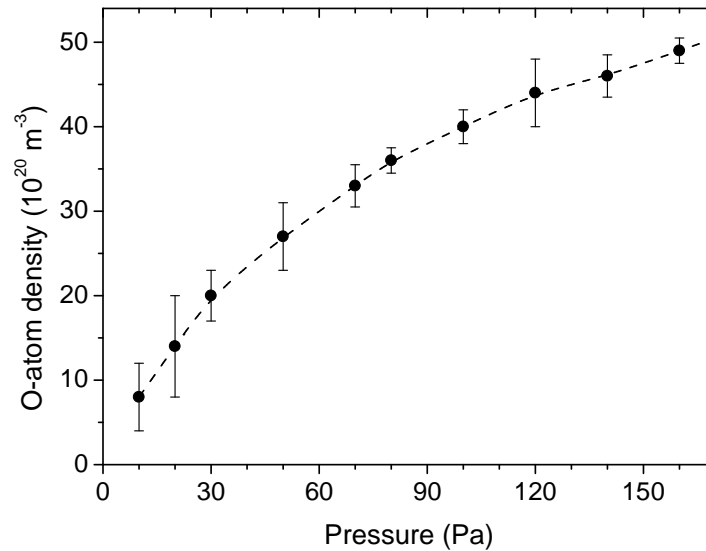


Figure 8: *Density of neutral O atoms*. Density of neutral O atoms measured with FOCP vs. pressure in the range from 10 Pa to 160 Pa.

Samples were exposed for different treatment times to plasma at pressures of 30, 75 and 150 Pa, where characteristic changes between plasma parameters are seen. In another control experiment, bacteria were exposed to vacuum conditions, but without plasma in order to detect possible changes caused by evacuation only and not by plasma.

3.2 Sample preparation and analyses

3.2.1 Bacteria and processing

The inactivation effect of the oxygen plasma was tested on the *Bacillus stearothermophilus* ATCC No. 7953 (Gram-positive bacteria), *Staphylococcus aureus* ATCC No. 25923 (Gram-positive bacteria) and on the *Escherichia coli* ATCC No.25922 (Gram-negative bacteria). These bacteria were obtained from the MicroBioLogics CE (MN, USA). Bacterial cultures were grown overnight on Colombia agar plates (Difco Laboratories, MI, USA) at 55°C for *Bacillus stearothermophilus* and 37°C for *Staphylococcus aureus* and *Escherichia coli*. Cells were picked up with a loop and re-suspended in sterile water. The 100 µl of this initial bacterial suspension was evenly distributed onto the surface of sterile glass, silicon or aluminium substrate with the dimensions of 4 cm × 1.25 cm and air dried in a laminar-flow hood. Bacteria on substrates remained un-treated (control), or were either exposed to one of the following: low pressure oxygen plasma, vacuum, or high-temperature dry heat.

3.2.2 Plate count technique

The plate count is one of the standards means of enumeration of viable microbes because it allows for a visual indicator for every cell in the specimen. The technique stems from Robert Koch's insight gained from viewing colonies growing on the surface of a spoiling slice of potato. In practice, a small aliquot of a liquid suspension of microbes is spread on the surface of solidified nutrient medium, which when incubated, leads to each cell 'developing' into a visible colony through repeated fission. By counting each colony, the total number of colony forming units (CFUs) on the plate is determined. By multiplying this count by the total dilution of the solution, it is possible to calculate the total number of CFUs in the original sample (Colins, 1995).

One major disadvantage of the viable plate count is the assumption that each colony arises from one cell. In species where cells grow together in clusters, a gross underestimation of the true population is resulted. This is why the term *CFUs per ml* is used instead of *bacteria per ml* for the results of such an analysis. It is a constant reminder that one colony does not equal one cell. Great care must also be taking during dilution and plating to avoid errors. Even a small error in dilution, can have large effects on the final counting numbers. The rate at which bacteria give rise to an observable colony can also vary and depends on incubation time. Some colonies may not rise if an incubation time is too short. The temperature of incubation and medium conditions must also be optimized to achieve the largest colonies possible in order to make counting easier. The disadvantage of this technique is that it is very time consuming. Depending on the organism, one day to several weeks are needed to determine the number of CFUs (Kaiser, 2005; Isenberg, 1992).

Despite its shortcomings, the viable plate count is a popular method for the determination of cell numbers. The technique is sensitive and has the advantage of only counting living bacteria, which is often the important issue. Any concentration of microorganism can be easily counted via this method. The plate count method is long and laborious, and is not very accurate. Replicate plates have discrepancies that can be attributable to uneven distribution of bacteria, pipetting, counting errors, and many other systems. One estimate is that the normal error in the plate count may be as large as 10% (Carpenter, 1978). Therefore results obtained via the plate count should be taken with some critical observations.

3.2.2.1 Cultivation of bacteria – CFU measurements

Before and after each treatment, the samples (bacteria on carriers) were aseptically placed in sterile containers with 2 ml 0.85% NaCl saline solution. The containers were then briefly vortexed in order to wash bacterial cells from carriers. The suspension was serially diluted (1/10) in saline to the required concentration range. A sample of 100 µl of the diluted suspension was inoculated onto Colombia agar plate and spread evenly with a sterile bent glass rod. Plates were then incubated at 37°C (for *Staphylococcus aureus* and *Escherichia coli*) and 55°C (for *Bacillus stearothermophilus*) for 24-48 h. Colony forming units were finally counted to determine the number of survivors of bacteria. Also, 100 µl of bacterial suspension (before dilution) was transferred to 5 ml Tryptic glucose yeast broth and incubated for 7 days, and

monitored daily for growth. When turbidity occurred in any container, we sub-cultivated it on Columbia agar plates and searched for nominated (or any other in the case of contamination) bacteria. After 7 days the contents of all containers were sub-cultivated on Columbia agar plates to prove absence of growth. The samples were thereafter declared sterile if no positive growth was observed.

3.2.2.2 Carriers

Pyrex glass rectangular substrate and aluminium sheets as well as silicon wafers Si (100) triangular were used as carriers for bacteria as mentioned above. In order to avoid charging effects during the electron microscope imaging, aluminium sheets and Si wafers were used for SEM analysis, while glass carriers were used during the stage when fluorescence or flow cytometry was applied. The typical surface of the glass sample was $4\text{ cm} \times 1.25\text{ cm} = 5\text{ cm}^2$, whereas Si and Al substrates for SEM imaging were about 1 cm^2 .

3.2.2.3 Preparation of carriers

All carriers were prepared prior to bacteria deposition by plasma activation of surface in order to avoid bacteria agglomeration, and to achieve uniform distribution of cells across the entire carrier. The activation process was performed by oxygen plasma treatment for 5 s. Plasma with the same characteristic parameters at 75 Pa was used for both the activation of carriers and for the treatment of bacteria. The bacteria were deposited on carriers from liquid solution within 1 minute after surface plasma activation.

3.2.3 Scanning Electron Microscopy (SEM)

Scanning electron microscopy (SEM) is a widely-used surface analytical technique that images surface topology. High resolution images of surface topography, with excellent depth of field can be achieved by using a highly-focused, scanning (primary) electron beam. The primary electrons enter a surface with an energy of 0.5 - 30 keV, and generate many low energy secondary electrons. The number of these secondary electrons entering the electron detector is largely governed by the surface topography of the sample. An image of the sample surface can thus be constructed by measuring secondary electron intensity as a function of the position of the scanning primary electron beam. High lateral resolution is possible because the primary electron beam can be focused to a very small spot ($< 10\text{ nm}$). High sensitivity to topographic features on the outermost surface ($< 5\text{ nm}$) is achieved when using a primary electron beam with an energy of $< 1\text{ keV}$ (Sampson, 1996; Goodhew et al., 2001).

The SEM allows for the observation and characterization of different organic and inorganic materials from a couple of nanometers to micrometer scale. For conventional imaging, SEM requires conductive samples in order to avoid charging effects due to static electric charge on the sample during electron irradiation. In such cases, non-conductive solid samples are coated with a layer of ultra thin electrically conductive material such as gold, gold/palladium alloy, platinum, tungsten or graphite (Goldstein et al., 2003; Murphy, 2001).

Our samples were imaged using field-emission scanning electron microscopy at a low kinetic energy of primary electrons. All oxygen plasma-treated bacteria, high temperature dry heat-treated bacteria, vacuum-treated bacteria (control) and untreated bacteria (control) on carriers were viewed with Carl Zeiss Supra 35 VP scanning electron microscope. Images were taken on Si or Al substrates at pressure of approx. 10^{-3} Pa and primary electron beam energy of 1 keV or 600 eV. No coating was needed!

3.2.4 Fluorescence Microscopy (FM)

Fluorescence microscopy allows visualization of specific molecules that fluoresce in the presence of excitatory light. Because of its great specificity and detection of molecules, fluorescence microscopy is today the most frequent method used in biomedical research. Fluorescence microscopes contain special filters and employ a unique method of illumination to produce images of fluorescent light emitted from excited molecules in a specimen. The filters are designed to isolate and manipulate two distinct sets of

excitation and fluorescence wavelengths. A band of shorter excitation wavelengths from the illuminator and filters is directed to the specimen, while a band of longer fluorescence wavelengths emitted from the specimen forms an image of the specimen in the image plane. To perform fluorescence microscopy effectively, the microscopist must be able to select the proper fluorochrome, filters, and illuminator for a given application and evaluate the quality of fluorescence signals (Murphy, 2001).

Molecules that are capable of fluorescing are called fluorescent molecules, fluorescent dyes, or fluorochromes. Fluorochromes exhibit distinct excitation and emission spectra that depend on their atomic structure and electron resonance properties. Fluorescent dyes usually contain several unconjugated double bonds. Molecules absorb light and re-emit photons over a spectrum of wavelengths (the excitation spectrum) and exhibit one or more characteristic excitation maxima. Absorption and excitation spectra are distinct, but usually overlap, sometimes to the extent that they are nearly indistinguishable. However, for fluorescein and many other dyes, the absorption and excitation spectra are clearly distinct. The widths and locations of the spectral curves are important, particularly when selecting two or more fluorochromes for labelling different molecules within the same specimen (Herman, 1998; Paustian, 2008).

The viability of microorganisms is crucial for the evaluation of plasma inactivation treatments. The advantages of the fluorescence technique for the rapid assessment of viability of microorganisms include: a high sensitivity (i.e., the number of cells needed for detection is low), a high time resolution (approximately 10^{-8} s), and the potential to analyze individual cells in combination with advanced flow cytometry analysis (Veal, 2000).

The development of improved fluorescence methods for the evaluation of viability of bacteria is focused to nucleic acid staining. DNA and RNA provide large number of intercellular sites for many nucleic acid binding stains that can be excited at different wavelengths. Multi-colour specific labelling increases the information available from the targets cells (Breuweer, 2000). A suitable method is dual staining with the LIVE/DEAD *BacLight* bacterial viability kit (Molecular Probes, The Netherlands). In this procedure, cells are treated with two different DNA-binding fluorescent stains (SYTO 9 and propidium iodide), and viability is estimated according to the proportion of bound stains. This dual staining method allows effective separation between viable and dead cells, which is far more difficult to achieve with single staining. Viability is determined according to the proportion of green and red fluorescence of bacteria (Boulos et al., 1999; Haugland, 2002).

3.2.4.1 Fluorescent labelling of bacterial cells

Fluorescently labelled low pressure oxygen plasma-treated bacteria, high-temperature dry heat-treated bacteria, vacuum-treated bacteria and un-treated bacteria on glass carriers were viewed using wide-field fluorescence microscopy. LIVE/DEAD *BacLight*TM bacterial viability kit L7012 (Molecular Probes, The Netherlands) was used to stain bacteria on glass carriers according to the manufacturer's procedure. For staining solution two DNA stains SYTO 9 (3.34 mM) and propidium iodide (PI, 20 mM), were mixed together (1.5 μ l + 1.5 μ l) and diluted with 1 ml of deionised sterile water. Bacteria were incubated with 20 μ l of staining solution at room temperature in the dark. After 15 min, cells were washed with deionised sterile water and viewed under the inverted fluorescence microscope Olympus IX71 with the camera - Olympus DP50. Green fluorescence signal of SYTO 9 and red fluorescence signal of PI were detected using U-M41001 (exc. 461 - 500 nm / em. 511 - 560 nm) and U-MWIY2 (exc. 545 - 580 nm / em. > 600 nm) Olympus filter cubes, respectively. Oil objectives \times 60 (N.A. = 1.40) and \times 100 (N.A. = 1.35) were used.

3.2.5 Flow cytometry

Flow cytometry is a technique for counting, examining, and sorting microscopic particles suspended in a stream of fluid. It allows for the simultaneous multiparametric analysis of the physical and/or chemical characteristics of single cells flowing through an optical and/or electronic detection apparatus. Modern flow cytometers are able to analyse several thousand particles every second in real time, and can actively separate and isolate particles having specified properties. A flow cytometer is similar to a microscope, except that instead of producing an image of the cell, flow cytometry offers "high-throughput" (for a large

number of cells) and an automated quantification of set parameters (Shapiro, 2003; Ormerod, 2000).

Fluorescence-activated cell sorting (FACS) is a specialized type of flow cytometry. It provides a method for sorting a heterogeneous mixture of biological cells into two or more containers, one cell at a time, based upon the specific light scattering and fluorescent characteristics of each cell. It is a useful scientific instrument as it provides fast, objective and quantitative recording of fluorescent signals from individual cells, as well as the physical separation of cells of particular interest. The acronym FACS is trademarked and owned by Becton Dickinson. This term is not a generic term for flow cytometry.

The data generated by flow-cytometers can be plotted in a single dimension to produce a histogram, or in two dimensional dot plots, or even in three dimensions. The number of cells is shown by the number of dots where each dot represents a single cell. The plots are often made on logarithmic scales. FACS instruments generate three types of data:

- Forward Scatter (FSC) - provides information about approximate cell size.
- Side Scatter (SSC) - provides information about cell complexity or granularity.
- Fluorescent Labelling (FL) - used to investigate cell structure and function.

Forward and side scatters are used for preliminary identification of cells, and to exclude debris and dead cells. Both FSC and SSC are unique for every particle, and combination of the two may be used to differentiate different cell types in a heterogenic sample. Fluorescent labelling allows investigation of a cell structure and a function. Cell auto-fluorescence is generated by labelling cell structures with fluorescent dyes. FACS collect fluorescence signals in one to several channels corresponding to different laser excitation and fluorescence emission wavelength. Because different fluorescent dyes have emission spectra overlaps, signals at the detectors have to be compensated electronically, as well as computationally (modern flow cytometry analytical software applies fluorescence compensation mathematics automatically, which simplifies matters considerably). The measurement from each detector is referred to as a “parameter” or forward scatter, a side scatter or fluorescence. The data acquired in each parameter are known as the “events” and refer to the number of cells displaying the physical feature or marker of interest (Rahman, 2005).

An important principle of flow cytometry data analyses is to selectively visualize the cells of interest whilst eliminating results from unwanted particles e.g. debris. This procedure is called gating. Cells have traditionally been gated according to physical characteristics. For instance, subcellular debris and clumps can be distinguished from single cells by size and estimated by forward scatter. Also, dead cells have a lower forward scatter and higher side scatter than living cells. The graphs representing a single measurement parameter (relative fluorescence or light scatter intensity) on the x-axis and the number of events (cell count) on the y-axis are known as single parameter histograms. The graphs that display two measurement parameters, one on the x-axis and one on the y-axis, and the cell count as density (dot) plot or contour map are known as two-parameter histograms. The parameters in these graphs can be SSC, FSC or fluorescence (FL) (Macey, 1994; Rahman, 2005).

Fluorescence measurements taken at different wavelengths can provide quantitative and qualitative data about fluorochrome-labeled cell-surface receptors or intracellular molecules such as DNA. Flow cytometers use separate fluorescence (FL) channels to detect light emitted. The number of detectors will vary according to the device and its manufacturer (Ormerod, 2000).

Accurate determination of live, dead and total bacteria is important in many microbiology applications. Traditionally, viability in bacteria is synonymous with the ability to form colonies on solid growth mediums, and to proliferate in liquid nutrient broths. These traditional, culture-based tests are time consuming and do not provide real-time results or timely information that is needed in applications such as this one (evaluation of plasma inactivation treatments). In particular, flow cytometry can be readily applied to the enumeration of viable bacteria in a sample (Veal, 2000). Significantly, plate counting is a measure of living cells only, whereas flow cytometry as used in this study, provides an indication of the total number of cells, further separated into living and dead cells.

Therefore, flow cytometry offers the prospect of real-time microbial analysis of individual microorganisms, without dependency on microbial culture. However, flow cytometry has not been

extensively used as a tool for routine microbial analysis. This has been mainly due to the high cost and complexity of instrumentation, the need for trained flow cytometrists and the lack of assay kits with appropriate biological reagents targeted for specific applications.

3.2.5.1 Viability analysis and quantitative determination of live/dead bacteria by flow cytometry

Viability of bacteria was determined with LIVE/DEAD BacLight Bacterial Viability Kit for microscopy and quantitative assay (Molecular Probes, L7012). Alternatively, viability of bacteria as well as the concentrations of live and dead bacteria was determined using LIVE/DEAD BacLight Bacterial Viability and Counting Kit (Molecular Probes, L34856). Both kits contain two stains, green-fluorescent SYTO9 and red-fluorescent propidium iodide (PI). SYTO9 stains both live and dead bacteria, whereas PI enters only dead bacteria. Live bacteria have green fluorescence, while dead bacteria have strong red fluorescence and also weak green fluorescence. The counting kit contains in addition a microsphere standard (beads), by which the volume of the analysed sample can be determined and thereby the concentration of bacteria in the sample calculated. In this way all initial concentrations of bacteria in suspension were determined prior experiments and deposition on sample carriers, as well as counted after the experiments. Counted bacterial cells in initial suspension before deposition on carriers is marked in latter text as initial suspension, whereas deposited and dried bacteria on sample holders are labelled as untreated.

After plasma treatment, glass carriers coated with a layer of bacteria were transferred to a 50 ml tube containing 2 ml of 0.85% NaCl, and bacteria were released from the carriers into a suspension by gentle shaking. To prepare a 1 ml sample for simple viability analysis, 1.5 μ l of each dye was added to 997 μ l of bacteria suspension. To prepare 1 ml of sample for quantitative analysis, 10 μ l of 10-time diluted microsphere standard (1.0×10^7 beads/ml, final concentration thus 1.0×10^5 beads/ml) and 1.5 μ l of each dye were added to 987 μ l of bacteria suspension. Before the analysis, samples were incubated for 15 min at room temperature. If necessary, 10-/ 50-/100-time diluted bacteria suspension was used to prepare samples for the analysis.

Samples were analysed by FACSCalibur flow cytometer (Becton Dickinson) using CellQuest software, version 3.3 (Becton Dickinson). Gates for beads and for bacteria were set using green or red fluorescence and side scatter parameters. The percentages of live and dead bacteria within the gate were calculated from a green fluorescence versus red fluorescence plot. The concentrations of live and dead bacteria were calculated using beads to measure the volume of suspension analysed as follows:

$$\text{Bacteria / ml} = \frac{((\# \text{ of events in bacteria gate}) \times (\text{dilution factors}))}{((\# \text{ of events in bead gate}) \times 10^5)} \quad (1)$$

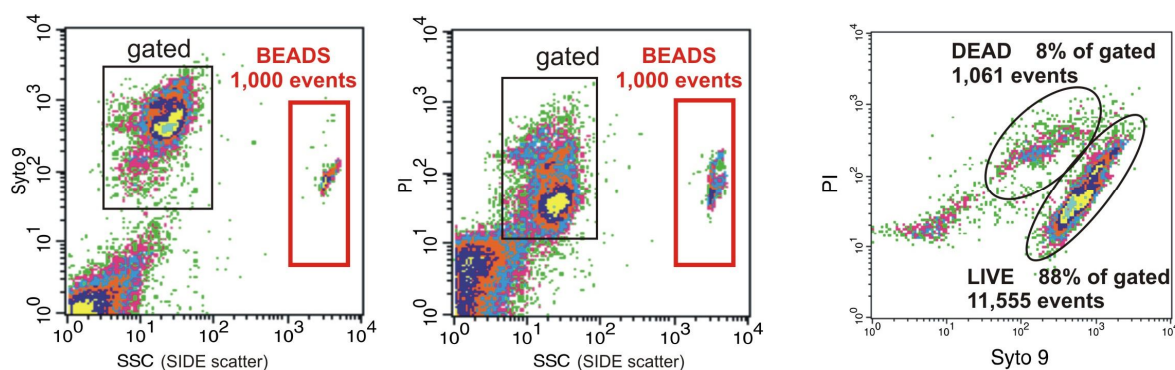


Figure 9: FACS results with gating protocol. The presented FACS images show the gating process protocol for measured stained live (Syto 9) and dead (PI) bacteria with counted beads as well as the joint result.

All experiments were performed with untreated cell suspension, which served as live cell controls as well as with 70 % isopropyl alcohol treated bacterial suspension which served as dead cell controls.

4 Results

4.1 Plasma characteristics and activation of carriers

Prior to experiments performed on bacteria, the parameters of low-pressure oxygen plasma were measured with a Fibre Optics Catalytic Probes and a double Langmuir probe in order to determine the density of neutral O atoms and ions, respectively. The neutral O-atom density was of the order of 10^{21} m^{-3} (Figure 8), the ion density was around 10^{16} m^{-3} (Figure 7) and the electron temperature was about 5 eV. The degree of dissociation of oxygen ($\text{O}_2(\text{g})$) to neutral O atoms ($\text{O}\cdot(\text{g})$) exceeded the ionization fraction by more than 5 orders of magnitude, allowing for almost entire plasma to interact as oxygen radicals with bacteria.

As stated in Experimental Section, the activation of carriers was done in the period of 5 s. Taking into account that in plasma the flux of O atoms was about $1 \times 10^{23} \text{ m}^{-2} \text{ s}^{-1}$, the dose of atoms which was received by carriers exceeded $5 \times 10^{23} \text{ m}^{-2}$, i.e. $5 \times 10^{11} \mu\text{m}^{-2}$. This flux of O atoms increased surface energy by mostly removing impurities from Al, Si and glass carriers. In this way, even distribution of bacteria cells on the entire carrier surface was achieved. Furthermore, X-ray photoelectron spectroscopy (XPS) analysis of thus activated Al, Si and glass carriers showed no traces of organic impurities, which could cause a decrease of surface energy and consequently uneven distribution of bacteria later on. Moreover, on the samples of aluminium and silicon a thin layer of oxide was created. Therefore, we can claim that bacteria were deposited on well activated carriers. Afterwards, the samples were then exposed to plasma separately for different periods of time. The plasma parameters were the same as previously used for the activation of the carriers.

4.2 The influence of substrate material on bacteria sterilization in an oxygen plasma glow discharge

During the processes of bacteria sterilization the reactive species didn't interact just with bacteria, but also with carriers or material being sterilized. To the best of our afford we could not find relevant data on the influence of carriers on bacteria inactivation, such as thermal effects due to heterogeneous neutral atom recombination on substrates, we performed systematic measurements to determine the influence of substrate material on plasma sterilization. Due to surface relaxation and recombination of neutral atoms, we can get extensive energy release causing local heating of material and its distortion including microorganism inactivation through unwanted heat (Cvelbar et al., 2006a).

The heating effect of material can be seen from Figure 10, where we measured the temperature of two different substrates (aluminium and glass) during continuous oxygen plasma treatments. We can see that aluminium substrate is heated above 350 K in about 10 s of plasma treatment, and the Al substrate temperature keeps rising for a minute when it reaches a fairly constant value of almost 700 K. On the other hand, the temperature of a glass substrate remains below the detection limit of our thermometer, i.e. 350 K for over than 3 minutes. The huge difference in heating rates is explained by different probability for oxygen atom recombination: the probability is extremely low for glass and moderately high for aluminium. The choice of substrate materials has therefore a tremendous influence on the process of material sterilization. The material overheating can cause sterilization itself! In order to clearly distinguish between "plasma" and "heating" effects, especially for biocompatible materials such as different polymers, the recombination coefficient has to be known.

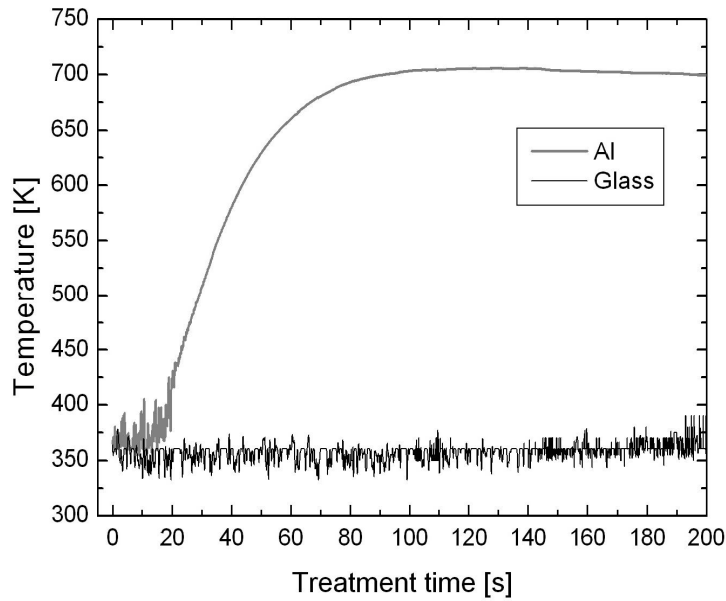


Figure 10: *Substrate heating in plasma.* The temperature of Al substrate (upper curve) and the glass substrate (lower curve) in continuum mode exposed to oxygen plasma glow discharge.

Let us explain the results presented in Figure 10 to some details. We measured the temperature of both substrates with an inert fibre optic catalytic probe immersed into sample holders. The aluminium holder is heated to approximately 620 K in the first 40 s of continues plasma treatment. Here, the heating rate near the origin is about 8 K/s. The temperature is stabilised after a minute of plasma treatment, because heating equals cooling by the thermal conductivity of surrounding gas. On the other hand the glass substrate is heated very slowly, and its temperature remains below the detection limit of the probe for a long time, more than 420 s. The probe detection limit of 350 K can be reached only after approximately 1000 s of plasma treatment. The plasma heating of glass substrate is therefore at least 100 times slower than for aluminium. Whereas for silicon activated samples, the heating is much slower than for aluminium, but still faster than for glass carriers. This difference is due to the recombination probability for oxygen O atoms given by coefficients listed in the Table 2.

Table 1: *Recombination of O atoms on material.* Recombination coefficients (γ) for neutral oxygen atoms on different materials with corresponding references.

Material	γ	Reference
Glass bacteria carrier	$\sim 10^{-4}$	
Pyrex, quartz, soda	$5 \times 10^{-3} - 1 \times 10^{-5}$	(Wickramanayaka, 1991a; Hacker, 1961; Morgan, 1960)
Al oxide (Al_2O_3)	0.02	(Mozetič, 2003)
Ti oxide (TiO_2)	0.03	(Legrand, 1997)
Teflon	7.3×10^{-5}	(Wickramanayaka, 1991b)
Copper (Cu)	0.3	(Shibata, 1996)
Nickel (Ni)	0.27	(Šorli and Ročak, 2000)
Slicon oxide	$< 1 \times 10^{-3}$	(Berkut et al., 1985)

Increased sample temperature helps O-atom radicals to sterilize material more effectively. Furthermore, the oxidation of bacteria is an exothermic process, so it would add to substrate the heating during plasma exposure. The combination of sample heating as a consequence of the surface O-atom recombination and etching atom by atom are therefore the most important mechanism for the effective oxygen plasma sterilization.

Temperature accelerates sterilization and it helps O-atoms to etch bacteria atom by atom. On the other side, it limits the allowed treatment time in oxygen glow discharge plasma, because of extensive heating

that comes from energy release due to recombination of oxygen atoms on the substrate surface. The problem may become extremely important when sterilizing biocompatible materials that do not stand high temperatures. Also, it can become problematic when sterilizing components made from different materials with different recombination coefficients. Some polymers and metals have high recombination coefficients, so their heating time in plasma is very short. In many cases the pulsed plasma treatment is needed in order to avoid overheating of substrates before sterilization is completed.

4.3 Analysis of oxygen plasma inactivation of bacteria by plate counting technique

The effects of low-pressure highly dissociated oxygen plasma were analyzed for all three types of bacteria tested: *Escherichia coli*, *Bacillus stearothermophilus*, and *Staphylococcus aureus*.

Samples were treated in low pressure oxygen plasma for different times, and viable counts of surviving cells were estimated via standard plate counting technique. Samples that had not been exposed to plasma were used as controls and kept at room temperature (marked as untreated samples). The survivors were counted as colony-forming units (CFUs) per carrier after incubation for 24-48 h, at 55°C for *Bacillus stearothermophilus*, and 37°C for *Staphylococcus aureus* and *Escherichia coli*.

4.3.1 Oxygen plasma inactivation of *Escherichia coli*

The samples of *Escherichia coli* (16×10^7 cells on glass carrier) were subjected to the low pressure highly dissociated oxygen plasma for various time periods of 0, 5, 10, 15, 20, 30, 50, 80, 120, and 240 s. The initial concentration was 16×10^8 cells per ml, but in 100 μ l bacterial suspensions deposited on carriers were only 16×10^7 cells. For details see section 3.2.1. The sterilization conditions were as follows: discharge power 180 W, pressure 75 Pa, the neutral oxygen atom density $3.5 \times 10^{21} \text{ m}^{-3}$, and the density of charged particles $1 \times 10^{16} \text{ m}^{-3}$. Samples were always mounted into the centre of the discharge region as indicated in Figure 6a. After the treatment results were obtained by the PCT method. The result of oxygen plasma treatment on the survival of the *Escherichia coli* bacteria as a function of plasma treatment time is presented in Figure 11.

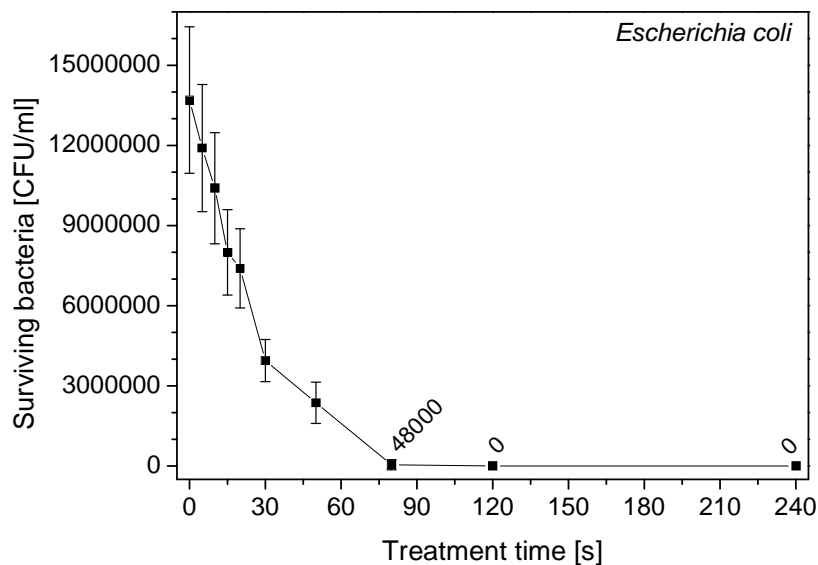


Figure 11: *Survival curve of Escherichia coli by PCT.* The graph represents CFUs of *Escherichia coli* vs. treatment time by oxygen plasma glow discharge at pressure of 75 Pa. The concentration of bacteria cells on glass substrate was 16×10^7 .

As can be seen from Figure 11, the number of CFUs decreases with an increasing treatment time. During the first 30 seconds it exhibits a very rapid drop in concentration of live bacteria. Complete sterilization of substrate was accomplished within approximately 120 s.

4.3.1.1 Influence of *Escherichia coli* concentration on plasma inactivation

Identical experiments to the previous one were performed with the 8×10^7 *Escherichia coli* cells on carrier (twofold less concentration). The results with mean values of surviving bacteria for both concentrations are presented in Figure 12 (the mean values without error bars were used for easier comparison of inactivation). The inactivation dynamics is very similar for both curves. The bacterium killing time is somehow shortened with decreasing of the original concentration of cells, and in this case sterilization was accomplished within 90 s.

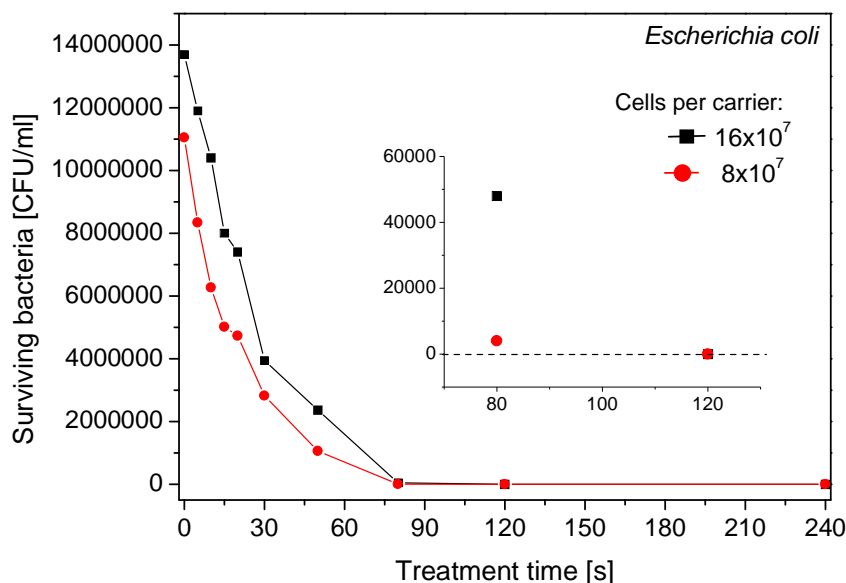


Figure 12: Survival curves of *Escherichia coli* by PCT. The graph represents CFUs of *Escherichia coli* vs. treatment time by oxygen plasma glow discharge at pressure of 75 Pa. The concentrations of bacteria cells on glass substrate were 16×10^7 and 8×10^7 .

4.3.2 Oxygen plasma inactivation of *Bacillus stearothermophilus*

The samples of *Bacillus stearothermophilus* were subjected to the low pressure highly dissociated oxygen plasma for various time periods, similar to previous experiment with *Escherichia coli*. The initial concentration of bacteria in suspension was 1.8×10^8 cells per ml, but in 100 μ l bacterial suspensions deposited on carriers were only 1.8×10^7 cells. For details see section 3.2.1. The plasma conditions were the same as in section 4.3.1.

The results of inactivation of *Bacillus stearothermophilus* in glass substrates containing 1.8×10^7 is shown in Figure 13. Within 240 s of plasma exposure 97.5 % cells of *Bacillus stearothermophilus* were killed, while longer treatment time was necessary to completely sterilize 1.8×10^7 cells. It is noticeable that longer plasma treatment time is required for sterilizing *Bacillus stearothermophilus* than killing *Escherichia coli*. Whereas, the survival curve of *Bacillus stearothermophilus* also differs from the previous one for *Escherichia coli*. This difference is attributed to the cell structure difference of *Bacillus stearothermophilus* from *Escherichia coli*.

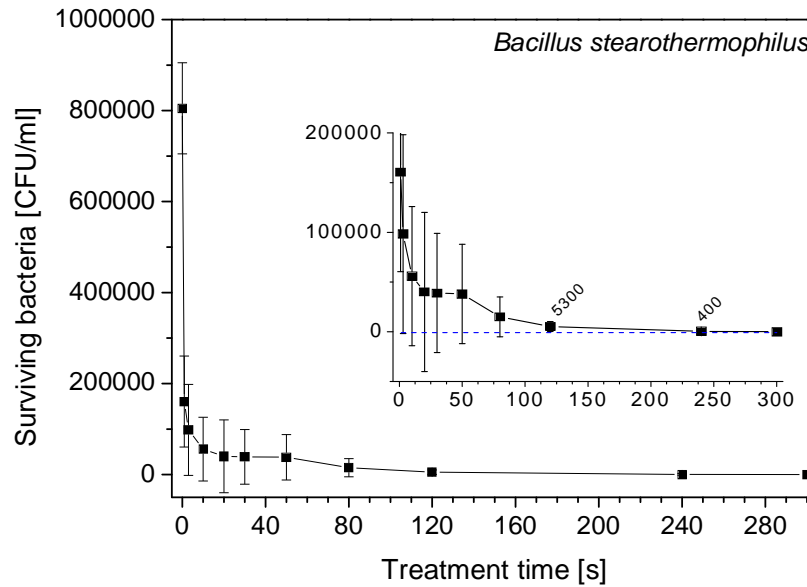


Figure 13: *Survival curve of Bacillus stearothermophilus by PCT.* The graph represents CFUs of *Bacillus stearothermophilus* vs. treatment time by oxygen plasma glow discharge at pressure of 75 Pa. The concentration of bacteria cells on glass substrate was 1.8×10^7 .

4.3.2.1 Influence of pressure on *Bacillus stearothermophilus* inactivation

In order to investigate the influence of plasma parameters on inactivation of *Bacillus stearothermophilus* bacteria, experiments were also performed at two other pressures (30 and 150 Pa). The pressure of 30 Pa is where the ion density is close to its maximal value, while 150 Pa is where O atom density is very high and the ion density extremely low at about $3 \times 10^{15} \text{ m}^{-3}$. The 1×10^7 cells of *Bacillus stearothermophilus* dispersed on glass carriers were treated in oxygen plasma for different treatment times and the results are presented in Figure 14.

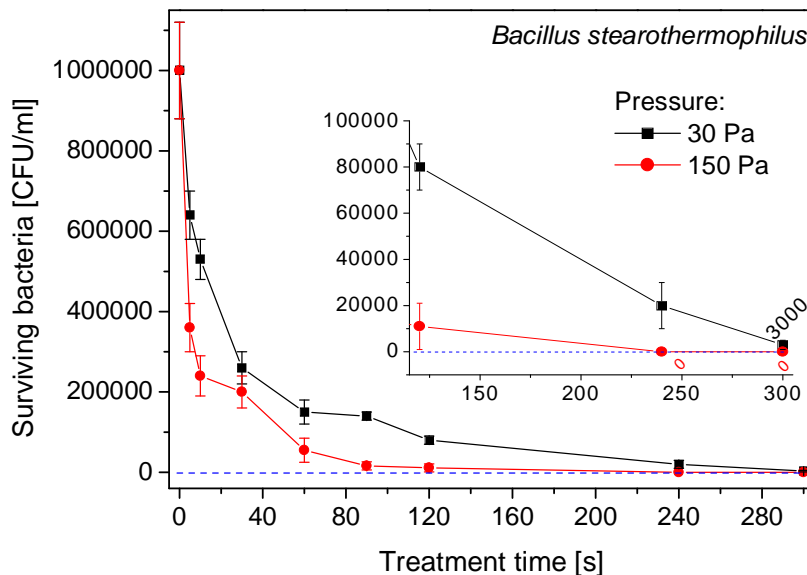


Figure 14: *Survival curves of Bacillus stearothermophilus by PCT.* The graph represents CFUs of *Bacillus stearothermophilus* vs. treatment time by oxygen plasma glow discharge at pressure of 30 Pa and pressure of 150 Pa. The concentration of bacteria cells on glass substrate was 1×10^7 .

In the use of 150 Pa, a much shorter plasma treatment time for inactivation of *Bacillus stearothermophilus* (< 240 s) is needed than for treatments at the pressure of 30 Pa. The survivor curves showed that treatment by oxygen plasma at higher pressure of 150 Pa was more efficient than at a lower pressure of 30 Pa. Therefore, the decreasing of bacteria killing time with the increase of the pressure can be observed.

4.3.2.2 Influence of afterglow treatment on *Bacillus stearothermophilus* inactivation

In order to determine the role of the neutral species (Figure 6b) on bacteria inactivation, we exposed *Bacillus stearothermophilus* (1×10^7) cells to the afterglow region for different periods of time. Compared to the discharge itself, the afterglow contains negligible amount of charged particles, but is rich with neutral oxygen atoms. The experiments were performed at the pressure of 75 Pa. In this experiment (Figure 15), only partial inactivation of *Bacillus stearothermophilus* was obtained. In contrast to an oxygen glow discharge (Figure 13), afterglow configuration produced less rapid inactivation than what is seen from the survival curve in Figure 15.

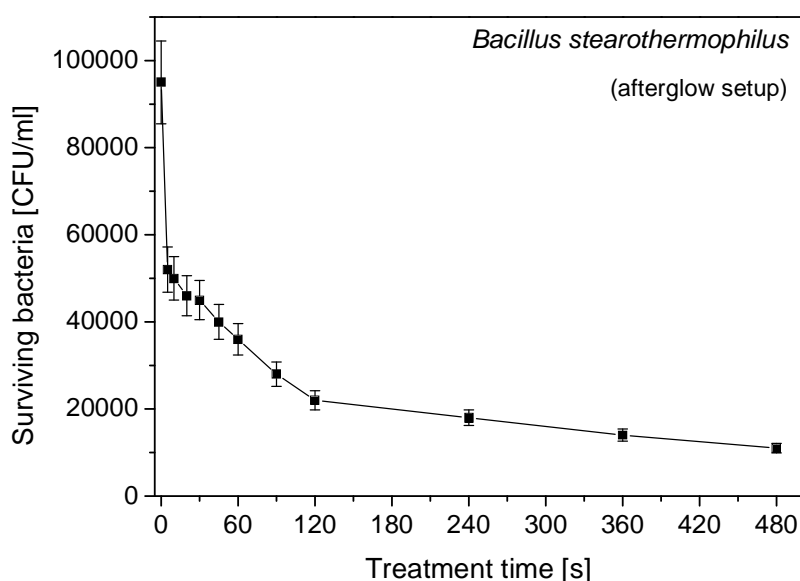


Figure 15: Survival curve of *Bacillus stearothermophilus* by PCT. The graph represents CFUs of *Bacillus stearothermophilus* vs. treatment time in oxygen plasma afterglow region of plasma reactor at pressure of 75 Pa. The concentration of bacteria cells on glass substrate was 1×10^7 .

4.3.3 Oxygen plasma inactivation of *Staphylococcus aureus*

Bacteria inactivation effects in low pressure oxygen plasma glow on *Staphylococcus aureus* cells were studied for various time periods. They were similar to previous experiments with *Escherichia coli* and *Bacillus stearothermophilus*. The plasma conditions were the same as in section 4.3.1. Sample carriers were treated at pressure of 75 Pa as well as for 30 Pa and 150 Pa. The concentration of bacterial cells per carrier was 1/10 of initial suspension, since 100 μ l was deposited on carriers. For details see section 3.2.1 or 4.3.1.

In the first experiment carried out at 75 Pa, the sample carriers with 1.7×10^8 cells of *Staphylococcus aureus* were exposed to glow discharge. This experiment results can be seen in Figure 16. The survival curve shows the very straight drop in viability of bacteria up to 5 s of plasma treatment. More than 90 % reductions of 1.7×10^8 *Staphylococcus aureus* cells population were observed after 20 s plasma exposure. The final sterilization of sample carriers is achieved after 90 s with an absence of any colony forming unit growth.

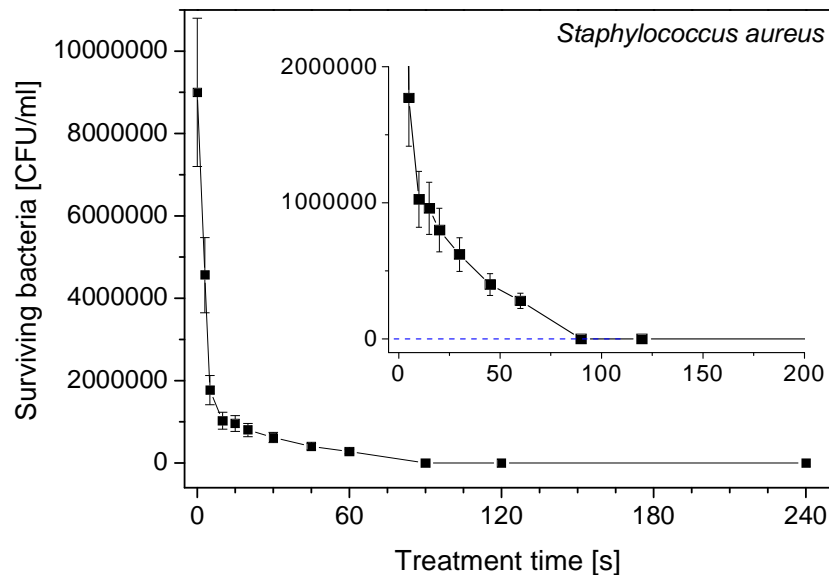


Figure 16: *Survival curve of Staphylococcus aureus by PCT.* The graph represents CFUs of *Staphylococcus aureus* vs. treatment time by oxygen plasma glow discharge at pressure of 75 Pa. The concentration of bacteria cells on glass substrate was 1.7×10^8 .

4.3.3.1 Influence of *Staphylococcus aureus* concentration on plasma inactivation

To determine the potential influence of bacteria concentration on the plasma inactivation process, two different volumes of 1.7×10^9 initial bacterial cell suspension was used to obtain different cell densities on the glass carrier surface. In the first series of measurements, a 100 μl suspension containing 1.7×10^8 cells were spread on the carrier; in the second series, 150 μl suspension containing 2.55×10^8 cells were used.

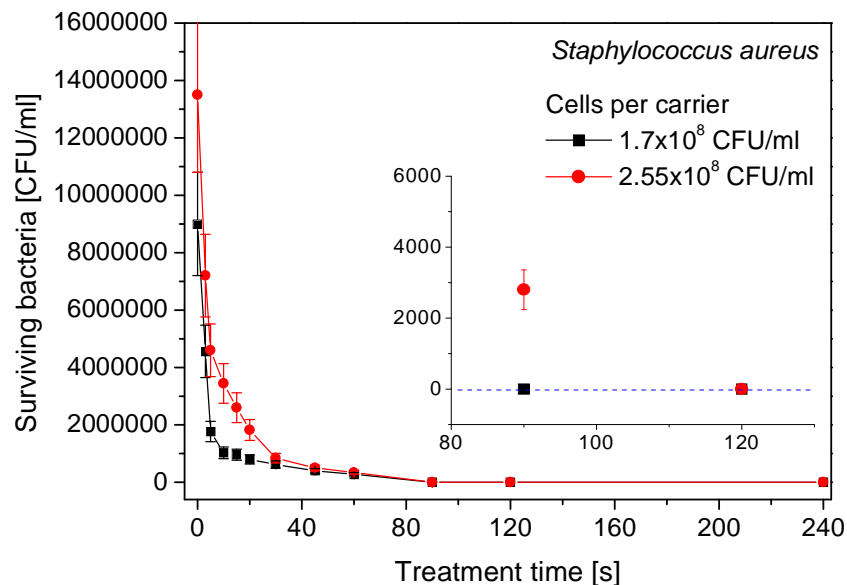


Figure 17: *Survival curves of Staphylococcus aureus by PCT.* The graph represents CFUs of *Staphylococcus aureus* vs. treatment time by oxygen plasma glow discharge at pressure of 75 Pa obtained with two different concentrations. The concentrations of bacteria cells on glass substrate were 1.7×10^8 and 2.55×10^8 .

The two surviving curves of bacteria don't show the same inclination degree (Figure 17). As expected, the higher concentrations require longer treatment times, similar as previously observed in inactivation of *Escherichia coli*. The complete inactivation of 1.7×10^8 *Staphylococcus aureus* cells was obtained within 90 s, while at least 120 s was needed to inactivate 2.55×10^8 cells. Therefore, shorter oxygen plasma treatment times are required at sterilization of a lower concentration of bacteria on the glass carriers.

4.3.3.2 Influence of pressure on *Staphylococcus aureus* inactivation

In order to compare the effect of plasma parameters on inactivation efficiency, we treated glass carriers with 7×10^8 cells of *Staphylococcus aureus* at two pressures: 30 Pa and 150 Pa at different exposure times. More on the plasma parameters under these two pressures can be found in section 4.3.2.1.

The result of inactivation of *Staphylococcus aureus* for two different pressures is presented in Figure 18. Both survival curves show two different trends in inactivation process. At higher pressure settings, bactericidal effects were much smaller than at lower pressure settings. Therefore, lower densities of neutrals and higher densities of charged particles, seems to accelerate the inactivation process of *Staphylococcus aureus*. This result is opposite phenomena from the inactivation of *Bacillus stearothermophilus*, and shows that different densities of plasma species can increase or decrease sterilization efficiency.

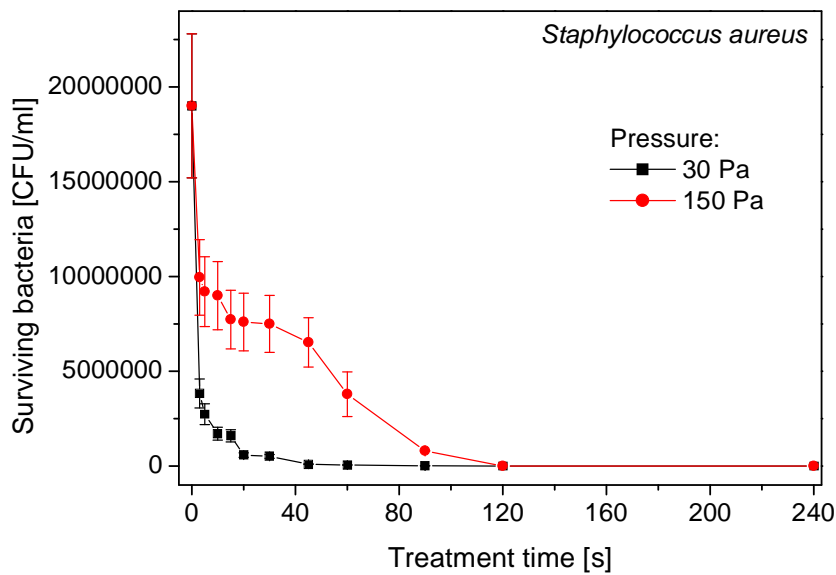


Figure 18: Survival curves of *Staphylococcus aureus* by PCT. The graph represents CFUs of *Staphylococcus aureus* vs. treatment time by oxygen plasma glow discharge at pressure of 30 Pa and pressure of 150 Pa. The concentration of bacteria cells on glass substrate was 7×10^8 .

4.3.3.3 Influence of afterglow treatment on *Staphylococcus aureus* inactivation

We also used afterglow for inactivation of 7×10^8 cells of *Staphylococcus aureus*. Again, experiments were performed at 75 Pa. Surprisingly enough, no strong effect on bacterial viability was observed up to 360 s (Figure 19). Since afterglow contains only neutral oxygen atoms, the interactions of them are not enough to perform efficient inactivation of bacterial cells. However, the oxygen plasma treatment still decreased the number of viable cells for one order of magnitude. This is also in agreement with the result seen in Figure 15.

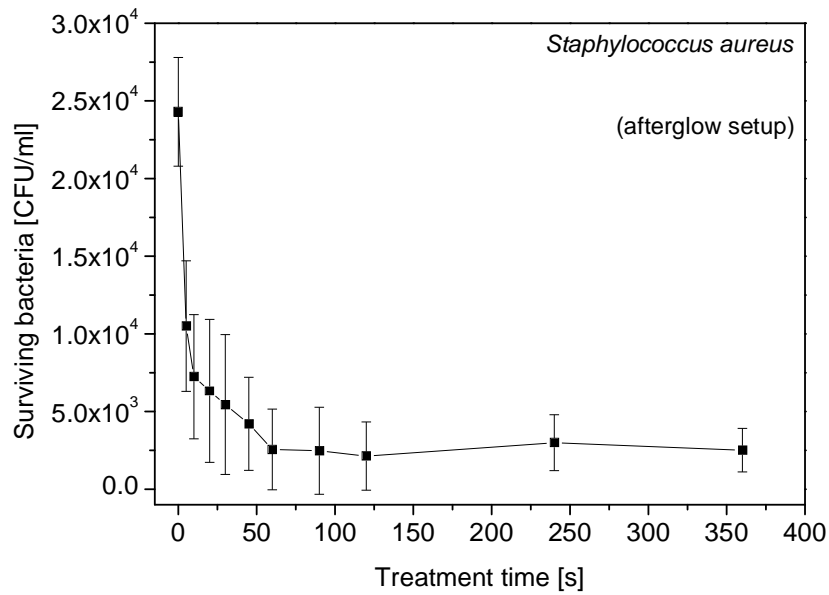


Figure 19: *Survival curve of Staphylococcus aureus by PCT in plasma afterglow.* The graph represents CFUs of *Staphylococcus aureus* vs. treatment time in oxygen plasma afterglow region of plasma reactor at pressure of 75 Pa. The concentration of bacteria cells on glass substrate was 7×10^8 .

4.4 Morphological changes caused by low-temperature oxygen plasma

In order to investigate the effects of oxygen plasma on the cell structure and its morphological changes during the inactivation process, we used Scanning Electron Microscopy (SEM). With SEM we obtained the micrographs of cells, including untreated and treated bacteria. Representative SEM micrographs of the untreated bacteria, bacteria treated with oxygen plasma, heat treated, and vacuum treated bacteria are shown.

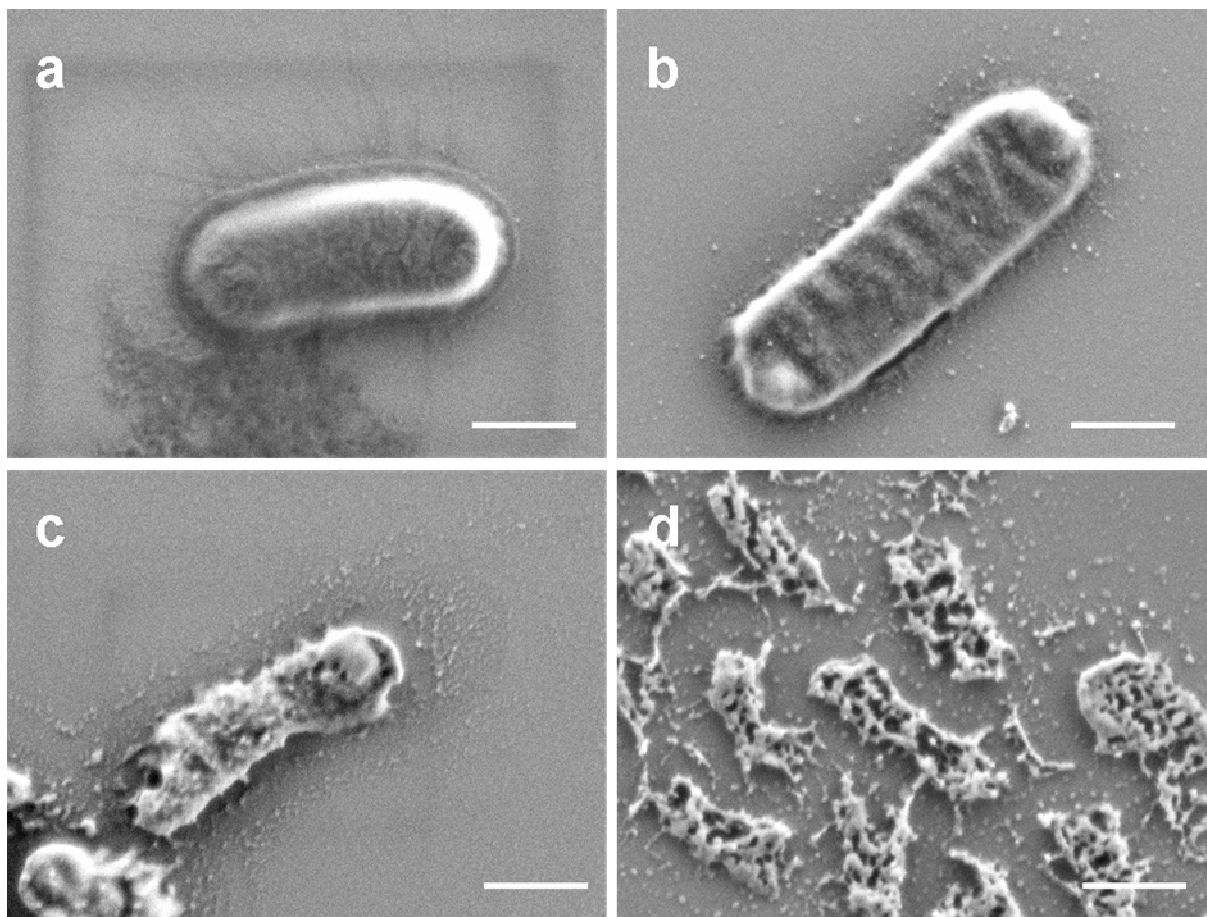


Figure 20: SEM micrographs of bacteria *Escherichia coli*. SEM images of *Escherichia coli* on Si substrate: (a) untreated; (b) treated with low-pressure highly dissociated oxygen plasma for 10 seconds; (c) 55 seconds; and (d) 240 seconds. Scale bar is 400 nm.

Gram-negative bacteria *Escherichia coli* were treated under the same experimental conditions as described before in the experimental section. Highly dissociated oxygen plasma at 75 Pa was used for different time treatments. Representative SEM micrographs of oxygen plasma treated *Escherichia coli* at 10 s, 55 s and 240 s are presented in Figures 20b, 20c, 20d, respectively. From the Figure 20b it can be seen that the short exposure to oxygen plasma for 10 s leads to disruption of bacterial envelope, predominantly of the cell wall. The smaller debris of envelope can be seen around bacteria. Prolonged treatment at 55 s leads to even stronger plasma etching effects on envelope, by destruction of cell wall and cytoplasmic membrane. At the same time cytoplasm is released and etched from the surface by oxygen atoms and ions. This probably causes certain death of bacteria, which can be seen from debris and cell deformation. After cytoplasm is released, the etching still continues by removal of bacterial residuals from surface until the surface is virtually free of any bacterial material. Representative micrograph of this process is shown in Figure 20d, taken after 240 s of plasma treatment.

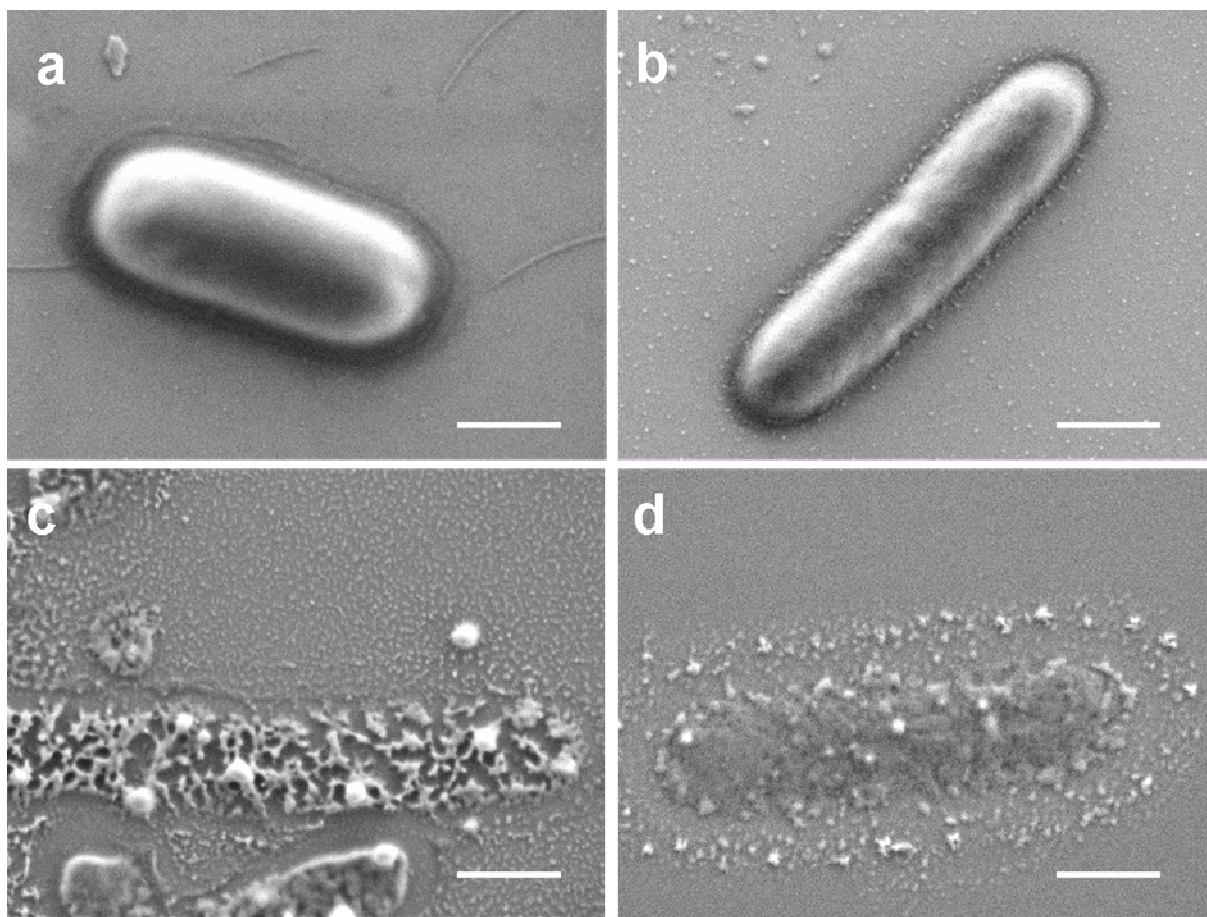


Figure 21: SEM micrographs of bacteria *Bacillus stearothermophilus*. SEM images of *Bacillus stearothermophilus* on Si substrate: (a) untreated; (b) treated with low-pressure highly dissociated oxygen plasma for 10 seconds; (c) 55 seconds; and (d) 240 seconds. Scale bar is 400 nm.

The untreated gram-positive bacteria *Bacillus stearothermophilus* and *Staphylococcus aureus* (Figures 21a and 22a) exhibit regular rod-shaped and coccoid form, respectively. Treatment with oxygen plasma at the same plasma parameters for shorter periods results in a slight reduction of cell size for *Bacillus stearothermophilus*, and modified surface morphology of *Staphylococcus aureus* (Figure 21b and Figure 22b) compared to the untreated controls of bacteria *Bacillus stearothermophilus* (Figure 21a) and *Staphylococcus aureus* (Figure 22a). The process is similar to the one seen for *Escherichia coli*. At first the cell wall of *Bacillus stearothermophilus* is to some extent damaged (Figure 21b). Then longer plasma exposure leads to even more cell structure damage; their cell membrane and cytoplasm were strongly eroded and ruptured (Figure 21c). Therefore, we can say that bacterial cells in plasma lose their cell integrity, because a cell wall and the bacterial cytoplasm became barely recognizable. Longer oxygen plasma treatments just continue to remove destroyed bacteria and the bacterial material from the surface (Figure 21d).

The process for *Staphylococcus aureus* on Si substrates is similar as the one presented for bacteria *Bacillus stearothermophilus* in Figure 21. Whereas for *Staphylococcus aureus* on Al substrates is even more intensive, additional heating of aluminium increases the destruction rate due in extra substrate heating. Representative images of this process are seen in Figure 22.

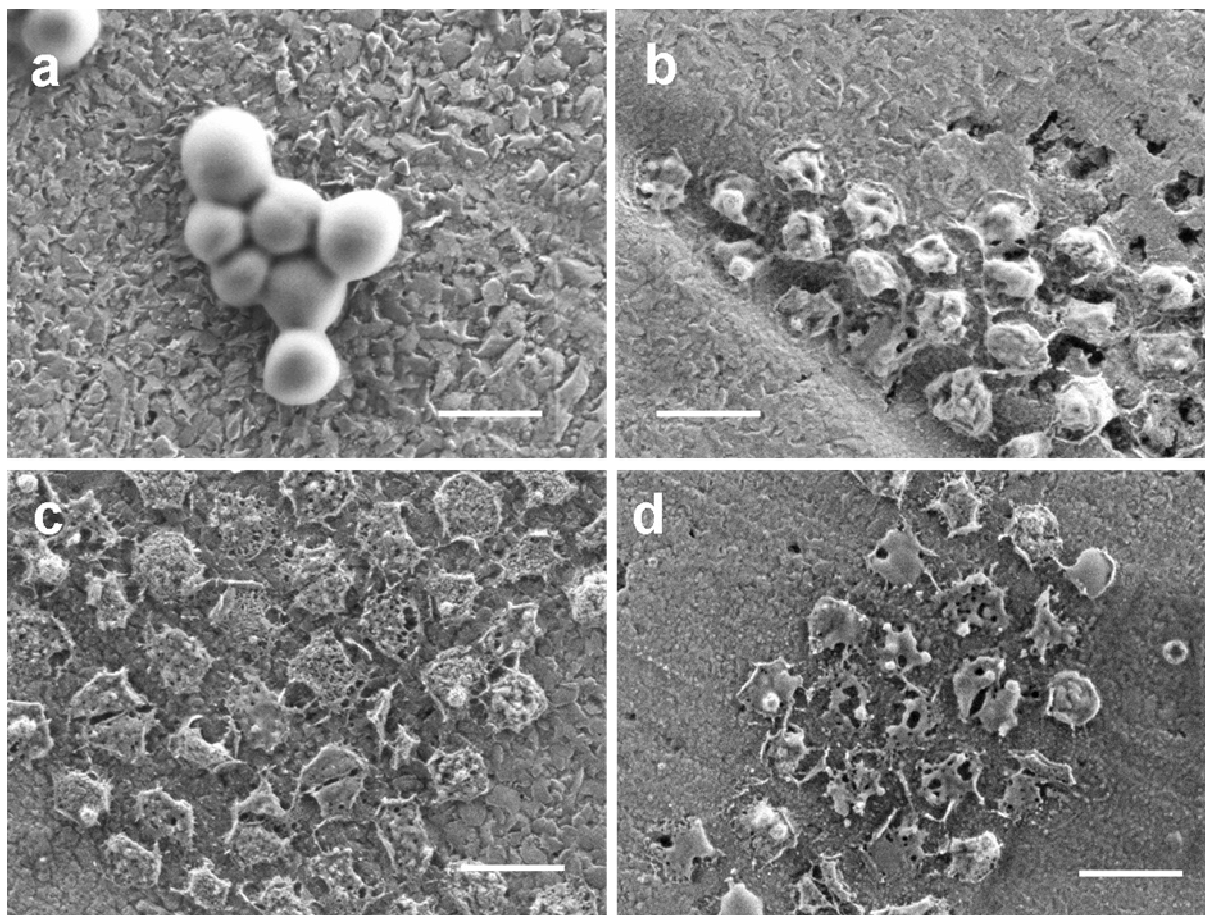


Figure 22: SEM micrographs of bacteria *Staphylococcus aureus*. SEM images of *Staphylococcus aureus* on Al substrate: (a) untreated; (b) treated with low-pressure highly dissociated oxygen plasma for 20 seconds; (c) 60 seconds; and (d) 240 seconds. Scale bar is 400 nm.

In order to compare temperature effects to oxygen plasma effects on the bacteria morphology, SEM micrographs were obtained after high temperature dry heat treatment of the samples *Bacillus stearothermophilus* and *Staphylococcus aureus* at 140 °C for 20 s and 10 min. Representative micrographs that show *Bacillus stearothermophilus* and *Staphylococcus aureus* are seen in Figure 23. As seen from images, the bacteria *Bacillus stearothermophilus* (Figure 23a) still retained its typical rod shaped form after 20 s exposure to dry heat, and *Staphylococcus aureus* (Figure 23b) still retained its actual coccoid form. Both represented bacteria after 20 s of heat treatment (Figures 23a and 23b) appeared quite similar to the untreated cells in the control experiments (Figures 21a and 22a). Nevertheless, some change in bacterial envelope morphology was observed after a prolonged treatment time for 10 min at 140 °C indicating a certain effect of high temperature on bacterial cells after a prolonged time. Minor changes in morphology of bacterial cell wall are seen (Figure 23c and 23d). Therefore, dry heat doesn't practically cause any morphological changes in the bacterial cell structure.

Another control experiment was performed with *Bacillus stearothermophilus*, *Staphylococcus aureus* and *Escherichia coli*. It was done in such a way that bacteria were exposed to the vacuum, but without plasma (Figure 24). This was done in order to control the change of cell morphology and the possible eruption of envelopes by vacuum, which can affect the bacteria prior plasma experiments when plasma reactor is pumped down and oxygen is leaked in at 75 Pa. The Figures 24a, 24b and 24c revealed that the size and the shape of bacteria did not depend on this pre-treatment under vacuum conditions. Furthermore, SEM did not confirm any notable changes on the surface of bacteria which would be caused directly by vacuum, used in a reactor prior or during plasma experiment.

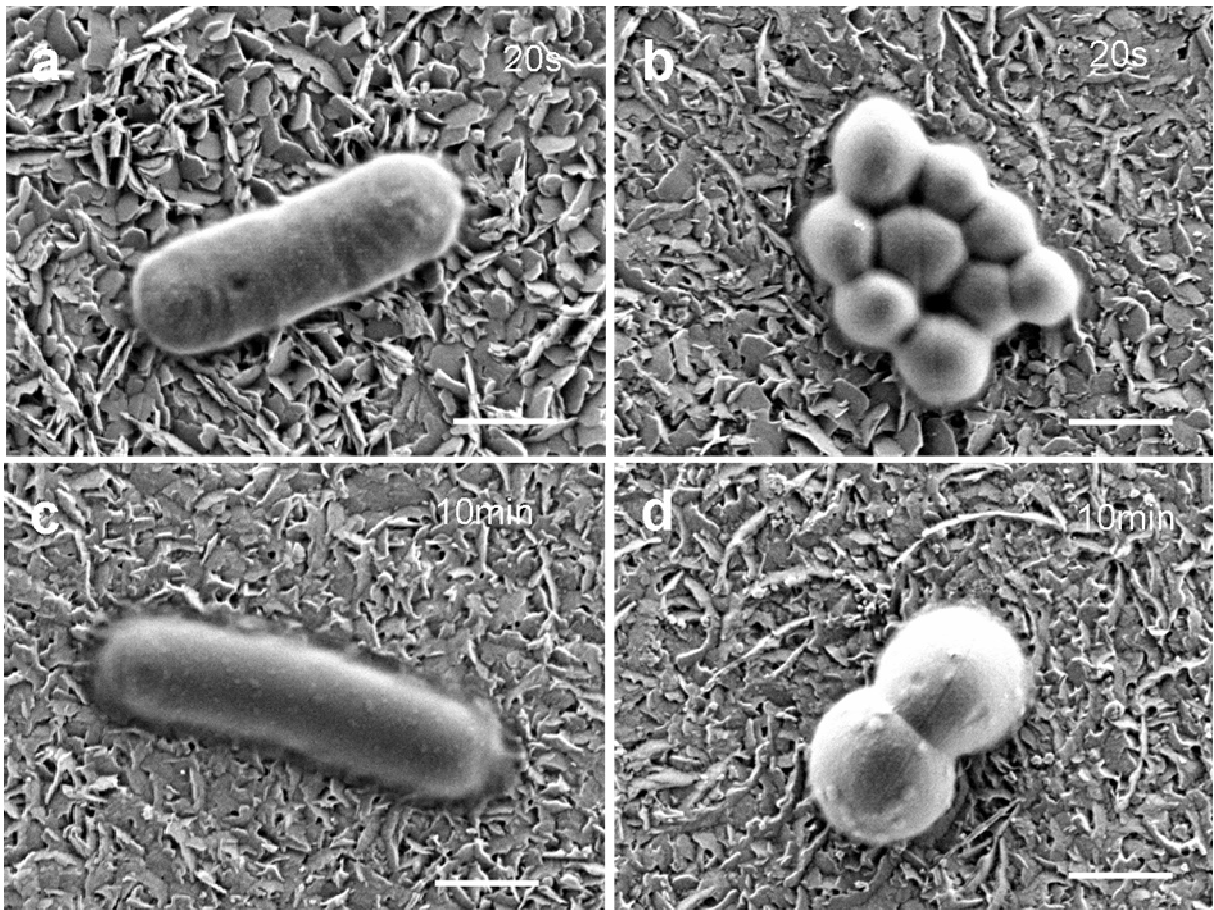


Figure 23: *SEM micrographs of heat-treated bacteria.* SEM micrographs of heat-treated bacteria at 140 °C on Al substrate: (a) of *Bacillus stearothermophilus* for 20 seconds; (b) *Staphylococcus aureus* for 20 seconds; (c) *Bacillus stearothermophilus* for 10 minutes; *Staphylococcus aureus* for 10 minutes. Scale bar is 400 nm.

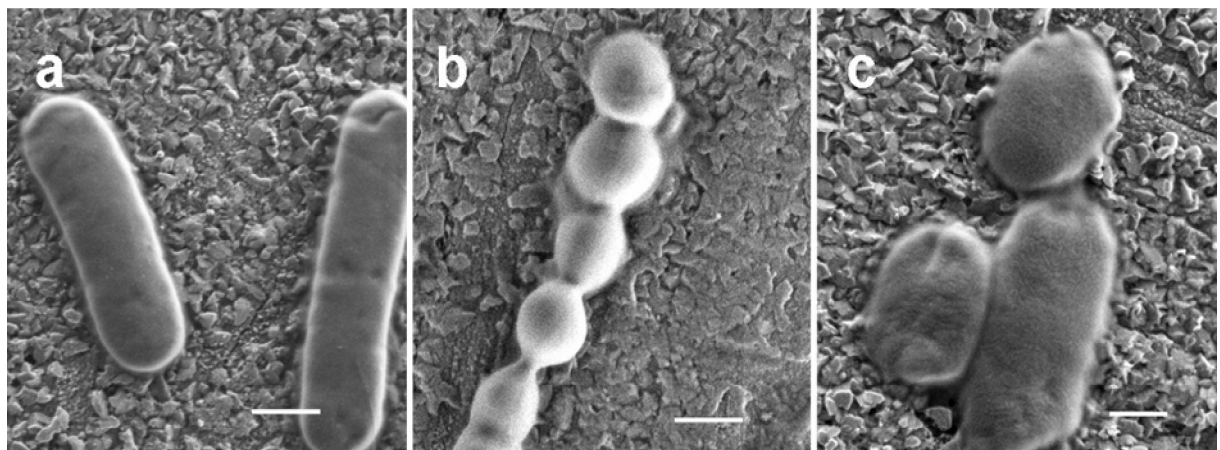


Figure 24: *SEM micrographs of vacuum-treated bacteria.* SEM micrographs of vacuum treated (a) *Bacillus stearothermophilus*; (b) *Staphylococcus aureus* and (c) *Escherichia coli*. Scale bar is 400 nm.

These results demonstrate that a strong etching process of bacteria in oxygen plasma is caused predominantly by plasma species (e.g. neutrals or charged species) and not vacuum or dry heat. Generally, the bacteria have been heavily damaged, and then reduced to microscopic debris. Eventually the envelope is ruptured and their cellular cytoplasmatic content is released on the substrate surface and etched away. This demonstrates that oxygen plasma has direct physical impact on the bacterial cells.

4.5 Fluorescence viability analysis of bacterial cells using SYTO 9 - PI dual staining

Viability of bacteria was assessed with the DEAD/LIVE *BacLight*TM Viability Kit L7012 (Molecular Probes, The Netherlands). It consists of two dyes, SYTO 9 can enter bacteria with intact cell membranes and emits green fluorescence, whereas propidium iodide (PI) penetrates only into bacterial cells with damaged membranes and exhibits red fluorescence. When bacterial cells are stained with a mixture of the two dyes, viable cells fluorescence bright green, while dead cells exhibit weaker green fluorescence and also fluoresce red. This differential staining was particularly obvious when cells were observed under the fluorescent microscope. Typically for this experiment, we used 10^4 - 10^5 bacterial cells per glass carrier in order to get separated cells and observe damages inflicted by plasma. The images of *Escherichia coli* (Figure 25), *Bacillus stearothermophilus* (Figure 26), and *Staphylococcus aureus* (Figure 27) binding of DNA dyes SYTO 9 and PI are shown for the untreated bacteria (a, d), the bacteria treated with high-temperature dry heat at 140 °C for 10 min (b, e) and the bacteria treated with low pressure highly dissociated oxygen plasma at 75 Pa for 20 s (c, f). Binding of DNA dyes to bacteria treated with high-temperature dry heat for 20 s at 140 °C is not shown, because no morphological changes of bacterial cell wall were observed with SEM after 20 s.

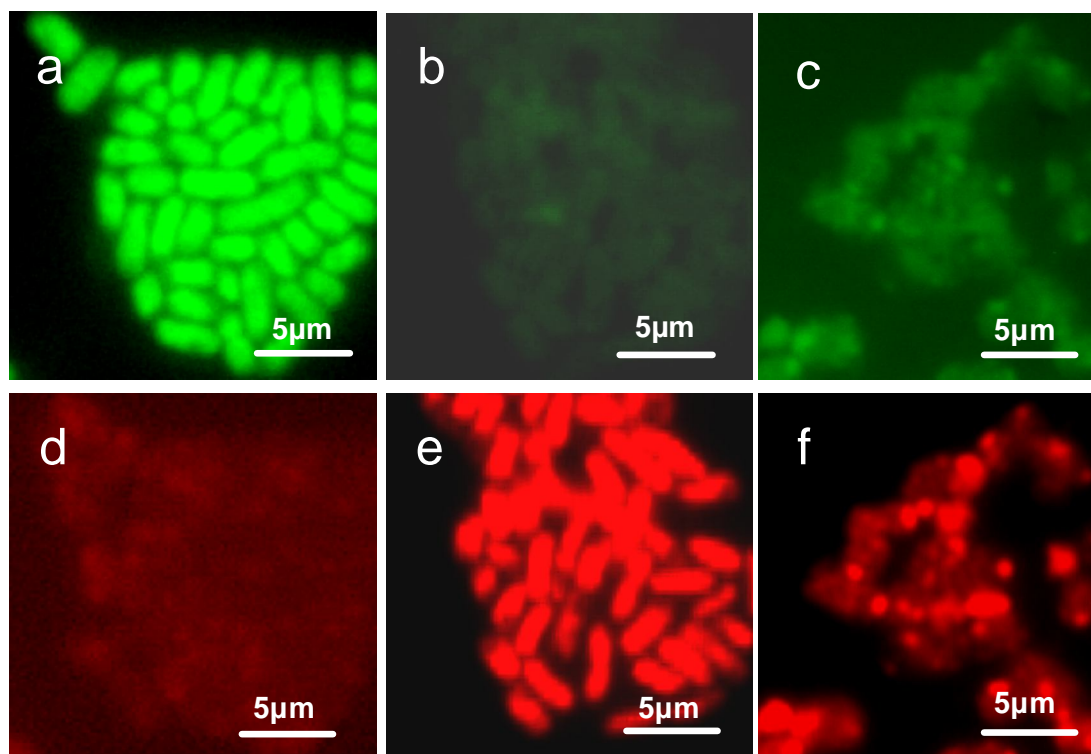


Figure 25: Fluorescence microscopy images of bacteria *Escherichia coli*. The bacteria *Escherichia coli* were labelled with DNA dyes SYTO 9 (green fluorescence in a, b and c) propidium iodide (red fluorescence in d, e and f). The images (a, d) show untreated bacteria, (b, e) bacteria treated with high-temperature dry heat for 10 minutes at 140 °C and (c, f) bacteria treated with oxygen plasma for 20 seconds. Untreated bacteria show strong SYTO 9 (a) staining (fluorescence), but weak propidium iodide (PI) staining (d). In high-temperature treated bacteria PI staining (red fluorescence) increased (e) compared to SYTO 9 (b). Plasma treated bacteria show poor or no SYTO 9 (c) or PI (f) fluorescence signal.

In our experiments, the untreated bacteria *Escherichia coli* showed strong SYTO 9 staining (green fluorescence, Figure 25a), but very weak or no PI staining (red fluorescence, Figure 25d). In high-temperature treated bacteria, the number of PI-stained cells stained increased compared to SYTO 9 only-stained cells (Figure 25b and 25e). Plasma-treated bacteria show neither clear SYTO 9 (Figure 25c) nor PI (Figure 25f) fluorescence signal. SYTO 9 and propidium iodide bind to the nucleic acids, then the absence of fluorescence could be explained by denaturation and/or fragmentation bacterial DNA.

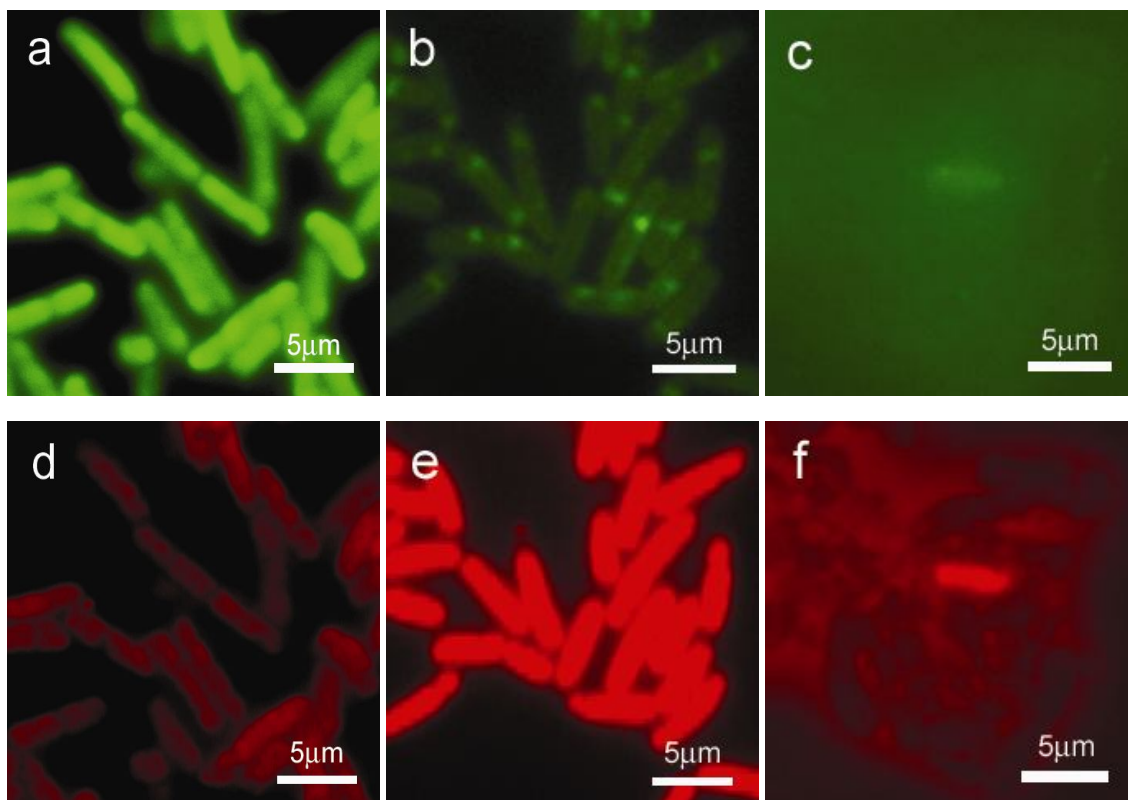


Figure 26: Fluorescence microscopy images of bacteria *Bacillus stearothermophilus*. The bacteria *Bacillus stearothermophilus* were labelled with DNA dyes: SYTO 9 (green fluorescence in a, b and c) and propidium iodide (red fluorescence in d, e and f). The images (a, d) show untreated bacteria, (b, e) bacteria treated with high-temperature dry heat for 10 minutes at 140 °C and (c, f) bacteria treated with oxygen plasma for 20 seconds. Untreated bacteria show strong SYTO 9 (a) staining (fluorescence) but weak propidium iodide (PI) staining (d). In high-temperature treated bacteria PI staining (red fluorescence) increased (e) compared to SYTO 9 (b). Plasma treated bacteria show poor or no SYTO 9 (c) or PI (f) fluorescence signal.

Fluorescence labelling of bacteria *Bacillus stearothermophilus* shown in Figure 26 exhibited the same profile as *Escherichia coli*, the untreated bacteria showed strong green labelling of living cells (Figure 26a), but very weak PI staining (Figure 26d, red fluorescence). Conversely, in high-temperature-treated bacteria the number of PI positive dead cells markedly increased (Figure 26e, red-fluorescence) and they were SYTO 9 negative (Figure 26b, green fluorescence). In high-temperature treated bacteria not a single green fluorescent cell could be detected but all cells were labelled red. As expected, plasma treated *Bacillus stearothermophilus* make poor or almost no more visible bacterial structures either in green (Figure 26c) or red fluorescence (Figure 26f) (the same as in previous case for *Escherichia coli*).

Binding of DNA SYTO 9 and PI in bacteria *Staphylococcus aureus* exhibited quite a similar way of staining (Figure 27). The untreated bacteria showed strong SYTO 9 staining (Figure 27a, green fluorescence). In contrast to the untreated bacteria *Bacillus stearothermophilus*, there were some PI-stained bacteria *Staphylococcus aureus* cells already in the untreated sample (Figure 27d). In high-temperature treated bacteria, PI-stained bacteria dominated (Figure 27e, red fluorescence) and only a few cells remained SYTO 9 positive (Figure 27b, green fluorescence) and PI negative (Figure 27e). Plasma treated bacteria *Staphylococcus aureus* showed neither clear SYTO 9 (Figure 27c) nor PI (Figure 27f) fluorescence, the same as *Bacillus stearothermophilus* or *Escherichia coli*.

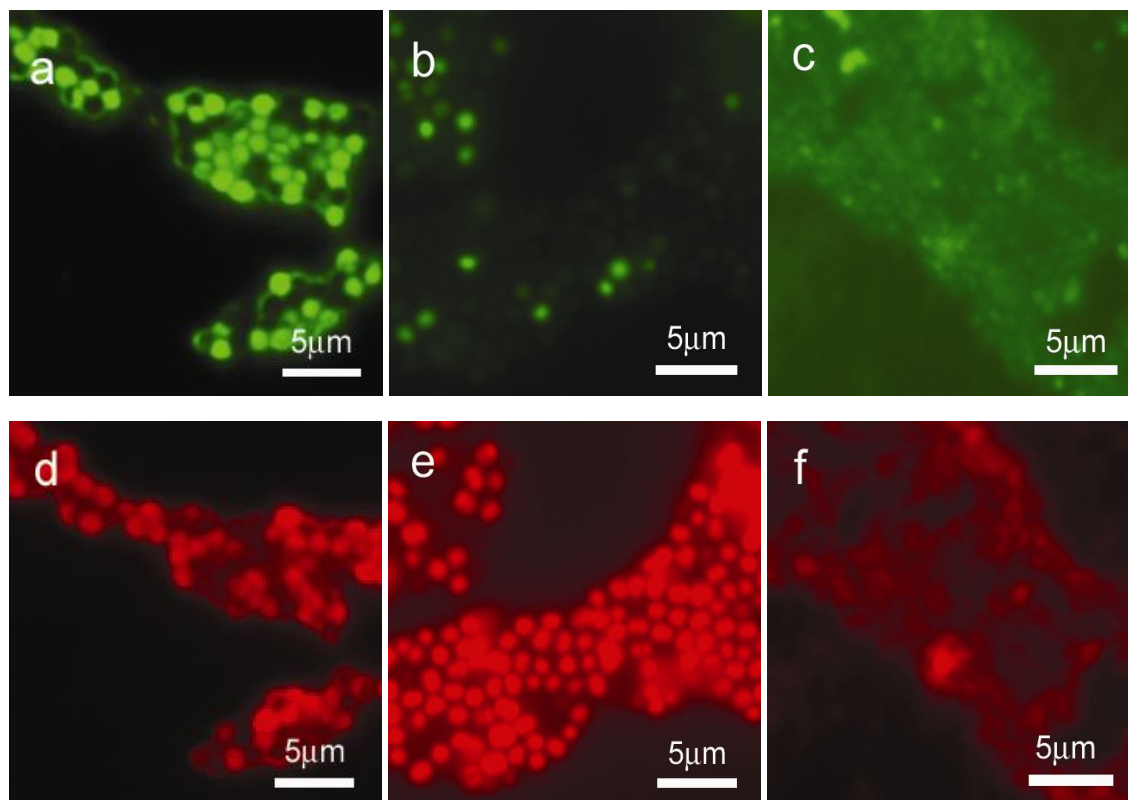


Figure 27: Fluorescence microscopy images of bacteria *Staphylococcus aureus*. The bacteria *Staphylococcus aureus* were labelled with DNA dyes SYTO 9 (green fluorescence in a, b and c) propidium iodide (red fluorescence in d, e and f). The images (a, d) show untreated bacteria, (b, e) bacteria treated with high-temperature dry heat for 10 minutes at 140 °C and (c, f) bacteria treated with oxygen plasma for 20 seconds. Untreated bacteria show strong SYTO 9 (a) staining (green fluorescence). In untreated bacteria, a certain percentage of SYTO 9 negative cells also show propidium iodide (PI) staining (d). In high-temperatures treated bacteria PI (e) staining (red fluorescence) increased compared to SYTO 9 (b). Plasma treated bacteria show poor or no SYTO 9 (c) or PI (f) fluorescence signal.

In the case of plasma-treated bacteria, the fluorescent microscopy showed that the original DNA is either heavily modified or fully oxidized, so there is practically no DNA left to assure stain binding where cell wall was destroyed. The emitted fluorescence is poor: stain is evenly distributed on the carrier showing no preference to the sites where bacteria reside. This confirms also to the nature of low temperature plasma sterilization, where neutral atoms interact chemically with bacteria material, as was suggested before in section 1.6.

4.6 Flow cytometric viability analysis

In addition to the microscopy, stained bacteria with SYTO 9 and PI were also analyzed by flow cytometry to quantitatively distinguish live and dead bacteria. This was done in order to compare and confirm results from the plate counting technique.

Initially we determined the viability of dry heated bacteria. Bacteria were either untreated, treated with dry heat at 140 °C for 20 s for 2 minutes or 10 minutes. Typically samples with about 2 or 4×10^8 bacterial cells per carrier were used. After the heat treatment, the bacteria were gently washed from the glass carriers in order to obtain a suitable suspension. The analysis gate was set in the untreated sample in a histogram of green (FL1, SYTO 9) and red (FL3, PI) fluorescence versus side scatter. Results for *Bacillus stearothermophilus* and *Staphylococcus aureus* are displayed in Figure 28.

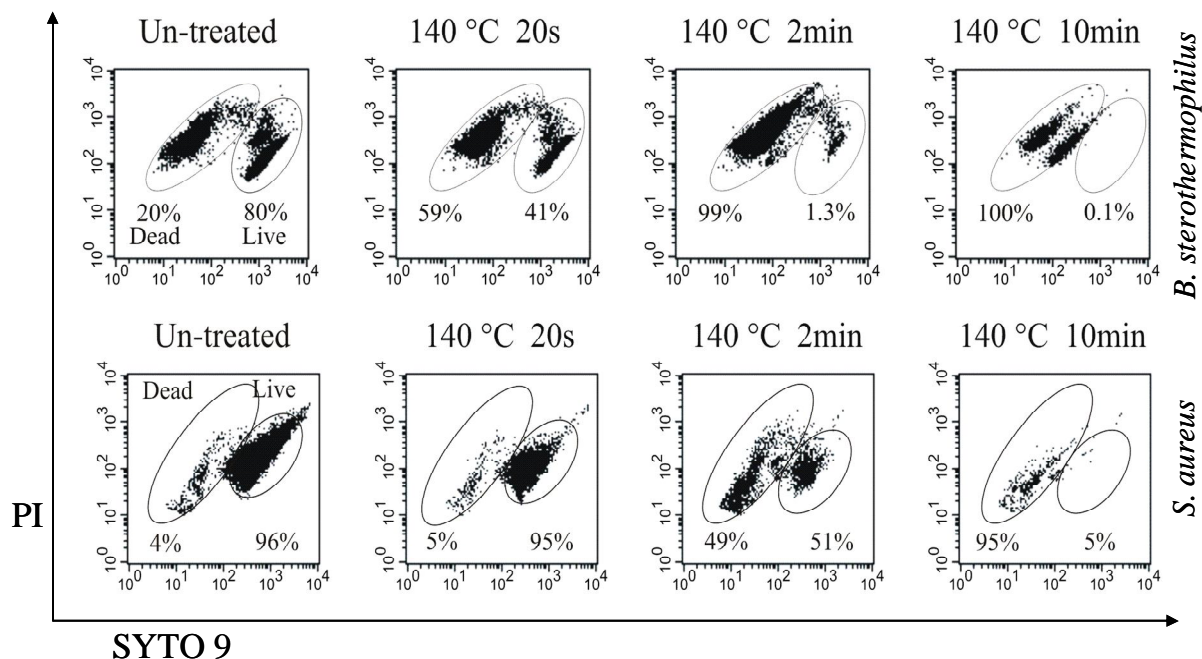


Figure 28: Flow cytometric plot analysis of *Bacillus stearothermophilus* and *Staphylococcus aureus* after dry heat treatment. *Bacillus stearothermophilus* and *Staphylococcus aureus* were analysed by flow cytometry after staining with LIVE/DEAD BacLight™ Bacterial Viability Kit (L7012) untreated samples, and samples treated with dry heat at 140 °C for 20 s, 2 min and 10 min.

Live and dead bacteria appeared as two populations of different intensity fluorescences. In *Bacillus stearothermophilus* (vegetative form), the untreated sample has 80% of viable cells from 2×10^8 cells in total (Figure 28). The viability was halved after 20 s exposures to 140°C, while after 2 minutes exposure at 140°C a large majority of cells died. After 10 minutes exposure to 140°C, the number of cells in the analysis gate was just additionally reduced to 0.1%.

For *Staphylococcus aureus*, the results were very similar. Although in the case of *Staphylococcus aureus* the process of inactivation is slower due to cell grouping and a larger number of cells on the carriers. The number of *Staphylococcus aureus* cells was doubled compared to *Bacillus stearothermophilus*. The viability of the untreated sample was above 95%. 20 s exposures to 140°C did not significantly affect the viability, whereas after 2 min the viability was almost halved, and after an exposure of 10 min exposure almost all of the cells left were dead.

After the inactivation experiment with dry heat, we also performed an oxygen plasma treatment of all three kinds of bacteria. At the same time we tested the initial suspension for live bacteria by flow cytometry, and then the dead cell control (bacteria killed with 70% isopropyl alcohol in accordance with recommendations of kit producer), as well as the untreated samples of bacteria, where bacteria were dried on carriers before plasma treated. Later, all plasma treated samples were analysed by flow cytometry in order to quantify live and dead bacteria. Three representative results of oxygen plasma treatment in glow discharge are shown in two-parameter histograms below.

The flow cytometric analysis of oxygen plasma treated (with the plasma parameters for 75 Pa pressure) *Escherichia coli* samples are shown in Figure 29. The first control of initial suspension shows that some bacteria are already dead, but most of them are still vital. Whereas, when we treated the initial suspension with isopropyl alcohol, no viable bacterium is detected. Although we can also see that many *Escherichia coli* bacteria died during sample preparation, which is seen from untreated sample. When bacteria are exposed to plasma for shorter periods, e.g. 10 s, very little happens in terms of viability, but the peak intensity of dead bacteria in two-parameter histogram becomes smaller. This means that some of bacteria cells and its envelopes were destroyed or removed. More pronounced inactivation occurs after longer treatments of 50 s. At that exposure, very little live bacteria are detected. After even longer treatments for 120 s, almost no vital bacteria are seen, and very little total bacterial cells are detected. This is probably due to the etching and degradation of bacterial cells with plasma.

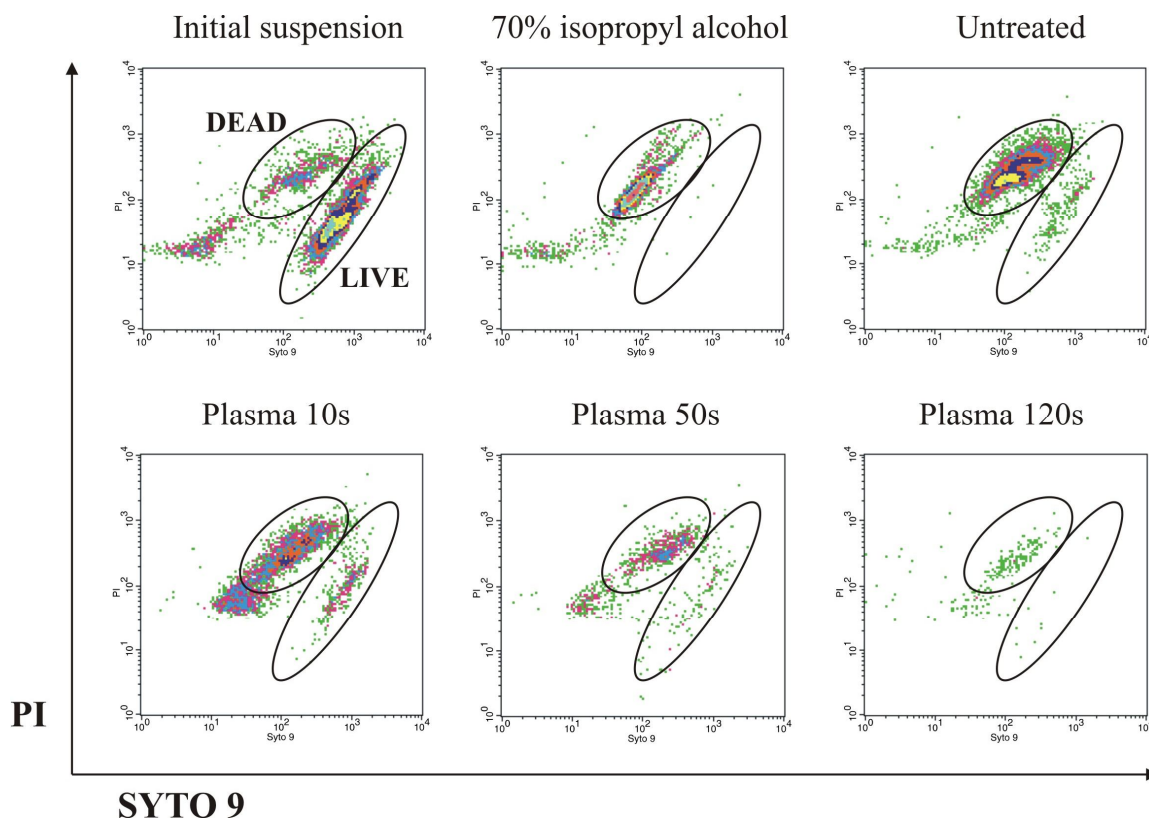


Figure 29: Flow cytometric plot analysis of *Escherichia coli* after plasma treatment. *Escherichia coli* was analysed by flow cytometry after staining with LIVE/DEAD BacLight™ Bacterial Viability Kit (L7012) initial bacterial suspension, dead cell control by 70% isopropyl alcohol, untreated samples, and oxygen plasma treated samples for 10 s, 50 s and 120 s.

The inactivation process of bacteria *Bacillus stearothermophilus* as seen from two-parameter histograms in Figure 30 is similar to the one for *Escherichia coli*. Initial bacterial suspension contains both live and dead bacteria. The dead cell control is in accordance with kit protocol. The shorter 10 s plasma treatment already kills a lot of bacteria compared to untreated samples. And more, a high number of cells are destroyed and can be viewed as debris under the gate for dead cells. Prolonged plasma treatment times increase the number of dead cells and the number of debris, as well as removed cells from the sample surface. After 240 s the surface is virtually free of any viable bacteria cell, and very little dead cells are detected.

For *Staphylococcus aureus* bacteria in Figure 31, the process is also similar to both previous results. In this case we have more vital bacteria in initial concentration as well as on untreated samples. The shorter treatment times of about 10 s already destroy a large number of cells, which are consequently removed from surface with a prolonged plasma treatment time. As a result, very little or no bacteria cells are left on the surface after 240 s.

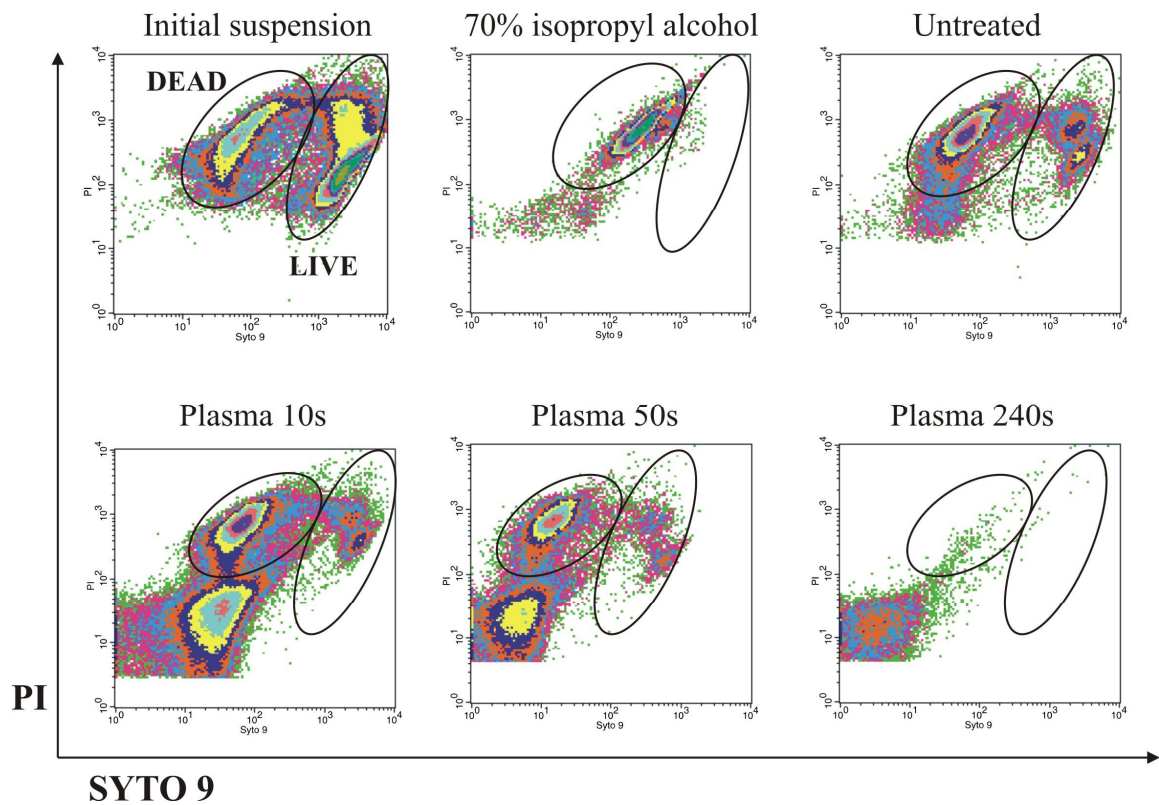


Figure 30: *Flow cytometric plot analysis of Bacillus stearothermophilus after plasma treatment. Bacillus stearothermophilus* was analysed by flow cytometry after staining with LIVE/DEAD BacLight™ Bacterial Viability Kit (L7012) initial bacterial suspension, dead cell control by 70% isopropyl alcohol, untreated samples, and oxygen plasma treated samples for 10 s, 50 s and 240 s.

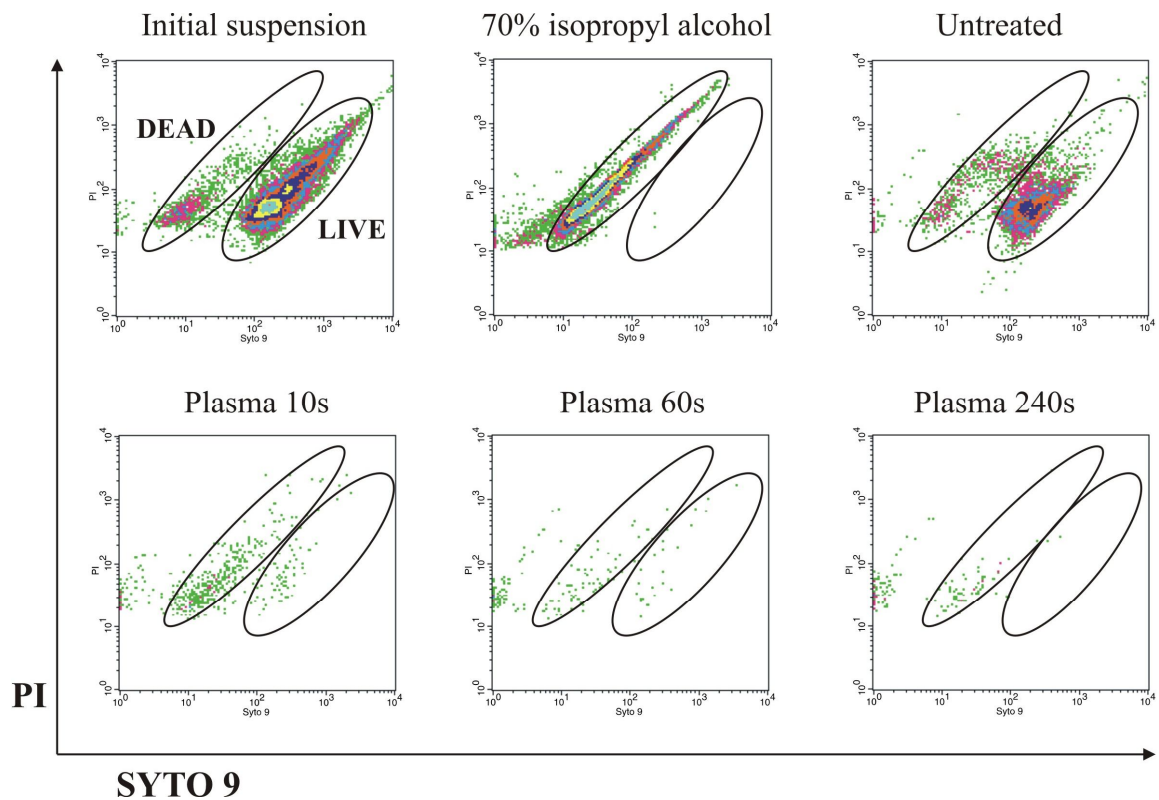


Figure 31: *Flow cytometric plot analysis of Staphylococcus aureus after plasma treatment. Staphylococcus aureus* was analysed by flow cytometry after staining with LIVE/DEAD BacLight™ Bacterial Viability Kit (L7012) initial bacterial suspension, dead cell control by 70% isopropyl alcohol, untreated samples, and oxygen plasma treated samples for 10 s, 60 s and 240 s.

The difference in the effectiveness of heat and plasma treatments was pronounced. In plasma treated samples, the percentage of live bacteria decreased faster than in heat-treated samples. Furthermore, the number of cells in the analysis gate has been significantly reduced already after 60 s, and there had hardly been any cells left after 2 min with plasma treatment. The results of this analysis suggest that low pressure oxygen plasma inactivation and final sterilization is not only capable of killing bacteria, but is also capable of removing the dead bacteria cells from the surface of the objects being sterilized (as seen also from previous results Figures 29, 30 and 31). This method proved to be very efficient monitoring method as well as quantifying method for detection of dead and live bacteria after the plasma treatment.

4.7 Quantitative viability analysis by flow cytometry

To quantify the results of surviving bacteria as well as the number of dead cells after oxygen plasma treatment we used the LIVE/DEAD[®] BacLight[™] Bacterial Viability and Counting Kit L34856 (Molecular Probes, The Netherlands) which allows the reliable distinguishing and quantifications of live and dead bacteria. The kit utilizes a mixture of two nucleic acid stains (green fluorescent SYTO 9 dye and red fluorescent propidium iodide) for viability determinations (provides an indication of the total number of cells, further separated into living and dead cells), and calibrated suspension of microspheres for accurate sample volume measurement. The calibrated suspension of microspheres serves as a reference standard for a sample volume. For absolute counts, a specific volume of the microsphere suspension is added to a specific volume of sample, so that the ratio of sample volume to microsphere is known. The volume of sample analyzed can be calculated from the number of microsphere events, and can be used with cell events to determine cell concentration. The samples of bacteria were prepared, stained and analyzed following the procedures described in detail earlier (see section 3.2.5.1).

4.7.1 Analysis of *Escherichia coli* after plasma treatment

To see how oxygen plasma interacts with bacteria *Escherichia coli*, we used two different concentrations of bacteria deposited on the carrier, and the plasma parameters for pressure of 75 Pa. The results of live and dead bacteria after plasma treatment as well as after control experiments were quantified using kit L34856. These results of quantitative viability analysis are presented in Figures 32, 33, and Figure 34, which show the dynamics of time dependence of bacteria inactivation.

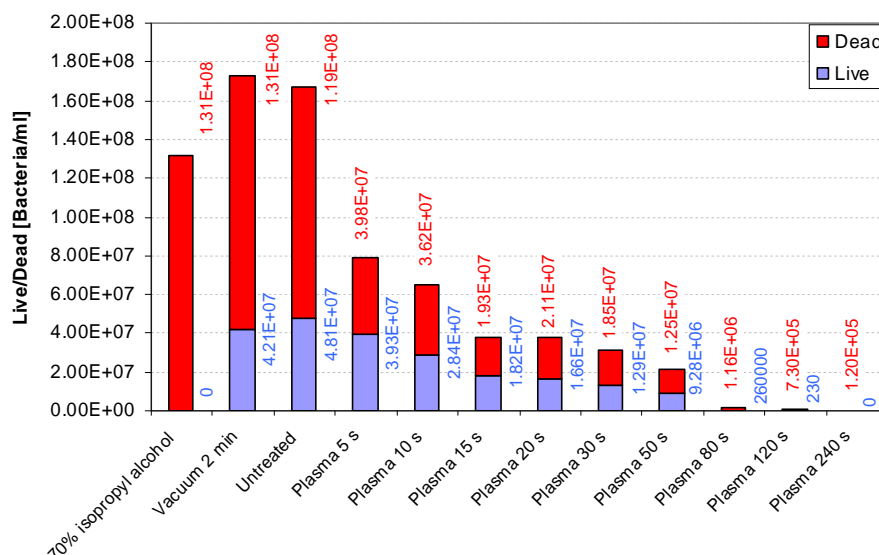


Figure 32: Quantitative viability analysis of *Escherichia coli* after plasma treatment. The number of live/dead *Escherichia coli* cells measured for various oxygen plasma treatment times at 75 Pa as well as in vacuum and 70 % isopropyl alcohol by flow cytometer. The concentration of bacteria cells per carrier was 16×10^7 .

As can be seen from the Figure 32, it was found that there were already a large number of dead *Escherichia coli* bacteria on untreated samples. This occurred during the sample preparation process. However, there were no notable changes in the number of live bacteria exposed to the vacuum in comparison to untreated bacteria which would be caused directly by influence of vacuum. The dead cell control was in accordance with the test. Furthermore, the number of living cells measured by flow cytometry decreased rapidly with increased plasma treatment time. As expected, this reduction of viable counts was matched by parallel increase in the number of dead cells. However, a decrease in the amount of dead cells was observed with increased plasma treatment time. So, the amount of live and dead *Escherichia coli* cells was decreasing along with the prolonged exposure to plasma. Similar results were obtained for the halved concentration of cells per carrier, which is presented in Figure 33.

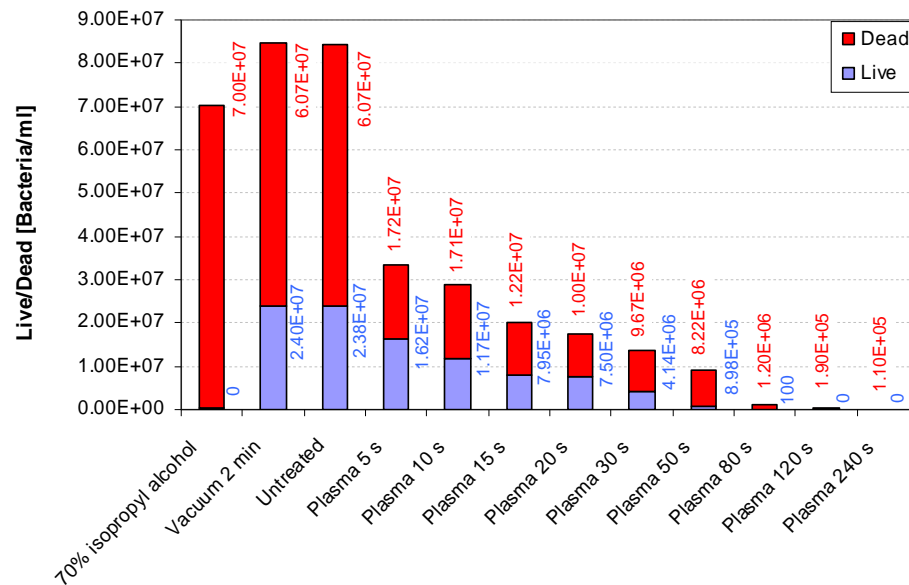


Figure 33: *Quantitative viability analysis of Escherichia coli after plasma treatment.* The number of live/dead *Escherichia coli* cells (with two-fold less initial concentration) measured for various oxygen plasma treatment times at 75 Pa, as well as in a vacuum and 70 % isopropyl alcohol by flow cytometers. The initial number of bacteria cells per carrier was 8×10^7 .

In the case of two-fold fewer concentrations of *Escherichia coli* cells per carrier, the experimental results demonstrated that for lower concentrations the bacteria killing time shortens. After a 80 s plasma treatment, the total number of cells (live and dead) declined significantly and almost all *Escherichia coli* cells were killed. After already 120 s, there were no live *Escherichia coli* cells left. In addition, the total number of all cells is significantly reduced. For longer treatment times, almost no cells are detected.

Typically three flow cytometry measurements for a single plasma exposure time were performed. These results are presented in a flow cytometry count graph, where both concentrations (8×10^7 and 16×10^7) are shown in the time scale (Figure 34). The survival curves as well as dead cell counts are both shown. The samples with 8×10^7 cells per carrier are characteristically inactivated at 80 s, whereas samples 16×10^7 are inactivated at 120 s of oxygen plasma exposure. The total number of (live and dead) bacteria declined significantly, which indicates plasma degradation process and the final removal of bacteria from the carrier surface.

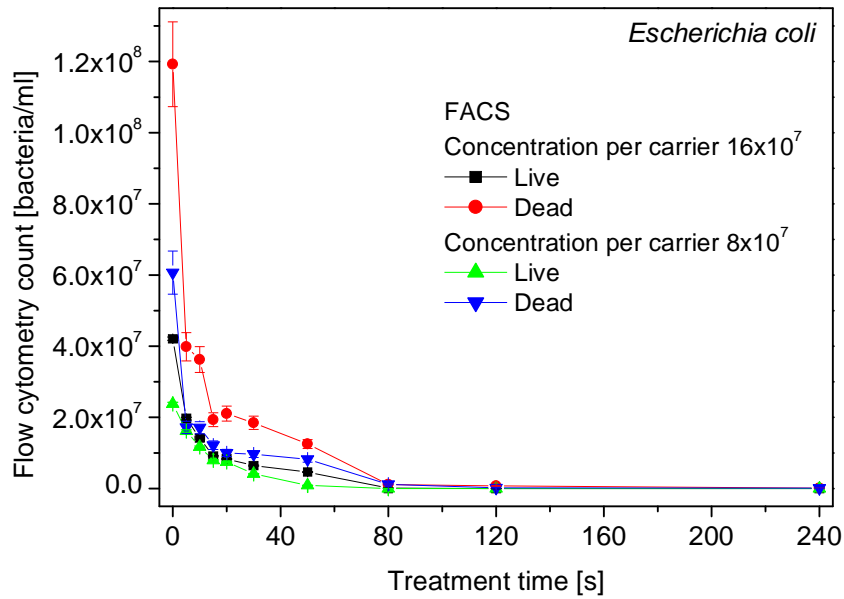


Figure 34: *Quantitative viability analysis of Escherichia coli for 2 concentrations after plasma treatment.* The number of live/dead *Escherichia coli* cells with two different concentrations on sample glass carriers is plotted versus oxygen plasma treatment times at 75 Pa. The initial numbers of bacteria cells per carrier were 8×10^7 and 16×10^7 .

4.7.2 Analysis of *Bacillus stearothermophilus* after plasma treatment

Similar experiment to the one with *Escherichia coli* was performed for two different concentrations of *Bacillus stearothermophilus*, where carriers with 5×10^8 and 1.8×10^8 cells have been exposed to oxygen plasma at 75 Pa (Figures 35, 36 and 37). And more *Bacillus s tearothermophilus* samples were exposed also to two additional pressures of 30 Pa and 150 Pa (Figure 38) as well as to afterglow (Figure 39) in order to study the influence of plasma species on inactivation process. We also used overnight dried samples to obtain vegetative forms with spores.

Two representative graphs with columns of a single FACS measurement for two concentrations of cells per carrier dried overnight are displayed in Figures 35 and 36. In Figure 35 the inactivation of carriers with 5×10^8 cells is shown, whereas in Figure 36 for 1.8×10^8 cells.

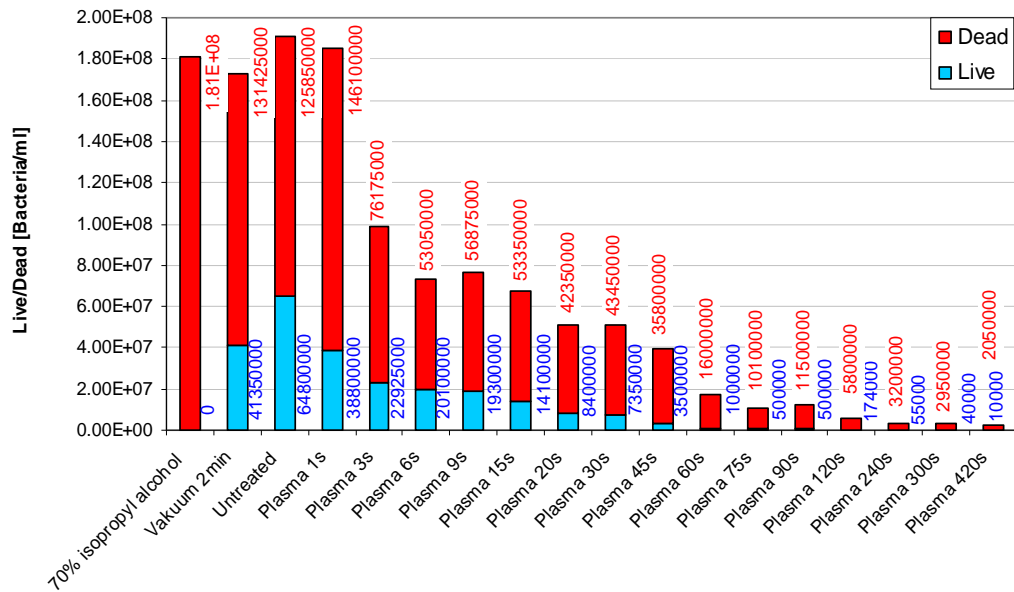


Figure 35: Quantitative viability analysis of *Bacillus stearothermophilus* after plasma treatment. The number of live/dead *Bacillus stearothermophilus* cells (vegetative form with spores) measured for various oxygen plasma treatment times at 75 Pa as well as in vacuum and 70 % isopropyl alcohol by flow cytometer. The concentration of bacteria cells per carrier was 5×10^8 .

Experimental results for *Bacillus stearothermophilus* in both graphs (Figure 35 and 36) were found similar to the one of *Escherichia coli*. The amount of live and dead *Bacillus stearothermophilus* cells was decreasing along with the prolonged exposure to plasma. Comparable data were obtained with the plate count technique (standard plate count), presented before. Characteristic of the *Bacillus stearothermophilus* inactivation process is a rather large number of debris that persists on the surface after the plasma treatment (as can be seen from Figure 30). Specific are some parts of bacteria cells that are rather large (Figure 21c) or spores persisting on the surface. This was seen in two parameter flow cytometry histograms (Figure 30) in addition to SEM analysis (Figure 21). Therefore, even if some cells are detected after 420 s plasma treatments then this can be an artefact of FACS analysis or spores, since we used bacteria in vegetative and in form with spores.

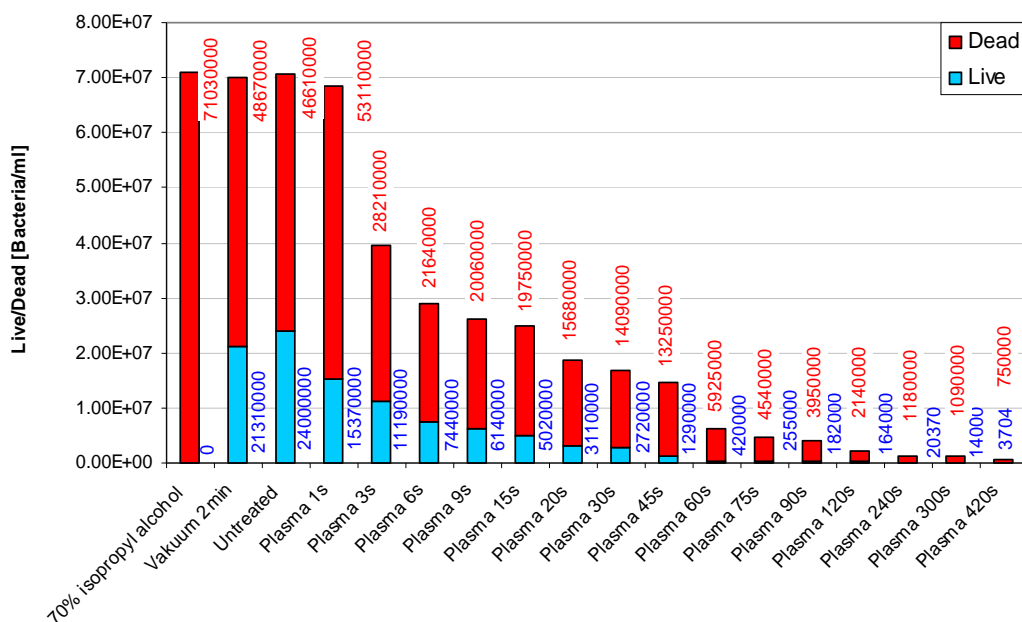


Figure 36: Quantitative viability analysis of *Bacillus stearothermophilus* after plasma treatment. The number of live/dead *Bacillus stearothermophilus* cells (vegetative form with spores) measured for various oxygen plasma treatment times at 75 Pa as well as in vacuum and 70 % isopropyl alcohol by flow cytometer. The concentration of bacteria cells per carrier was 1.8×10^8 .

When only vegetative forms are used (Figure 37), the inactivation trend is similar to the previous two results in Figures 35 and 36. However, the inactivation is much faster than in previous two cases. Reason for this is probably the absence of rather resistant spores.

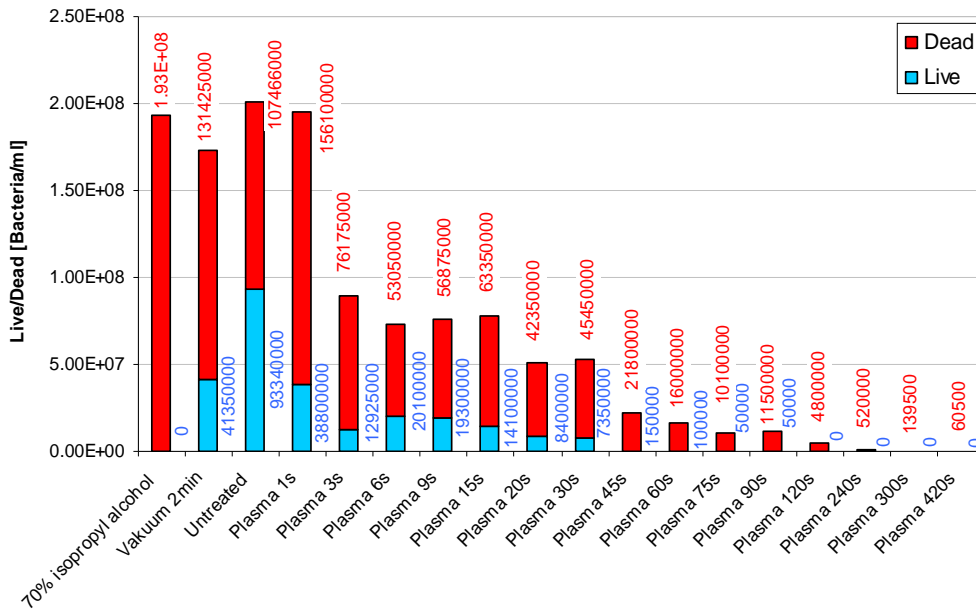


Figure 37: Quantitative viability analysis of *Bacillus stearothermophilus* after plasma treatment. The number of live/dead *Bacillus stearothermophilus* cells (vegetative forms only) measured for various oxygen plasma treatment times at 75 Pa as well as in vacuum and 70 % isopropyl alcohol by flow cytometers. The concentration of bacteria cells per carrier was 5×10^8 .

For three FACS measurements at the same exposure time, and for two concentrations of bacteria cells per carrier, the survival curves of *Bacillus stearothermophilus* with spores are presented in Figure 38. The figure shows that the inactivation and removal of bacterial cells from the surface is faster for lower concentrations of bacterial cells per carrier. This was observed also before, for other bacteria. The number of 1.8×10^8 bacterial cells is reduced for two orders of magnitude in 45 s, whereas the one with 5×10^8 cells in approximately 60 s. There was no final inactivation of bacteria covered surface within 420 s.

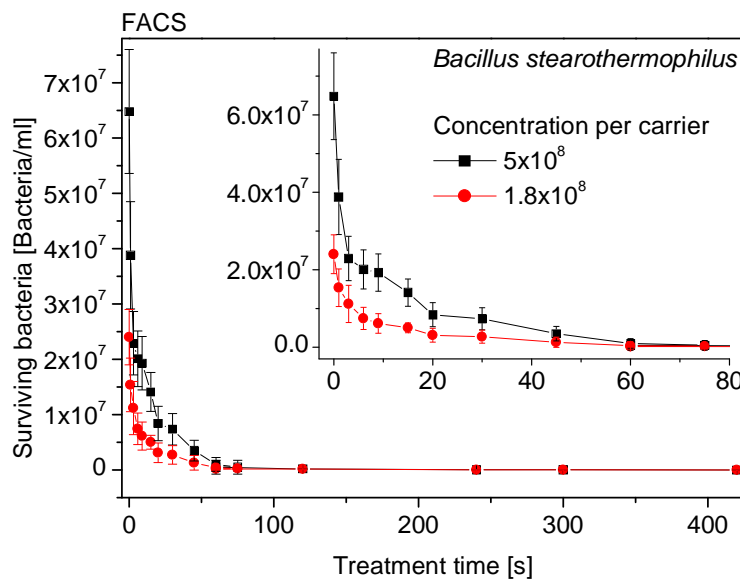


Figure 38: Survival curve of *Bacillus stearothermophilus* for 2 concentrations. The number of live *Bacillus stearothermophilus* cells (vegetative form with spores) with two different concentrations on sample glass carriers is plotted versus oxygen plasma treatment times at 75 Pa. The initial numbers of bacteria cells per carrier were 5×10^8 and 1.8×10^8 .

To study how the change in ratio between charged and neutral oxygen plasma species influences bacterial inactivation, we used two additional pressures: 30 Pa and 150 Pa. In this experiment 7×10^8 cells per carrier were used, as well as triple FACS runs per given treatment time. The survival curves for both pressures are presented in Figure 39. A higher oxygen pressure at 150 Pa in a plasma reactor chamber with a higher density of neutral O atoms and a lower amount of O ions more effectively inactivates sample surfaces contaminated with bacteria. Although, there is not much difference in survival curves (Figure 39), sterilization at pressure 150 Pa is somewhat faster than at 30 Pa. The difference is more significant for inactivation at 75 Pa, but smaller for the number of bacteria per carrier.

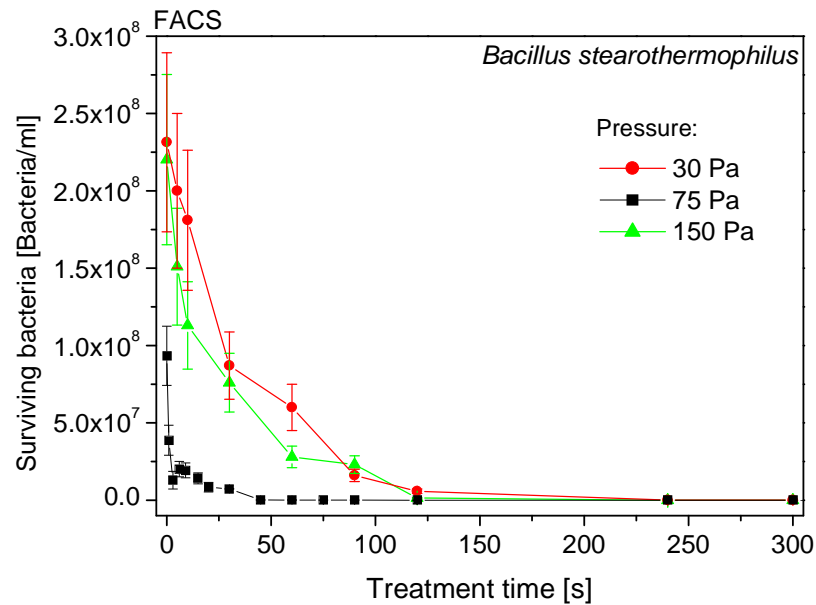


Figure 39: Survival curve of *Bacillus stearothermophilus* for 2 pressures of plasma treatment. The number of live *Bacillus stearothermophilus* cells (in vegetative form) on sample glass carriers is plotted versus oxygen plasma treatment times at two pressures; 30 Pa and 150 Pa. The initial number of bacteria cells per carrier was 7×10^8 for 30 Pa and 150 Pa, and 5×10^8 for 75 Pa.

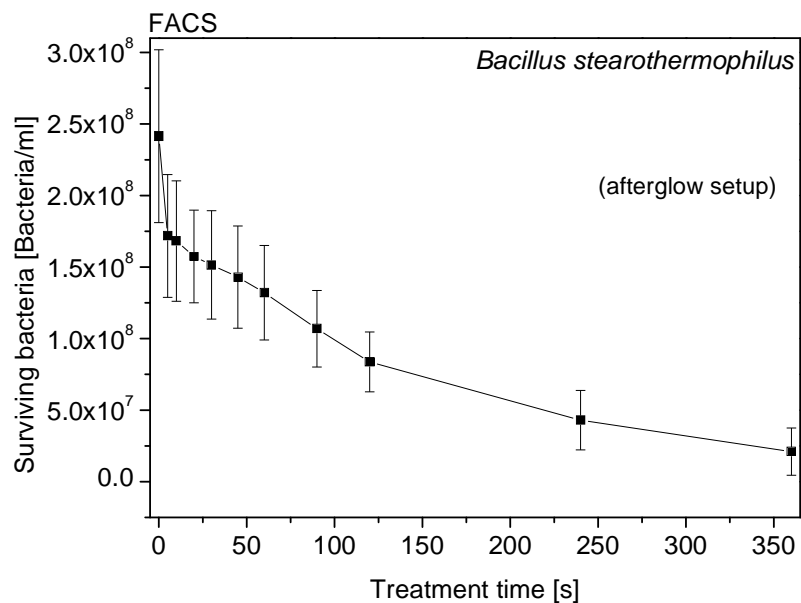


Figure 40: Survival curve of *Bacillus stearothermophilus* for afterglow plasma treatment. The number of live/dead *Bacillus stearothermophilus* cells on sample glass carriers is plotted versus oxygen plasma treatment times at 75 Pa in afterglow region of the reactor. The initial number of bacteria cells per carrier was 7×10^8 .

In the afterglow with only neutral O atoms, inactivation of 7×10^8 cells is much slower than in glow discharge, and the sample is not inactivated even after 350 s (Figure 40). Therefore, when using only oxygen atoms in treatment of *Bacillus stearothermophilus* the inactivation process is not as efficient as in the case of glow discharge treatment. The kinetic of inactivation process measured by FACS is very similar to the one for PCT.

4.7.3 Analysis of *Staphylococcus aureus* after plasma treatment

The quantitative viability analysis with flow cytometry was performed also for *Staphylococcus aureus*. We performed three types of experiments: the first were with two concentrations at the same pressure (75 Pa), the second contained the same concentration of cells per carrier and treatment with two different pressures (30 Pa and 150 Pa), and the third treatment was in afterglow.

Two representative graphs with columns of a single FACS measurement for two concentrations of cells per carrier are displayed in Figures 41 and 42. The inactivation of carriers with 1.7×10^8 cells is presented in Figure 42, whereas the inactivation of carriers of 2.55×10^8 cells is presented in Figure 43.

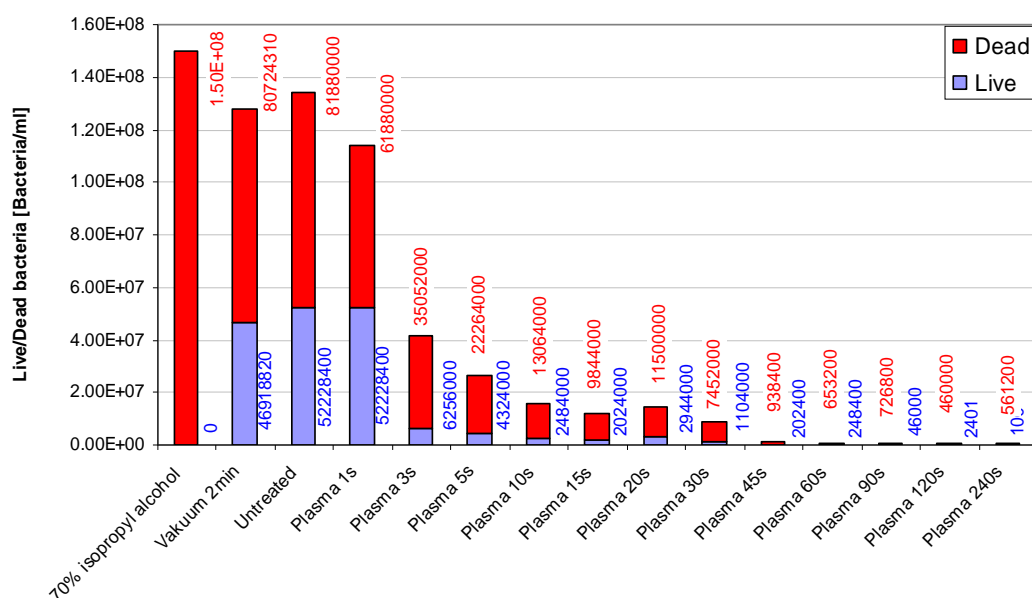


Figure 41: Quantitative viability analysis of *Staphylococcus aureus* after plasma treatment. The number of live/dead *Staphylococcus aureus* cells measured for various oxygen plasma treatment times at 75 Pa, as well as in a vacuum and 70 % isopropyl alcohol by flow cytometer. The concentration of bacteria cells per carrier was 1.7×10^8 .

After short plasma treatment times the number of viable cells reduced rapidly and seven orders reduction of *Staphylococcus aureus* cells was detected within 100 s, which is shown in Figure 41. The total cell number (dead and live) is falling rapidly with plasma treatment time. Similar inactivation is seen for higher *Staphylococcus aureus* concentrations (cell density) on carriers exposed to oxygen plasma glow discharges (Figure 42). The inactivation trend is the similar to the one for 1.7×10^8 cells, except that the sterilization time is slightly prolonged, disregarding the fact that some bacterial counts can be artefacts of debris.

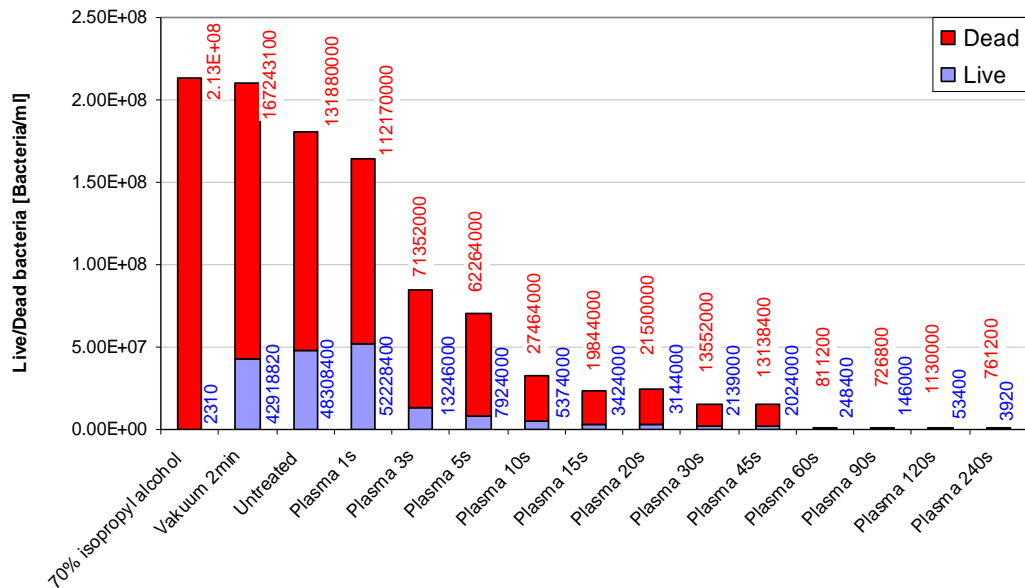


Figure 42: Quantitative viability analysis of *Staphylococcus aureus* after plasma treatment. The number of live/dead *Staphylococcus aureus* cells measured for various oxygen plasma treatment times at 75Pa as well as in a vacuum and 70 % isopropyl alcohol by flow cytometer. The concentration of bacteria cells per glass carrier was 2.55×10^8 .

For triple FACS measurements at single exposure time, and two concentrations of *Staphylococcus aureus* cells per carrier, the survival curves are presented in Figure 43. The figure shows that the inactivation and removal of bacterial cells from the surface is slightly faster for lower concentrations of bacterial cells per carrier. The same effect was observed before for *Bacillus stearothermophilus*. The samples with 1.7×10^8 and 2.55×10^8 cells were not fully inactivated within 240 s.

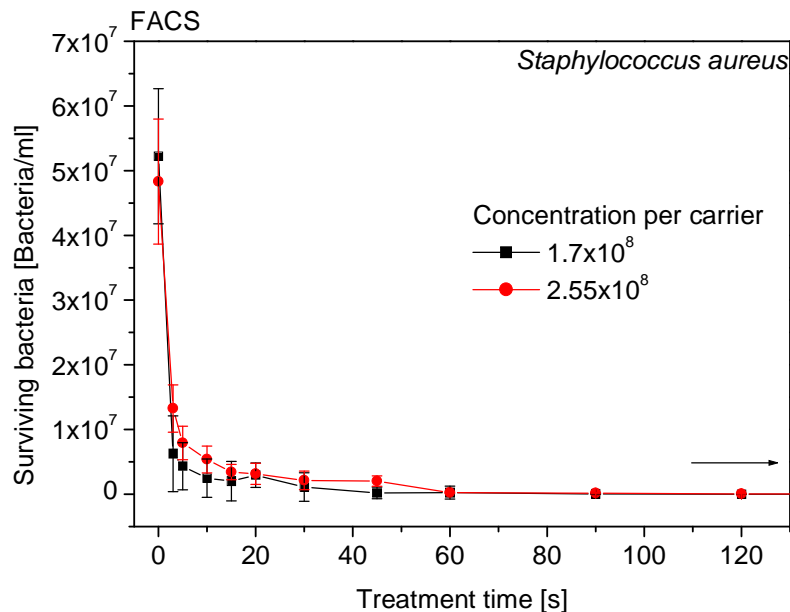


Figure 43: Survival curve of *Staphylococcus aureus* for 2 concentrations. The number of live *Staphylococcus aureus* cells with two different concentrations on sample glass carriers is plotted versus oxygen plasma treatment times at 75 Pa. The initial numbers of bacteria cells per glass carrier were 1.7×10^8 and 2.55×10^8 .

The same concept of measurements for 2 different concentrations (Figure 43) was applied for 2 different pressures. The constant cell number on carriers was used, and pressure was changed to 30 Pa and 150 Pa. Again, the inactivation was faster for 30 Pa treatments for PCT where the samples were inactivated within 90 s. The samples were inactivated on an average within 120 s for oxygen plasma treatments at 150 Pa.

Therefore, 30 Pa treatments are more efficient as 150 Pa treatments.

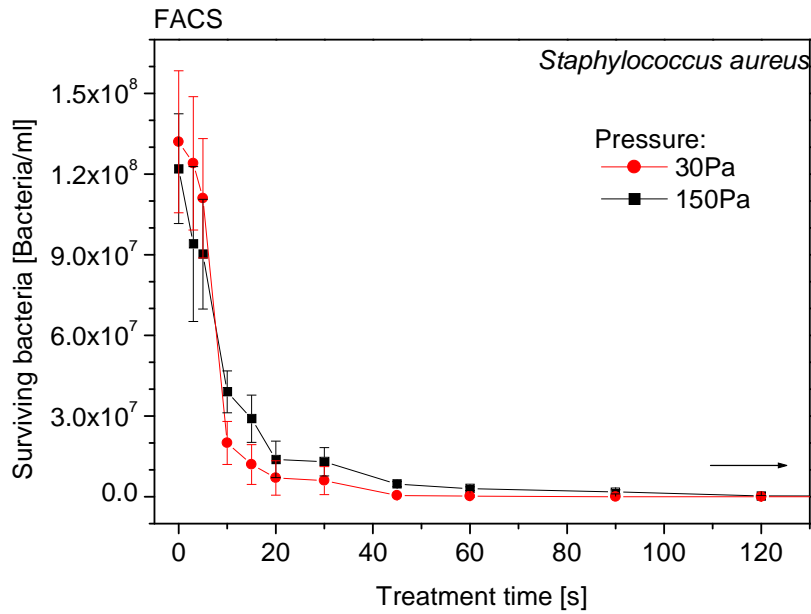


Figure 44: Survival curve of *Staphylococcus aureus* for 2 pressures of plasma treatment. The number of live *Staphylococcus aureus* cells on sample glass carriers is plotted versus oxygen plasma treatment times at two pressures; 30 Pa and 150 Pa. The initial number of bacteria cells per carrier was 7×10^8 .

When oxygen plasma afterglow is used, then rather small bactericidal effect of *Staphylococcus aureus* bacteria is observed (Figure 45). The survival curve shows some decrease in viability for one order of magnitude within 100 s of treatment. Although later exposure times to plasma, show only a diminished inactivation process. The sterilization is not achieved within 500 s plasma treatments.

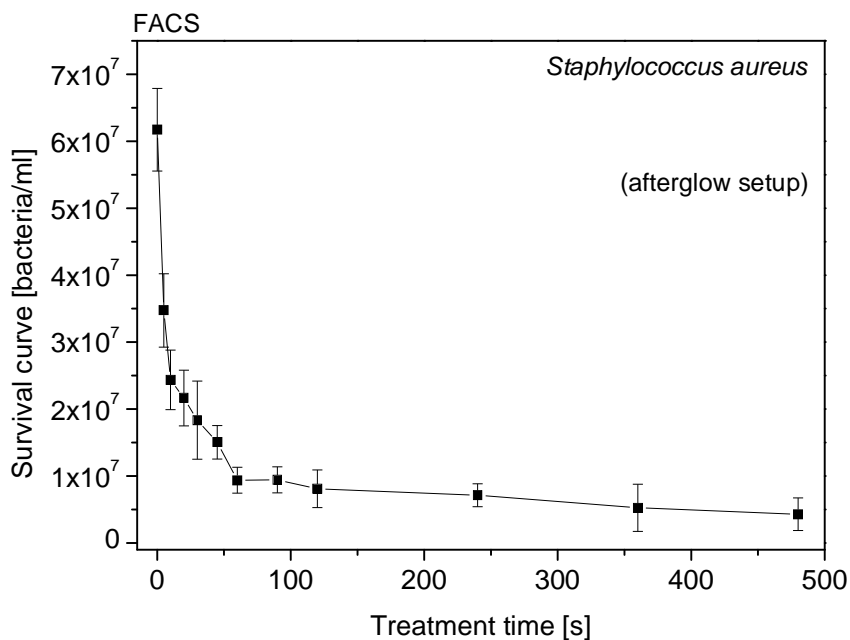


Figure 45: Survival curve of *Staphylococcus aureus* for afterglow plasma treatment. The number of live *Staphylococcus aureus* cells on sample glass carriers is plotted versus oxygen plasma treatment times at 75 Pa in plasma afterglow. The initial number of bacteria cells per carrier was 7×10^8 .

4.8 Optical emission spectroscopy during bacteria treatment

Optical emission spectroscopy (OES) enables qualitative study of chemical and physical processes in plasma, and is used for investigation of many plasma processes. We used optical emission spectroscopy for the characterization of plasma, which proved very suitable to monitor the bacteria degradation during sample treatment with oxygen radicals in a plasma glow discharge. Optical emission spectroscopy was applied for characterization of inductively coupled RF oxygen plasma at the pressure between 30 to 150 Pa (Vujošević et al., 2006)

Optical emission spectroscopy was performed at different conditions. First, it was performed in the empty discharge tube to recognize spectral features. As plasma ignited, several impurities are detected due to desorption from the walls. After a few seconds, the emission becomes constant and is taken as the background. Then the samples of bacteria *Escherichia coli* were treated in oxygen plasma at different pressures. All samples were exposed for 250 s, and the evolution of different spectral features was measured during plasma treatment. The survey spectra measured from plasma loaded with bacteria were not remarkably different from the corresponding spectra measured in the empty discharge vessel. Namely, atomic lines from oxygen were predominant with hydrogen atom lines, as well as with OH band. The difference was only observed after systematic and detail examination of the time evolution of a particular range of spectra where CO and N₂ bands are expected. A comparison for the case of nitrogen molecular band of a spectral feature for an empty and loaded discharge vessel is plotted in Figure 46.

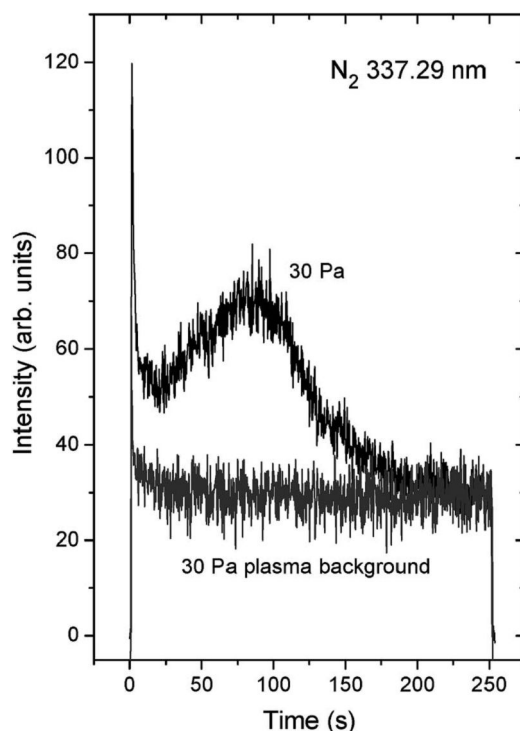


Figure 46: *Optical emission of molecular nitrogen from plasma and during the process.* Time evolution of N₂ peak during oxygen plasma treatment of 10¹⁰ cell/ml *Escherichia coli* at the pressure of 30 Pa and the corresponding background measured in an empty glow discharge chamber.

Organic materials, especially bacteria, usually contain hydrogen, carbon, oxygen, and nitrogen atoms. During plasma treatment, they react with oxygen radicals forming different compounds. Obviously, only those compounds with spectral features in the spectrometer range are suitable for monitoring reactions between the plasma radicals and bacteria. In our case, we are showing results for nitrogen molecules and carbon monoxide. Hydrogen and OH molecules may also be useful for monitoring the bacteria degradation, but since the residual atmosphere in our vacuum system is largely water vapour, the results of H and OH monitoring might be doubtful. The appearance of nitrogen is monitored by measuring intensity of the peak

corresponding to the second positive band $C^3\Pi_u - B^3\Pi_g(0,0)$ at 337.29 nm. The time evolution of this peak during plasma sterilization is plotted in Figure 47 for different pressures.

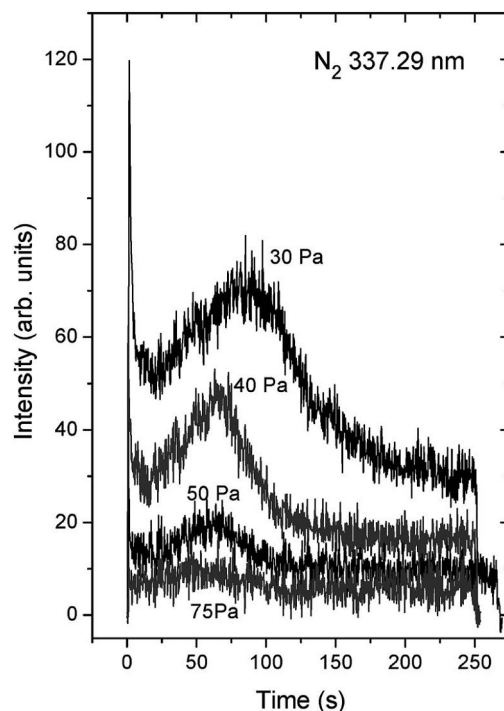


Figure 47: Optical emission of molecular nitrogen during the plasma treatment process. Time evolution of N_2 C–B (0,0) peak during oxygen plasma treatment of *Escherichia coli* 10^{10} CFUs/ml at pressures of 30, 40, 50, and 75 Pa.

The evolution of the nitrogen peak during treatment of bacteria is shown in Figure 47. The intensity of the C–B (0,0) transition was measured at different pressures. As expected, the nitrogen peak is the highest at 30 Pa, where both electron temperature and density are high. At the origin, the peak is very high probably due to desorption of nitrogen molecules from the walls facing plasma. In the next few seconds, a minimum is observed. As the treatment proceeds, the peak increases and reaches a rather broad maximum. The position of the maximum depends on pressure: at low pressure it is shifted to longer times. At 30 Pa the maximum nitrogen radiation is observed for about 85 s of treatment time, and at 40 Pa it is at about 70 s, while at 50 Pa it is at about 60 s. The shift in the maximum radiation is explained by different etching rates. At low pressure, the density of neutral oxygen atoms (that are major reactants in plasma) is rather low, so the time needed for bacteria destruction is rather high. As the pressure is increased, the etching rate is also increased. The increased etching rate causes a shift of the nitrogen emission, as observed from Figure 47. At higher pressures, the peak would be probably shifted even to lower time, but the emission becomes too weak. As mentioned before, the electron density and temperature at high pressure are too low to provide enough molecular excitation. Similar observation is found for the case of CO emission presented in Figure 48.

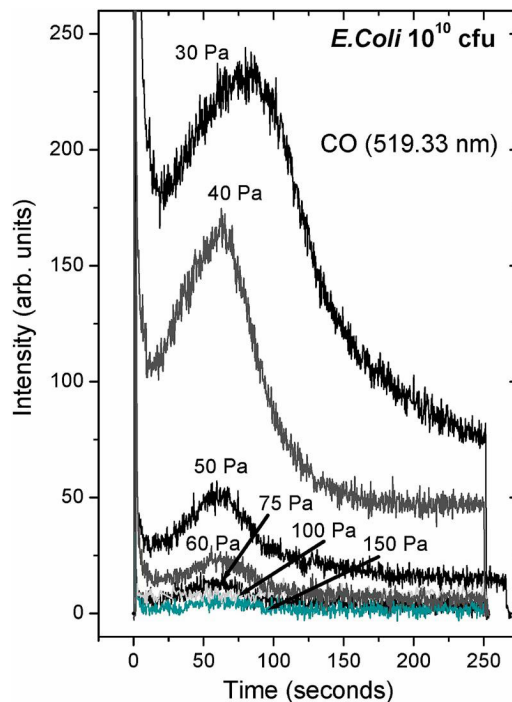


Figure 48: *Optical emission of carbon dioxide during the plasma treatment process.* Time evolution of CO Angstrom band (0,0) peak during oxygen plasma treatment of *Escherichia coli* 10^{10} CFUs/ml at pressures of 30, 40, 50, 60, 75, 100, and 150 Pa.

The CO line is more intense than the nitrogen, so the peak in this line is detectable up to the pressure of about 75 Pa. The time evolution of the CO peak corresponds to the evolution of the nitrogen peak: the maximum is after about 85 s of plasma treatment for the pressure of 30 Pa, 65 s for 40 Pa, 60 s for 50 Pa, and it fairly remains at this position for higher pressure.

To confirm the spectral results, SEM analyses and bacteria culturing (CFU measurements) were performed for various treatment times at designated plasma parameters. The corresponding SEM images are seen in Figures 20. The SEM images confirm that the appearance of the nitrogen and CO peaks probably originates from bacteria oxidation and etching. Figure 20c represents the SEM image of bacteria after 55 s of plasma treatment at 75 Pa. The bacteria are already badly damaged: the cell wall still persists, but it is so badly damaged that the cytoplasm has already escaped. The cytoplasm consists of water mainly (80%), and the rest are proteins, lipids, polysaccharides, and minerals. These materials are easily evaporated in a vacuum, and they enter the plasma when the cell wall is damaged enough to become permeable. As this occurs, a sharp peak should be observed in Figures 47 and 48. However, the peak is not all that sharp. This is explained by slight differences of cell wall erosion for particular bacteria: some bacteria are eroded before others resulting in the peak broadening.

When inner parts of bacteria have been removed, there are still the remains of the cell wall to be etched by oxygen radicals. As stated above, the etching rate is poor, and that is probably the reason for long exponential-like tails observed in Figures 47 and 48. In any case, there are some remains to be oxidized even after 240 s of plasma treatment at 75 Pa (Figure 20d). However, the bacteria themselves have been devitalized well before. This was also proven by determination of viable counts of surviving cells using a standard plate technique. The survivors were counted as colony-forming units (CFUs) per carrier after incubation at 37 °C for 24-48 h. It was confirmed that *Escherichia coli* does not survive within 200 s. So, it can be concluded that the bacteria are damaged enough as soon as the peak intensity of the N_2 and CO peaks is reached.

5 Discussion

5.1 The choice of plasma parameters

The survey of relevant literature on plasma sterilization is presented in the Introduction to this thesis. Authors of the scientific papers presented their results on the destruction of bacteria as a function of the discharge parameters. As a general rule, they spent little words on exact configuration of their experimental setups, so it is difficult if not impossible to compare their results. Furthermore, they usually stated only some discharge parameters like the type of the gas used for plasma generation, the pressure and/or the flow of gas through the vacuum system, the discharge power and/or the discharge voltage and current. And they often did not mention either the exact dimensions of the discharge chamber or the materials facing plasma, let alone the surface finish of plasma facing materials and substrates.

As already mentioned in Introduction, the discharge itself does not interact with bacteria or the substrates, but it is the reactive plasma species which interact with bacteria. Thus, the proper description of the sterilization effects should be obtained by studying the influence of plasma parameters on the destruction of bacteria. The plasma parameters are densities and temperatures (or average energies if energy distribution function is not Maxwellian) of all reactive species in plasma.

There are so many collisions taking place in non-equilibrium plasma that no general theory on the behaviour of plasma at different discharge parameters currently exists. Therefore, plasma parameters should be measured for a particular set of discharge conditions. Unfortunately, the methods for measuring plasma parameters are scarce and many of them are qualitative rather than quantitative. Obviously, the exact evaluation of plasma parameters is currently still beyond the current knowledge. In order to avoid the uncertainties in plasma description, many authors use plasma at such conditions where one or a few parameters are predominant, so measuring these parameters is sufficient to the interaction of plasma with solid materials. The right choice of discharge parameters may therefore result in the creation of plasma with a few important parameters that the problem of plasma characterization is manageable. One such example is plasma created in a glass tube by an inductively coupled RF discharge. This is the main reason why we chose such plasma.

Plasma created in a glass tube with pure oxygen at pressure of around 100 Pa by inductively coupled RF discharge at the frequency of the order of 10 MHz is characterized by the following features:

- Acceleration of electrons in entire volume of plasma reactor due to the induced electric field;
- No positive ion acceleration in the induced electric field;
- Very small DC self-biasing;
- High probability for neutralization of charged particles on the walls facing plasma;
- Extremely high probability for super-elastic collisions between vibration ally excited molecules and atoms;
- Good coupling between rotational and translational states;
- Low and temperature independent probability of surface recombination of oxygen atoms;
- Low probability for volume recombination of neutral oxygen atoms.

These features that are well explained in literature (Ricard, 1996) allow for the creation of plasma with the following parameters:

- Electron temperature of several 10000 K;
- Positively (and also negatively) charged oxygen close to the temperature of reactor walls. If walls are cooled it is often room temperature.
- Neutral oxygen species (molecules, atoms, ozone) temperature close to room temperature;
- Vibrational temperature of oxygen molecules close to room temperature;
- Rotational temperature of oxygen molecules close to room temperature;
- Rather low density of electrons and singly charged positive ions;
- Extremely low density of multiple charged positive ions;
- Rather low density of ozone molecules;
- Very high density of neutral oxygen atoms.

Knowing these general features of our plasma that is created in a forced air cooled glass tube with pure oxygen at pressure of around 100 Pa by inductively coupled RF discharge at the frequency of 27.12 MHz (Figure 6), the list of plasma parameters that should be determined in order to understand interaction with bacteria and substrates shortens to the following ones:

- Electron temperature;
- Charged particles density;
- Plasma potential;
- Density of neutral oxygen atoms.

The electron temperature (thereafter T_e) and density of charged particles (thereafter n_i) was measured with a double Langmuir probe. Plasma potential (or, more precisely, the difference between plasma potential and floating potential) is calculated from measured T_e and n_i using the following equation (Swift, 1969):

$$V_p - V_f = \frac{kT_e}{2e_0} \ln\left(\frac{m_+}{2m_e}\right) \quad (2)$$

Here, V_p is plasma potential, V_f is floating potential, k Boltzmann constant, T_e electron temperature, e_0 elementary charge, m_+ ion mass and m_e electron mass. The numerical value of plasma potential is 15 V for an electron temperature of $kT_e = 3$ eV, and 25 V for electron temperature of $kT_e = 5$ eV.

The density of neutral oxygen atoms in our plasma was measured with a catalytic probe (Mozetič et al., 2003; Cvelbar et al., 2005; Mozetič et al., 2005; Drenik et al., 2005; Mozetič et al., 2006; Drenik et al., 2006; Cvelbar et al., 2008). Our plasma is therefore well characterized (all relevant plasma parameters are known) and therefore suitable for a decent study on interaction with bacteria.

Our experimental results on plasma characterization show that the density of neutral oxygen atoms exceeds the density of ions for the factor of between 3×10^4 and 1×10^6 at pressures of 10 and 150 Pa (Figure 7). Since we postulated that the major reactants are neutral oxygen atoms, the majority of experiments were performed at the pressure of 75 Pa where the dissociation fraction of oxygen molecules is around the highest value (Figure 8). We avoided higher pressures than 75 Pa, because at higher pressures the neutral particles start heating due to inelastic as well as elastic collisions with low energy electrons. In cases where we were interested in the role of ions, we performed experiments at the extreme pressures 150 Pa and 30 Pa. At 150 Pa the density of neutral atoms is huge compared to the ion density, and the plasma potential is very small, so ions are easily neglected. The other opposite should be at very low pressure of about 10 Pa where the ion density reaches its maximum. We chose 30 Pa for the following reason: the ultimate pressure is about 7 Pa so gas at this pressure contains more water vapour rather than oxygen. However, at 30 Pa the ion density is still high, but the concentration of oxygen is high enough to assure the negligible effect of residual atmosphere.

5.2 Preparation of bacteria and substrates

Once the right conditions for plasma treatment of bacteria were chosen, we continued with the preparation of bacteria and substrates. Bacteria are normally cultivated in liquid Nutrient Broth. If Nutrient Broth containing bacteria is deposited onto a substrate together with bacteria, non volatile compounds from the broth would remain on the substrate partially covering bacteria. This would lead to the underestimation of the destruction efficiency of plasma treatment, since the remains of the compounds would have to be removed before bacteria themselves are exposed to plasma radicals. In order to overcome this problem, a protocol for bacteria harvesting from Columbia agar plates and then resuspending in sterile water was elaborated. The protocol is described to details in Materials and Methods Section of this thesis (section 3.2.1). The protocol was so elaborated that even traces of such impurities were not observed on samples deposited with bacteria.

Bacteria tend to agglomerate. Many of them form capsule, which allows for the good sticking of bacteria into small groups with roughly spherical shape. The formation of such groups results in the overlapping of bacteria on substrates. Again, this effect would lead to the underestimation of plasma efficiency. In order to overlap this particular effect, the substrates were carefully prepared prior to the deposition of bacteria. The agglomeration effect is mostly pronounced if the water solution of bacteria is placed onto substrates with a low surface energy; the water is not evenly distributed but forms drops, which after evaporation lead to localized agglomerates of bacteria. The surface properties of substrates should therefore be modified. The best method is definitely the application of oxygen plasma. Plasma removes traces of impurities (that cause substrates hydrophobic), so a protocol for removal of such impurities was elaborated. We found that 5 s of plasma treatment at 75 Pa effectively modifies our substrates (which are pre-cleaned before) to become highly hydrophilic. Since such hydrophilic surface tends to attract organic molecules that are always found in air at tiny concentrations, the effect is not permanent. In the protocol elaborated in this thesis the allowed time between plasma activation of substrates and bacteria deposition is only a few minutes.

Such treatment of the substrates prior to deposition of bacteria should assure for a rather uniform distribution of bacteria in a monolayer. Still, it has to be mentioned that bacteria can never be distributed perfectly uniformly. At large numbers of bacteria we have to take into the account of not only the possible agglomeration, but also the finite size of the bacteria. The size of sample holders is about $5 \text{ cm}^2 = 5 \times 10^8 \mu\text{m}^2$. A typical size of bacteria used at our experiments is almost $1 \mu\text{m}^2$. If bacteria form a perfect monolayer, there is obviously room to accommodate at least 5×10^8 bacteria on the sample holder. Most experiments were actually performed with roughly this number of bacteria.

5.3 Effect of plasma treatment on bacteria inactivation

Once the protocols for both bacteria and substrate preparation were elaborated, systematic experiments were performed. The evaluation of bacteria after treatment with plasma at different conditions was performed by Scanning Electron Microscopy, Fluorescence Microscopy, Fluorescence Activated Cell Sorting and Plate Count Technique. SEM was used to observe morphological changes of bacteria and to double-check the damages on bacteria cells after plasma treatment. Therefore only badly damaged bacteria are shown. The FM method was used to determine the viability of bacteria, but turned out to not be appropriate for the case of plasma sterilization.

The quantitative techniques that proved suitable for determination of bacterial survival curves after plasma treatments are FACS and PCT. As explained to details in Materials and Methods section of this thesis, the PCT never gives results in terms of the absolute number of live bacteria, but rather in terms of CFUs. Happily enough, the CFUs are often linear with the number of bacteria, so relative survival curves should give a good insight in the sterilization efficiency (Block, 2001). On the other hand, FACS is an absolute counting method, which is calibrated with well defined beads.

FACS proved to be a relatively reliable method in our experiments. To the best of our knowledge this method has never used by any other author for evaluation of plasma sterilization. FACS allows for the

determination of bacteria (live or dead), as long as their size is within certain brackets. Plasma destroyed bacteria lost their typical size and shape, so it is not surprising that the number of dead cells decrease with increasing plasma treatment time. This is a general rule and was observed for all bacteria treated by plasma for reasonable times.

5.4 Inactivation of *Escherichia coli*

Let us now discuss the results obtained with *Escherichia coli*. The results of bacterial survivals as determined by FASC are summarized in Figures 32, 33 and 34. The first 3 columns in Figure 32 represent the number of bacteria as detected by FACS after treatment with isopropyl alcohol, bacteria exposed to vacuum for 2 minutes, and for untreated bacteria. The original number of bacteria per carrier should be 1.6×10^8 . In a short treatment time of 5 s the number of survived bacteria is lowered by a factor of $3.9/4.8 = 0.81$, so we can conclude that about 20% of bacteria is killed in 5 s. Surprisingly enough, the number of dead bacteria is lowered much more: $4/12 = 0.33$. This rapid drop of dead bacteria could not be attributed to the inaccuracy of the FACS technique, which has just been found pretty well at about 20%. Furthermore, SEM images do not show complete degradation of any bacterium after 5 s of plasma treatment. This rapid drop in the number of dead bacteria after a few seconds of treatment with oxygen plasma cannot be simply attributed to a general error, but should be explained. The handiest explanation is the charging effect caused by plasma treatment. As long as bacteria are alive, they can stick to the surface with pili. Once dead they do not stick that actively, but rather by electrostatic forces. When such bacteria are placed into plasma for a short time, both bacteria and the carrier are charged negatively. The electrostatic force between the bacteria and the carrier is thus repelling, so death bacteria can be just detached from the substrate in a short time of plasma treatment. Of course, not all death bacteria can be removed since this force is weak. Apparently, this is a possible explanation for a quick drop of the death bacteria after plasma treatment of *Escherichia coli* for 5 s.

Further exposure of bacteria to plasma leads to the continuous decrease of the number of death bacteria. This observation is attributed to destruction of bacteria because the size as well as the shape of dead bacteria is changed so much that FASC cannot detect them – rather the remains of bacteria are detected as debris. This explanation is sound with SEM images of bacteria that show bad damages after about a minute of plasma treatment (Figure 20c)

Let us now consider the number of live *Escherichia coli*. As expected, bacteria exposed to isopropyl alcohol are all dead. Interestingly enough, the number of live bacteria for untreated samples is pretty low – only about 28% of bacteria are found live on untreated samples. This is a result of improper handling with such delicate experimental materials. The number of survived bacteria after exposure to vacuum or exposure to plasma for 5 s is further decreased by about 25%. There is a small difference between the number of live bacteria for vacuum and plasma treated samples. This difference is hardly attributed to plasma action, since also SEM images do not show serious damage of *Escherichia coli* after 5 s of plasma treatment. The first substantial fall of the number of live bacteria is observed after 10 s of plasma treatment. Obviously, this is due to the damage of the bacterial cell wall. Knowing the plasma parameters, it is possible to calculate the dose of O atoms required for substantial damage of the cell wall. The O atom density at 75 Pa is $3.5 \times 10^{21} \text{ m}^{-3}$. The flux of O atoms onto the surface of bacteria is given with:

$$j = \frac{1}{4}nv \quad (3)$$

where n is the density of neutral oxygen atoms as measured with the catalytic probe, and v is the average of the absolute velocity of thermallized oxygen atoms.

$$v = \sqrt{\frac{8kT}{\pi m}} \quad (4)$$

Here, T is the kinetic temperature of neutral gas in the vicinity of our sample (measured in Kelvin), k

Boltzmann constant, and m the mass of oxygen atom. Taking into account numerical values, i. e. $k = 1.38 \times 10^{-23} \text{ JK}^{-1}$, $T = 300 \text{ K}$, $m = 16 \text{ emu} = 2.66 \times 10^{-26} \text{ kg}$, the velocity is

$$v = 6.3 \cdot 10^2 \text{ ms}^{-1} \quad (5)$$

The flux of oxygen atoms onto bacteria during treatment with plasma at the pressure of 75 Pa is thus:

$$j = 5.5 \cdot 10^{23} \text{ m}^{-2} \text{ s}^{-1} \quad (6)$$

The dose bacteria receive during treatment with plasma for a period of t is:

$$D = jt \quad (7)$$

For the case of bacteria treated at pressure of 75 Pa for 10 s the dose is $5.5 \times 10^{24} \text{ m}^{-2} = 5.5 \times 10^{12} \mu\text{m}^2$. This is the result of our experiments with *Escherichia coli*, and can be generalized to any plasma system with a known (measured) density of neutral oxygen atoms.

Prolonged treatment of *Escherichia coli* with oxygen plasma caused bad damage of bacteria and eventually their inactivation. The treatment time, needed from the detection of an un-measurably low number of bacteria, depends slightly on the concentration of bacteria on samples, and is within 100 s. The absolute sterility of plasma treated samples cannot be determined precisely by FACS, but rather by PCT. Happily enough, both techniques give similar results (Figures 49 and 50), so we can conclude that the absolute sterility is obtained after (to be on the safety side) to be about 150 s. The required dose of oxygen atoms to obtain full destruction of *Escherichia coli* is calculated using equation (7) and is found to be:

$$D_{EC} = 8.25 \cdot 10^{25} \text{ m}^{-2} = 8.25 \cdot 10^{13} \mu\text{m}^2 \quad (8)$$

More precisely the calculated dose of oxygen atoms for total inactivation measured by PCT and FACS is plotted in Figures 49 and 50, respectively. The sterilization of *Escherichia coli* is achieved after the dose of $6.6 \times 10^{25} \text{ m}^{-2}$ or at the most after $1.3 \times 10^{26} \text{ m}^{-2}$ for double concentration of bacteria cells.

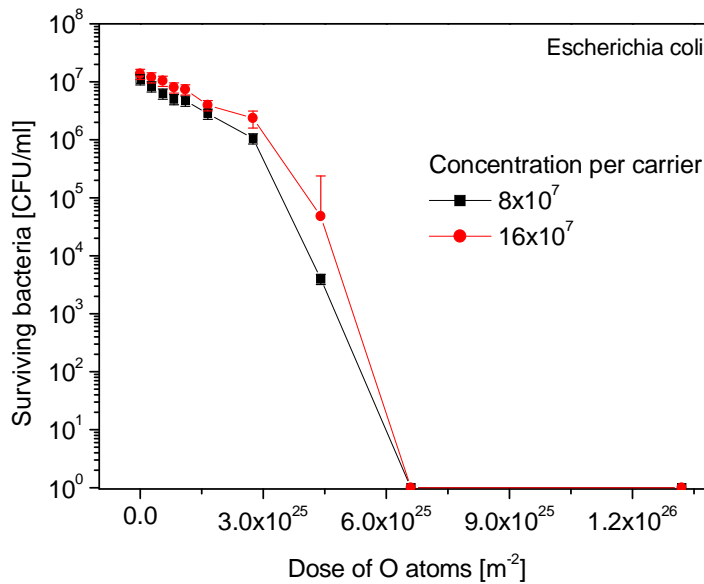


Figure 49: Survival curve of *Escherichia coli* for received dose of O atoms (measured by PCT). The number of surviving bacteria CFUs *Escherichia coli* in respect to received dose of neutral oxygen atoms. The two initial concentrations were used: 8×10^7 and 16×10^7 cells per carrier.

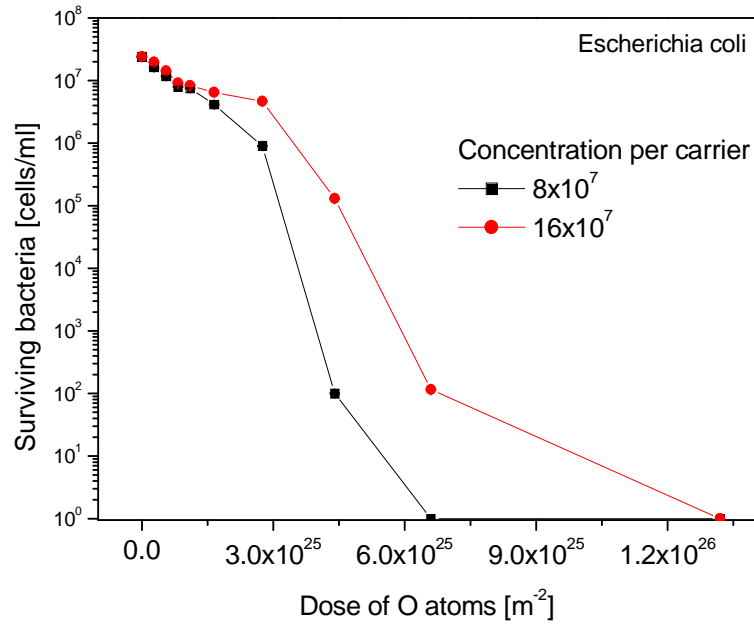


Figure 50: *Survival curve of Escherichia coli for received dose of O atoms (measured by FACS).* The number of surviving bacteria *Escherichia coli* cells in respect to received dose of neutral oxygen atoms. The two initial concentrations were used: 8×10^7 and 16×10^7 cells per carrier.

Contrarily, there are some discrepancies in survived bacteria between results obtained by PCT and FACS method (see Figures 49 and 50). The reason for this is that under certain conditions, bacteria having compromised membranes may recover and reproduce even though such bacteria may score as “dead” in LIVE/DEAD BacLight assay. However, more often bacteria with intact membranes may be unable to reproduce in a nutrient medium, yet be scored as “live” in FACS analysis (Molecular Probes, L34856).

In section 4.2 of this thesis we elaborated the influence of oxygen atoms on substrates (carriers) themselves. We showed that the materials with a high recombination coefficient tend to heat during prolonged plasma treatment. Let us now calculate the required properties of materials that would be heated for less than 30 K after receiving the dose which is fatal for *Escherichia coli*, i.e. $D_{EC} = 8.25 \times 10^{25} \text{ m}^{-2} = 8.25 \times 10^{13} \text{ } \mu\text{m}^2$. In the following calculation, the substrate to be sterilized is of a spherical shape. A sphere of radius r made from material with the density of ρ , the specific heat capacity of c_p , and the coefficient for heterogeneous surface recombination of γ is heated at the rate of:

$$P = \frac{1}{2} \gamma j W_D 4\pi r^2 = \rho \frac{4}{3} \pi r^3 c_p \frac{\Delta T}{\Delta t} \quad (9)$$

The critical radius of the sample to be heated for $\Delta T = 30 \text{ K}$ depends on the recombination coefficient:

$$r = \frac{3\gamma D W_D}{2\rho c_p \Delta T} \quad (10)$$

Taking into account measured values as well as typical values of constants for delicate organic materials, i.e. $\gamma = 0.005$, $D_{EC} = 8.25 \times 10^{25} \text{ m}^{-2}$, $W_D = 8.3 \times 10^{-19} \text{ J}$, $\rho = 2 \times 10^3 \text{ kg m}^{-3}$, $c_p = 1000 \text{ J kg}^{-1} \text{ K}^{-1}$ and $\Delta T = 30 \text{ K}$, the minimum radius of our sample to avoid substantial heating is 0.017 m. Spherical samples with radiuses larger then 1.7 cm are therefore suitable for sterilization with our plasma, as long as they are contaminated with *Escherichia coli*. In the upper calculation we did not take into account the cooling of the sample by thermal conductivity of the surrounding gas. On the other hand, actual samples are usually not spherical, so the overestimation of the critical radius due to neglecting cooling is compensated by less favourable actual shapes of samples. The upper calculation therefore just gives some directions about possible the application of sterilization with our plasma source: large samples can be effectively sterilized without bothering heating effects; smaller samples, on the other hand, would overheat after receiving the

lethal dose of oxygen atoms, so they should be kept on cooled holders to avoid overheating.

The upper calculation takes into account a typical value for the recombination of the coefficient of oxygen atoms on polymer materials, i.e. $\gamma = 5 \times 10^{-3}$. If our sample is made from a metal with moderate catalytic activity (i.e. $\gamma = 5 \times 10^{-2}$), the required radius is 10 times larger, i.e. $r = 17$ cm. For highly catalytic materials, the required radius to avoid overheating is even larger than the active cooling when plasma sterilization is required.

All upper results are valid for *Escherichia coli*. Although, the formulae presented in equations (2, 3, 4, 5, 7, 9 and 10) can be applied for any bacteria.

5.5 Inactivation of *Bacillus stearothermophilus*

Let us now consider *Bacillus stearothermophilus*. These bacteria are well known for their capability to survive in unpleasant environment, and are often used as a standard to determine the efficiency of various sterilization techniques, especially autoclaves. They may form spores – extremely resistant modes of bacteria – that can survive for long time in an unpleasant environment.

The FACS results on plasma degradation of *Bacillus stearothermophilus* follow those obtained for *Escherichia coli*. Approximately a third of bacteria are found alive on untreated samples. Exposure to a vacuum for 2 minutes causes the drop of this number for another third, so the percentage of bacteria surviving preparation procedure and evacuation is about 24%.

However, there is a certain discrepancy between the results obtained by FACS and PCT methods. Namely, the PCT method shows pronounced plateau in the number of vital bacteria between, say, 30 and 60 s (Figure 13), while such behaviour is not as pronounced for the case of FACSs. This discrepancy can be explained by taking into account the spore formation during sample preparation and sensitivity of both methods. Vegetative forms of bacteria are not as resistant as the spores and are etched at the similar efficiency as *Escherichia coli*. However, the spores are only slightly damaged after receiving a moderate dose of O atoms. The moderate dose is, according to upper calculations, about $2 \times 10^{26} \text{ m}^{-2}$. This dose is high enough to kill practically all vegetative bacteria, but is not at all high enough to destroy the spores.

Interestingly, even prolonged treatment times do not destroy all bacteria as in the case of *Escherichia coli* in some cases. The reason for this can be one order higher density of *Bacillus stearothermophilus* cells on a carrier surface compared to *Escherichia coli* carriers, as well as the fact that *Bacillus stearothermophilus* is much more resistant bacteria compared to *Escherichia coli*. An additional reason is that the sporulation of *Bacillus stearothermophilus* during the overnight drying before plasma experiments. Some spores should be extremely resistant to plasma environment. As shown by SEM images, vegetative forms of *Bacillus stearothermophilus* are almost perfectly destroyed after a few minutes of plasma treatment. In contrary, the presence of bacteria spores prolongs plasma treatment (Figures 35, 36 and 38).

The dose needed for the full sterilization of objects contaminated with a substantial amount of *Bacillus stearothermophilus* spore cannot be calculated from experiments performed within this work. Namely, larger treatment times (probably much more than 10 minutes) are needed to fully destroy the bacteria as well as spores of these bacteria. The required treatment time does not depend significantly on the initial number of bacteria on samples. In the Results section, we present systematic research with 2 different initial concentrations (which have spores) analysed with FACS: 1.8×10^8 and 5×10^8 (Figures 35 and 36, respectively). The corresponding number of live bacteria after 300 s of plasma treatment is 14000 and 40000 for initial number of 1.8×10^8 and 5×10^8 , respectively. The ratio between the initial numbers of bacteria is $1.8/5 = 0.36$, while the corresponding ratio after 300 s of plasma treatment is 0.35. The ratio after 420 s of plasma treatment is 0.37. These numbers clearly show that the initial concentration does not play any role in sterilization efficiency for *Bacillus stearothermophilus*, especially if the experimental error is taken into account.

Any extrapolations in science are doubtful and it applies also for our experiments. Still, if we take into

account the above mentioned numbers and try to extrapolate the survival curves to longer treatment times, we would find that an extremely long treatment time would be needed to sterilize the substrate completely (here, sterilization is defined to 1 cell only). Taking into account exponential decay $N = N_0 \exp(-t/\tau)$ we can calculate the decay time τ as

$$\tau = -t \ln^{-1} \left(\frac{N}{N_0} \right) . \quad (11)$$

Taking into account the numerical values, i.e. $t = 120$ s, $N/N_0 = 1/4$, the characteristic decay time is $\tau = 86$ s. Full sterilization is achieved when $N/N_0 = 1/40000$, so the sterilization time is $t_{str} = 86 \text{ s} \times 10.6 = 911$ s. Here we have to add the time needed to obtain 40000 live bacteria, which is 300 s, so the entire treatment time assuring sterilization of our substrate would be about 1000 s. This means that the received dose of O atoms at given parameters for sterilization of a sample contaminated with *Bacillus stearothermophilus* (vegetative form with spores) should be around $5.5 \times 10^{26} \text{ m}^{-2}$. The exact values in this paragraph are calculated for the case of 5×10^8 initial bacteria. As mentioned before, this is just an extrapolation of bacteria survival curve and the exact result is doubtful. Still, it gives a useful if rough estimation of required plasma treatment time to sterilize objects contaminated with *Bacillus stearothermophilus*. A valuable conclusion drawn from the experiments and discussion is that one should be extremely careful when dealing with plasma sterilization of bacteria that make spores.

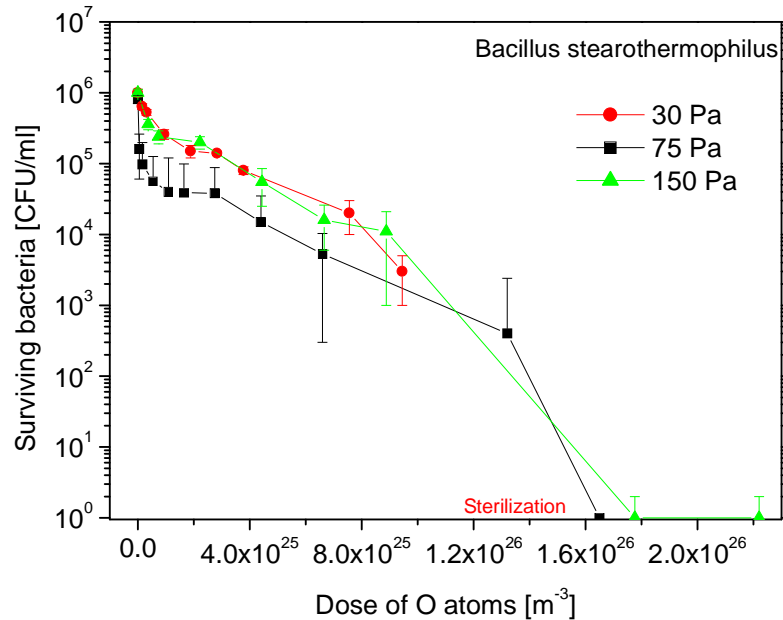


Figure 51: Survival curve of *Bacillus stearothermophilus* for received dose of O atoms (measured by PCT). The number of surviving bacteria (CFUs) *Bacillus stearothermophilus* (vegetative form only) in respect to received dose of neutral oxygen atoms at 3 different pressures. The two initial bacterial concentrations used were: 7×10^8 (at 30 Pa, 150 Pa) and 5×10^8 cells per carrier (at 75 Pa).

Contrarily, the *Bacillus stearothermophilus* in vegetative form only can be inactivated rather quickly. If oxygen plasma is used with plasma parameters validated for 75 Pa pressure, then the substrates can be sterilized within the O atom dose of $1.65 \times 10^{26} \text{ m}^{-2}$ (Figure 51). When bacteria *Bacillus stearothermophilus* were treated additionally at two pressures, i.e. 30 and 150 Pa, no significant difference was observed on PCT survival curves. The inactivation process is slightly faster for treatments at 75 Pa, compared to 150 Pa, where a larger dose is needed to achieve sterilization. However, there is no significant difference between 30 Pa and 150 Pa for inactivation trend. Although the differences are more clearly visible at FACS measurements, the most efficient inactivation of bacteria is performed with for plasma treatment at 75 Pa, secondly at 30 Pa, and lastly at 150 Pa (Figure 52). This leads to conclusion that the charged species influence the efficiency of bacterial inactivation. It seems that charged species, predominantly oxygen ions act synergistically with neutral O atoms and influence bacterial destruction. Thus, the exact role of ions as well as electrons is not yet fully resolved, but there are several indications of their importance.

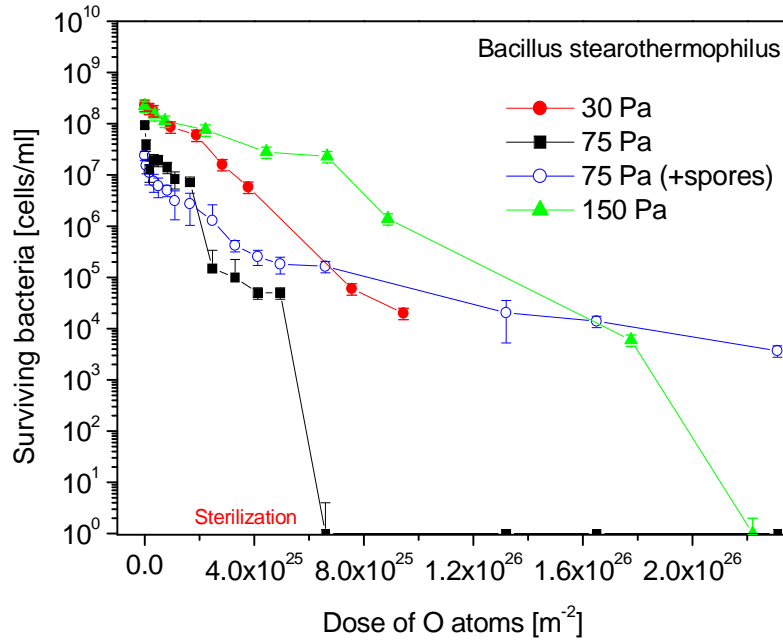


Figure 52: Survival curve of *Bacillus stearothermophilus* for received dose of O atoms (measured by PCT). The number of surviving bacteria *Bacillus stearothermophilus* cells (vegetative form and vegetative plus spores) in respect to received dose of neutral oxygen atoms at 3 different pressures.

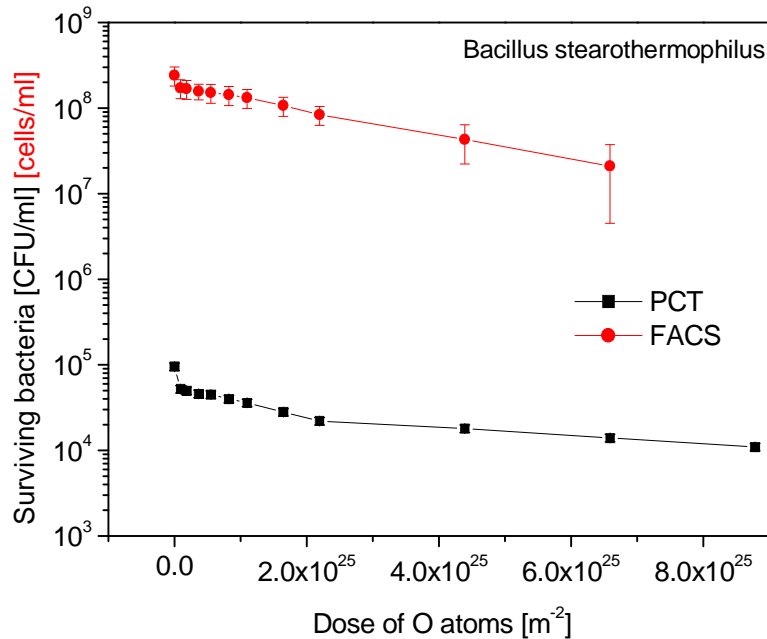


Figure 53: Survival curve of *Bacillus stearothermophilus* for received dose of O atoms in afterglow. The number of surviving bacteria *Bacillus stearothermophilus* cells (vegetative form) in respect to received dose of neutral oxygen at 75 Pa. The graphs presents PCT and FACS results of inactivation.

More interesting are results on survival curves in the afterglow. In this case, ions from plasma are absent and the density of neutral oxygen atoms are smaller than in plasma itself (glow discharge) by a factor of about 3. The survival curve for *Bacillus stearothermophilus* in the afterglow is just impressive: about 2×10^7 out of initially live 2.4×10^8 bacteria survived treatment with oxygen atoms for 360s! Both FACS and PCT methods show excellent survival of *Bacillus stearothermophilus* in the oxygen plasma afterglow and viability reduction for only one order (Figure 53). As mentioned earlier, such huge number of survived bacteria can be explained by the absence of synergetic actions between ions and atoms. Whereas the specific action of oxygen atoms on bacteria is rather slow etching of very resistant bacterial

envelope. This also confirms the conclusion that combined interactions of charged species and atoms can inactivate bacterial cells faster.

Although high efficiency in plasma glow cannot be ascribed solely to the role of electrons and ions (because in the case of indirect exposure in afterglow, the fluxes of uncharged active species are rather low), one can think of charge-induced mechanisms that contribute to bacterial killing in direct exposure. The negative charging of the cell wall by plasma electrons (in analogy to the charging of dust in complex plasmas) was considered by Laroussi (Laroussi et al., 2003). Mechanical stress induced by charging was under certain conditions that are sufficient to cause rupture in gram negative, but not in gram positive, bacteria. However, the contribution of charge to bacterial inactivation may be more prominent than concluded in (Laroussi et al., 2003), because the considered situation was somewhat idealized. The model was based on spherical bacteria (thus applicable to cocci), and only cell death by mechanical rupture was considered. Possibly, in nonspherical objects such as rods and spirals, the electrostatic repulsion of the surface charge induces more stress than in the case of regularly shaped spheres; these microbes may be easier to kill by rupture than cocci. Furthermore, inflicting mechanical damage is not necessarily the only way to destroy the cell. The nature of the bacterial cell wall allows many kinds of electrostatic interactions; one of them is disturbing the surface charge equilibrium (Bayat et al, 2004), which may kill the cell without actually tearing it apart.

The bacterial cell wall carries a natural negative charge, because it consists of strongly electronegative components. These components are teichoic acids linked to peptidoglycan (in gram positive) and electronegative carbohydrate ends of the lipopolysaccharide (in gram negative). The bacterial surface with a negative charge and a positive cationic cloud around it form an electric double layer. Typical zeta potentials are on the order of 30–50 mV; thus, the corresponding surface potentials are about 100 mV (Bayat et al, 2004). With the electrical capacitance of a spherical cell with a diameter of 1 μm ($C = 4\pi\epsilon\epsilon_0R \approx 4.4 \times 10^{-15}$ F, with $R = 5 \times 10^{-7}$ m and $\epsilon = 80$ for the permeability of the extracellular fluid), an estimated charge on the cell surface is 4.4×10^{-16} C, or about 3000 elementary charges. Bacteria are very sensitive to changes in their surface charge, considering that the changes violate the wall integrity. For example, the neutralization of the negative charge leads to cytoplasm leakage and cell death (Campanhã et al., 1999). This can easily occur in our case when positive oxygen ions from plasma glow hit the sample surface which is negatively charged (naturally as well as by inset into plasma onto floating potential).

Therefore, there may be a contribution of charged species in bacterial inactivation, but only in direct plasma treatment in glow discharge, and not in afterglow. And more this holds only for vegetative bacteria that are on or close to the sample surface. In this case charging accelerates the inactivation process, although the main reason for destruction of the cell wall is etching atom by atom (seen from almost linear decrease of survival curve) until the envelope is eroded, and followed by fast bacteria kill. Whereas for spores, charging doesn't play any important role as seen from Figure 52. The almost linear decrease of survival curve becomes flattened (after receiving dose of 6×10^{25} m^{-2}), when plasma starts interacting only with spores and vegetative forms are already devitalised. A similar claim was supported by Stoffels for inactivation of bacteria in cold atmospheric plasma (Stoffels et al, 2008).

5.6 Inactivation of *Staphylococcus aureus*

We already discussed important differences in plasma sterilization of gram negative bacteria *Escherichia coli* and gram positive bacteria *Bacillus stearothermophilus*. Let us now discuss the results obtained with another type of gram positive bacteria - *Staphylococcus aureus*. These bacteria have a form of almost perfect spheres. The spheres are always covered with a capsule that, among other functions, allows bacteria to stick to surfaces and form clusters. They do not form spores.

SEM images of *Staphylococcus aureus* are shown in Figure 22. As expected, live untreated bacteria are found in clusters which are covered with a rather thick capsule. SEM images also illustrate rapid degradation of such bacteria in oxygen plasma. Even 20 s of treatment at 75 Pa is enough for bad damages of bacteria (Figure 22b). SEM images also show that a minute of plasma treatment at 75 Pa is enough for transformation of original spheres to debris with indistinguishable size and shape (Figure 22c). SEM images therefore reveal pretty effective destruction and inactivation of bacteria by oxygen plasma.

The SEM images are sound with the number of dead bacteria counted by FACS; after about a minute of

plasma treatment the number of dead bacteria falls to an extremely small number. This is of course due to the measuring principle of FACS of bacteria viability as well as cell damages, which were described to details before.

PCT experiments (Figures 16, 17) on survival of *Staphylococcus aureus* are also sound with SEM images: absolute sterility was obtained after 90 s or 120 s of plasma treatment at 75 Pa. These values belong to the initial number of 1.7 and 2.55×10^8 bacteria, respectively. The results of PCT measurements are therefore good illustrations of SEM images. From the PCT results we can estimate the required dose of O atoms needed to sterilize objects contaminated with *Staphylococcus aureus*: it is close to those for *Escherichia coli*, i.e. about:

$$D_{SA} = 7 \cdot 10^{25} m^{-2}. \quad (12)$$

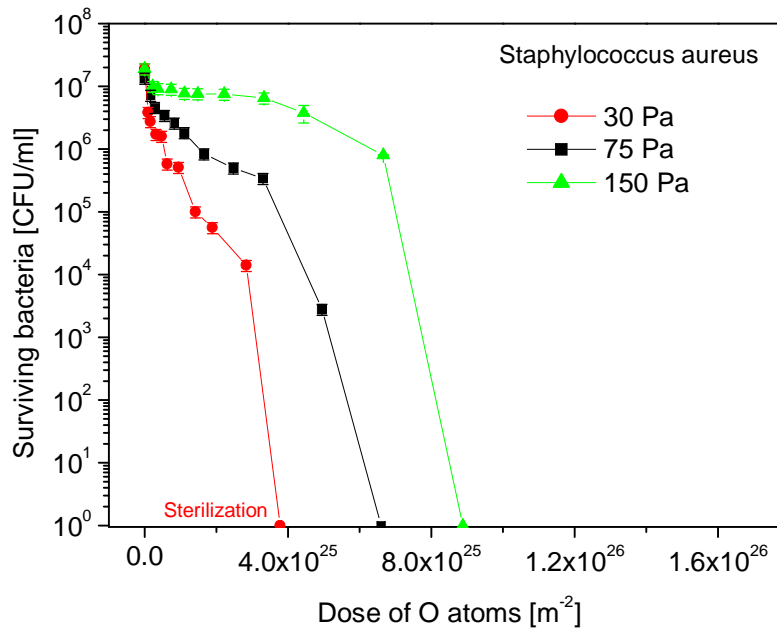


Figure 54: Survival curve of *Staphylococcus aureus* for received dose of O atoms (measured by PCT). The numbers of surviving bacteria (CFUs) *Staphylococcus aureus* in respect to received doses of neutral oxygen atoms at 3 different pressures. The two initial bacterial concentrations used were: 7×10^8 (at 30 Pa, 150 Pa) and 2.55×10^8 cells per carrier (at 75 Pa).

The PCT results on live *Staphylococcus aureus* are not at all supported with the FACS results for samples treated with plasma parameters at 75 Pa, which is more than surprising. Namely, FACS also detected live bacteria on carriers exposed to plasma at 240 s. The number is small - 100 live bacteria on the sample of 1.7×10^8 initial bacteria and 3900 on the sample of 2.25×10^8 initial bacteria, but for the case of *Escherichia coli* no live bacteria was found on samples treated by plasma at the same conditions. This inconvenient effect might be well explained by the clustering of bacteria on the surface of our carriers or as disadvantage of PCT for counting *Staphylococcus aureus* bacteria. One major disadvantage of the viable plate count is the assumption that each colony arises from one cell. Therefore where cells grow together in clusters, a gross underestimation of the true population results. *Staphylococcus* is known to form clusters of microorganisms in solution. Each cluster is therefore counted as one colony. At the same time, to the best of our effort we never found three dimensional clusters of *Staphylococcus aureus* on the prepared carrier surfaces imagined by SEM. Therefore we have only 3 possible explanations for the discrepancy of PCT with FACS results: we failed to count three dimensional clusters on the surface grown with PCT, the FACS does not recognize live *Staphylococcus aureus* correctly, or the bacteria was damaged to such an extent that bacteria was unable to reproduce, yet scored still lived. To the best of our effort we cannot exclude any of the upper options. Happily enough, the PCT experiments confirmed the SEM observations. Since the PCT is a common and most frequently used technique to determine sterility, we do trust its results. And, as we emphasized before, the PCT results are supported with SEM images.

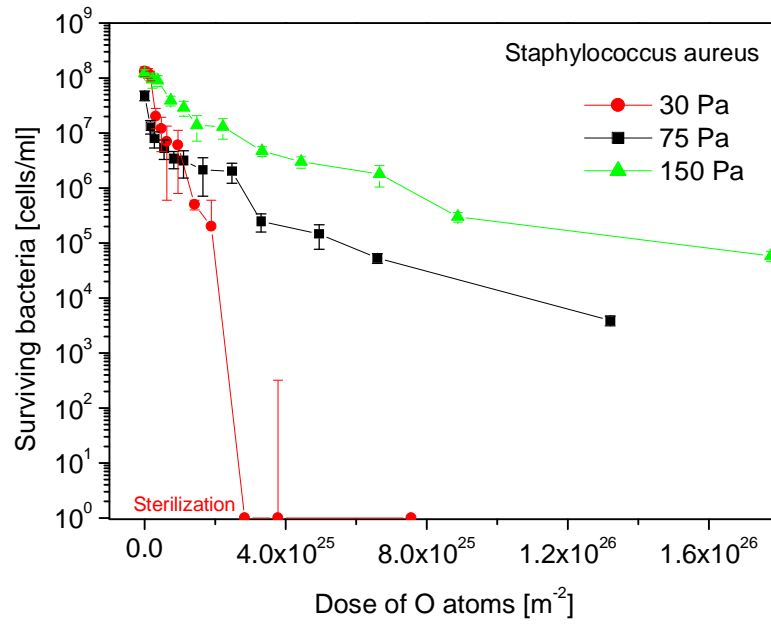


Figure 55: Survival curve of *Staphylococcus aureus* for received dose of O atoms (measured by FACS). The number of surviving bacteria *Staphylococcus aureus* cells in respect to received dose of neutral oxygen atoms at 3 different pressures. The two initial bacterial concentrations used were: 7×10^8 (at 30 Pa, 150 Pa) and 2.55×10^8 cells per carrier (at 75 Pa).

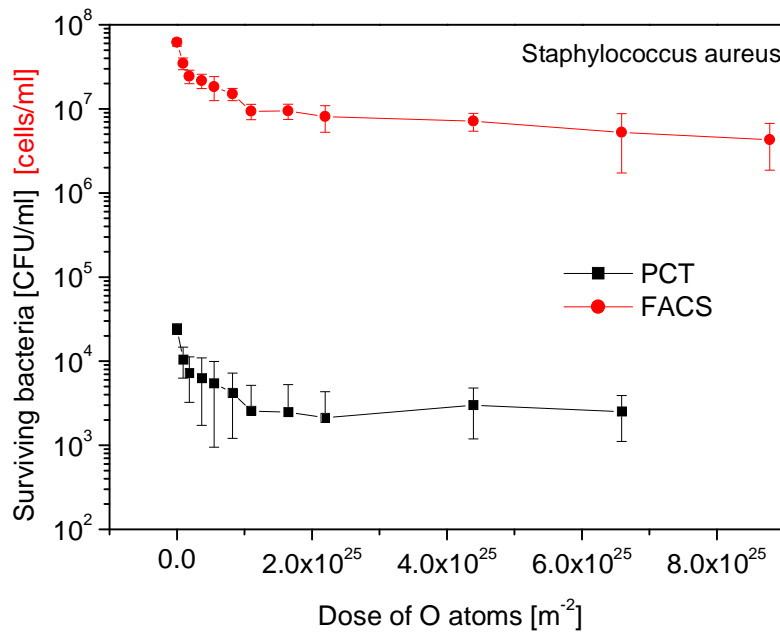


Figure 56: Survival curve of *Staphylococcus aureus* for received dose of O atoms in afterglow. The number of surviving bacteria *Staphylococcus aureus* cells in respect to received dose of neutral oxygen at 75 Pa. The graphs presents PCT and FACS results of inactivation.

Change of plasma parameters revealed a striking result that sterilization efficiency for *Staphylococcus aureus* doesn't depends only on O atoms, but also strongly on the density of charged species in plasma. At lower pressure of 30 Pa with plasma parameters $n_i=3 \times 10^{16} \text{ m}^{-3}$ and $n_o=2 \times 10^{21} \text{ m}^{-3}$, the bacteria on carriers was inactivated very fast and only after the dose of $3\text{-}4 \times 10^{26} \text{ m}^{-2}$ (Figures 54 and 55). This is the lowest dose required to sterilize any treated bacteria in our experiment. Whereas, the treatment with oxygen plasma glow discharge at 75 Pa ($n_i=1 \times 10^{16} \text{ m}^{-3}$ and $n_o=3.5 \times 10^{21} \text{ m}^{-3}$), and 150 Pa ($n_i=3 \times 10^{15} \text{ m}^{-3}$ and $n_o=4.7 \times 10^{21} \text{ m}^{-3}$) are much slower then the one at 30 Pa (Figure 54). All survival curves follow the same almost linear trend with an elbow representing the abrupt of cell wall and fast inactivation. As previously seen

and discussed for *Bacillus stearothermophilus*, the afterglow with predominantly neutral oxygen, inactivates bacteria rather slow (Figure 56). This further confirms our conclusions on the role of charged species, since the discharge with more charged species is more efficient. The destruction mechanism of bacteria is similar to all three cases, since curve trends match.

5.7 Optical emission spectroscopy of plasma inactivation process

All above mentioned techniques are *ex-situ* and time consuming so none are suitable for routine monitoring of the plasma sterilization process. It is practically impossible to apply a technique to determine the sterility *in situ*. Searching for a suitable in-direct method we arrived back to plasma characterization. As described in the beginning of the Discussion Section, the most important parameters of plasma created in inductively coupled discharge are the electron temperature and density, plasma potential, and the density of neutral oxygen atoms. None of this parameters are influenced by the presence of bacteria to a measurable extend.

The interaction between oxygen atoms and bacteria causes oxidation of the organic material and thus the formation of oxidation products such as water, vapour and carbon oxides. Small quantities of these gaseous components can be monitored by mass spectroscopy, light absorption techniques, and emission spectroscopy. Mass spectrometry is difficult if not impossible to apply since modern mass spectrometers should be differentially pumped, and may be destroyed due to the oxidation of the cathode or due to high frequency interferences. Optical absorption techniques are rather complicated and very expensive so the only technique left is optical emission spectrometry (OES). A decade ago, this technique was also expensive and pretty slow, but with recent spectrometers the price has dropped for orders of magnitude and so was the typical characterization time. Modern spectrometers are able to detect the entire spectrum in a fraction of a second. The problem is their offset – they are not suitable for monitoring weak peaks of gaseous impurities. Happily enough we overcame this problem using pretty long acquisition times allowing the main peaks to over-saturate. Using this procedure we developed a unique technique for monitoring the sterilization process using OES. The applicability of our method with *Escherichia coli* is described in the Results Section of this thesis. Let us here briefly discuss the limitations of OES for monitoring sterilization process.

OES can detect traces of excited gaseous molecules if:

- They are good emitters of photons in the range from about 250 to 1100 nm;
- The concentration of the molecules created at oxidation of bacteria is above the background;
- The light emitted by these molecules do not overlap with major peaks;
- The absolute number of photons is high enough to allow for reasonable acquisition time (few seconds at most).

The products of oxidation include H₂O, CO₂, CO and perhaps OH. It also includes small quantities of N, P, Ca, Na, and other microelements. H₂O represents the residual atmosphere in vacuum systems so water molecules are not candidates to monitor sterilization. CO₂ has rich continua and some bands are difficult if not impossible to distinguish from the background. CO is more perspective since it has strong emission bands, and many “lines” within these bands do not overlap with O or O₂ lines and bands. N₂ molecules are also a perspective since they have strong bands in UV; luckily not all of them are entirely overlapping with OH bands. We also tested lines of microelements, but found them undistinguishable from the background.

The evolution chosen “lines” of CO and N₂ bends was measured in order to monitor the evolution of the sterilization process. The experiments for the case of *Escherichia coli* were presented to details in this thesis. The technique is probably pretty useful for monitoring *Staphylococcus aureus* because rapid degradation by plasma was observed. For the case of *Bacillus stearothermophilus* this technique could give nice results for the destruction of bacteria vegetative forms, but not the spores, due to spores being pretty resistant to oxygen radicals. They remain on the surface of our carriers long after all vital bacteria were destroyed. Since the destruction of the spores is slow, the CO and N₂ would be well below the detection limit of OES. OES is thus not suitable for monitoring sterilization if objects are contaminated with spores.

The emission intensity depends on electron temperature and its density. The best results are obtained at low pressure, where we have the maximal T_e and n_i (see above). So in principle, this technique would be useful in plasma reactors operating at a much lower pressure. Unfortunately, as stressed in this thesis, lower pressure also means lower O density and thus longer treatment times.

6 Conclusions

Systematic experiments on the sterilization efficiency of low pressure oxygen plasma were performed. Three different types of microorganisms were used: *Escherichia coli* (gram negative bacteria), *Bacillus stearothermophilus* and *Staphylococcus aureus* (both are gram positive bacteria). The evaluation of plasma effects on microbes was performed using different methods, including Scanning Electron Microscopy (SEM), Fluorescence Microscopy (FM), Plate Count Technique (PCT), and Fluorescence Activated Cell Sorting (FACS). SEM is a standard technique for the visualization of small objects. In our experiments it was only used as an illustration of the bacteria degradation. Namely, SEM is not a technique to monitor the sterilization process and the interpretation of images in sterilization view is heavily arbitrary. As described in the Introduction Section, bacteria have revitalization ability; although they visually look damaged they may revitalize. On the other hand, a well preserved shape of bacteria definitely does not mean the bacteria are live. The standard technique for medical test on bacteria viability is PCT. We used this technique at our experiments and the results were conclusive enough to determine the critical dose of oxygen atoms needed for sterilization. Although the PCT method is regarded quantitative method in order to determine the number of survived bacteria, but doesn't count dead or damaged bacteria. Therefore other methods should be applied. One of them which have been reported to be applied by other authors is FM. The observation of treated samples under a fluorescence microscope allows for the evaluation of the number of dead (stained red with PI) and live (stained with SYTO 9) cells. Considering that counting large numbers of cells is troublesome, dilution steps are usually necessary. However, the FM technique was not accurate enough and appropriate for larger number of plasma treated samples as well as for large concentrations of bacteria used in our experiments. Searching for an alternative method brought us to FACS. To the best of our knowledge, FACS has never been reported to be used for measuring the concentration of dead or live bacteria after plasma treatment. FACS performed extremely well so we can conclude that this is a recommended method for monitoring the sterilization process.

All mentioned techniques are *ex-situ*. For practical application, an *in-situ*, real-time method for monitoring the sterilization progress should be invented. For the first time, we used optical emission spectroscopy (OES) to this end, and the results were sound with the classical *ex-situ* methods. Another important conclusion drawn from our experiments is that OES represents a powerful (if not the only available) method for real-time monitoring of the sterilization process. However, the limitation of the OES method for monitoring sterilization is that it works well just for larger quantities of bacteria larger from 10^6 cells per carrier, and it depends on operating pressure. The method performed better at lower pressures where we got more signal from oxygen plasma.

From the plasma (chemical) point of view, inactivation agents that cause bacterial death or injury were roughly classified as follows:

- heat;
- shear stress and desiccation;
- UV radiation;
- free radicals;
- charging.

Thermal damage is usually not an important mechanism of bacteria injury, considering that most low pressure plasma created with radiofrequency discharge are mostly low temperature plasmas with ambient temperature of molecular gases. However, we showed that the sterilizing material plays an important role and should be taken under consideration when sterilizing bacteria. Namely, neutral atoms interacting with surface can heat different materials at various rates. Therefore, in such cases it is always recommended to control sample heating. Shear stress and desiccation of bacteria mainly due to vacuum can be disregarded; however, it can play an important role when sterilizing the thin cell wall bacteria like gram negative. UV

radiation is normally a very important parameter, but in our case of oxygen plasma at operating pressures between 10 and 200 Pa doesn't play any role and can be disregarded. Short-living free radicals, particularly the reactive oxygen species (O, OH), are considered to be the prime plasma-borne disinfectants. The antimicrobial function of reactive oxygen species including oxygen radicals on living organisms was proven in our experiments. Lethal effects were largely ascribed to chemical erosion (e.g., damage to the cell wall or to the spore coat in case of spore inactivation). Characteristic changes to the cell walls of treated bacteria were shown in the thesis. Interestingly, the best efficiency was achieved in the presence of charged species (e.g. positive ions and electrons) from plasma glow discharge. It looks that charging bacteria plays an important role in the inactivation process of bacteria. The charging effect gives synergetic efficiency with neutral atoms, and can depend on bacteria structure. Since the structure of bacteria differs from type to type, we used two types of bacteria: gram positive and gram negative. However, our systematic work revealed that the plasma sterilization efficiency depends also on another bacteria characteristic – the ability to form spores, as well as the type and density of plasma species used. The results showed significant difference in required doses of radicals for sporulating bacteria and non-sporulating ones; therefore, it is between gram positive and gram negative bacteria. This conclusion obviously has practical consequence.

Yet another conclusion deals with the usefulness of oxygen plasma for sterilization of delicate materials. The results summarized in this thesis clearly show that thermal effects should be taken into account when interpreting the sterilization efficiency. Same bacteria on aluminium substrates are destroyed with much lower doses of plasma radicals than on glass substrates. This conclusion can be generalized: sterilization efficiency depends on the surface properties of substrates, the most important one being the coefficient for heterogeneous surface recombination of neutral oxygen atoms. Our calculations showed that materials with a very low recombination coefficient need a rather high dose to be sterilized, but on the other hand they do not heat appreciably during plasma treatment. This effect is extremely important in the case of sterilizing the delicate biocompatible materials that do not stand heating to moderate temperatures. The conclusion drawn from our experiments show that such materials (especially if the recombination coefficient is above, say 0.005) should be either actively cooled or treated in plasma pulses. The required time between subsequent plasma pulses should be high enough to allow for material to cool down to the initial (usually room) temperature. The results summarized in this thesis allow for calculation of the recommended pulse duration if plasma parameters and the recombination coefficient are known. To the best of our knowledge, such critical approach to plasma sterilization has not been reported so far.

It was found and confirmed that plasma parameters with different densities of plasma species actively influence the sterilization efficiency of different types of bacteria. This has been mostly disregarded by many authors, which normally report only on discharge parameters versus treatment time. Generally, inactivation time depends on the bacteria density per carrier and its vegetative/spore form, what we also shown in this thesis. However, the sterilization efficiency for bacteria depends primarily on the dose of neutral O atoms to the surface as well as on the influx of charged species (positive O ions). In the case of *Staphylococcus aureus* the efficiency of process was achieved when we had a higher density of ions ($n_i=3\times 10^{16}\text{m}^{-3}$) and moderate density of neutral atoms ($n_o=2\times 10^{21}\text{m}^{-3}$). Whereas for *Bacillus stearothermophilus*, the best efficiency was achieved by the balanced flux of positive ions and atoms to the surface at densities of $n_i=1\times 10^{16}\text{m}^{-3}$ and $n_o=3.5\times 10^{21}\text{m}^{-3}$. Therefore, the density of different plasma species and their influx to the surface gives different sterilization efficiencies depending on bacteria and their form. Moreover, charging bacteria from plasma glow, predominately by ions, accelerates the inactivation process. Although the main reason for the destruction of the cell wall is still chemical etching by reactive neutrals, atom by atom, until envelope is eroded and followed by fast death. This upgrades the inactivation model presented by Moisan (Moisan et al., 2001), and proves the thesis of Laroussi and Mendis that charged particles play an important role in the plasma sterilization of bacteria. Therefore we have proven our hypothesis.

7 Acknowledgements

Many people have helped me in the course of my research and I would like to acknowledge their help and support.

First of all, I wish to thank my supervisor Prof. Dr. Miran Mozetič for introducing me to the new plasma technology and for his valuable guidance, constructive comments, and support throughout this work.

I want to express my special gratitude towards co-advisor A/Prof. Dr. Uroš Cvelbar for helping me out in all aspects during my work. He has been actively interested in my work and has always been available to advise me. I warmly thank Dr. Cvelbar for his valuable advices, patience and friendly help.

I also wish to express gratitude to Ad Futura - Science and Education Foundation of the Republic of Slovenia, Public Fund, for providing the financial support of this work through program "Scholarships for Doctoral Studies of Foreign Citizens in Slovenia in academic year 2005/2006".

I would like to thank the members of the Evaluation Board, A/Prof. Dr. Aleš Podgornik, A/Prof. Dr. Janez Kovač and Prof. Dr. Cristina Canal for their valuable and useful comments, criticisms and suggestions.

Many thanks go to the group at the Department for Surface Engineering F4, Jožef Stefan Institute: Tatjana, Janez, Ita, Sašo, Tjaša and Kristina for providing a great work environment and helping me with my experiments. Especially, I want to express my sincere thanks to Ruža Bolte for logistic support; her assistance was more than precious. I am very grateful for their hospitality.

My special thanks Dr. Urška Repnik from Department of Biochemistry, Molecular and Structural Biology, Jožef Stefan Institute, for performing FACS analyses. Her assistance and valuable suggestions have been very helpful for this study.

Thanks to Dr. Tina Zavašnik from Department of Biochemistry, Molecular and Structural Biology, Jožef Stefan Institute for the help in carrying out of fluorescence microscopy.

I express thanks Dr. Marta Klanjšek-Gunde and her assistant Nina Hauptman as well as Dr. Marjan Bele from National Chemistry Institute, for arranging and conducting the examination with scanning electron microscope.

Also, thanks to Dr. Slobodan Milošević and his assistant Nikša Krstulović from Institute of Physics in Zagreb, for optical emission spectroscopy measurements and relevant discussions.

I am very grateful to all my colleagues and friends from the Center for Medical Microbiology at the Institute of Public Health, Montenegro, for their friendships and encouragements. At the same time I want to thank the Director of Institute of Public Health Dr. Boban Mugoša, for his understanding and unconditional support.

Lastly, I would like to thank my family and my friends for all their love, faith and encouragement.

8 References

- American Medical Association. Report of the Council on Pharmacy and chemistry: use of the terms “sterile,” “sterilize”, and “sterilization.” *JAMA* **107**, 381936, (1999).
- ANSI/AAMI/ISO 11737-1-1995. Sterilization of medical devices-microbiological methods, Part 1: estimation of population microorganisms on product. 1-16 (AAMI, Arlington, VA, 1995).
- Ashman, L. E.; Menashi, W. P. Treatment of surfaces with low pressure plasmas. *US Patent* 3 701, 628, (1972).
- Bayat, O., Arslan, V., Bayat, B., Poole, C., Application of a flocculation-ultrafiltration process for bacteria removal from industrial plant process water. *Biochem. Eng. J.* **18** (2), 105 (2004).
- Bell, A.T. Techniques and applications of plasma chemistry. In: Hollahan, J. R.; Bell, A. T. (ed.) *Fundamentals of plasma chemistry*. 1-56 (Wiley-Interscience, New York, 1974).
- Berkut, V. D.; Kovtun, V. V; Kudryavtsev, N. N.; Novikov, S. S.; Sharovатов, A. I.; Determination of the time-resolved probabilities of heterogeneous recombination of atoms in shock-tube experiments. *Int Comm Heat Mass Transfer.* **12**, 567 (1985).
- Bithell, R. M. Package and sterilizing process for same. *US Patent* 4 321, 232 (1982).
- Block, S.S. Sterilization. In: (ed.) *Encyclopedia of Microbiology*. 87-103 (Academic Press, New York, 1992).
- Block, S. S. Definition of Terms. In: Block, S. S. (ed.) *Disinfection, Sterilization, and Preservation*. 19-28 (Lippincott Williams & Wilkins, Philadelphia, 2001).
- Bol'shakov, A. A., Cruden, B. A.; Mogul, M. V. V. et al. *AIAA J.* **42**, 823 (2004).
- Boucher, R. M. Seeded gas plasma sterilization method. *US Patent* 4 207, 286 (1980).
- Boulos, L.; Prevost, M.; Barbeau, B.; Coallier, J. LIVE/DEAD® BacLight™: application of a new rapid staining method for direct enumeration of viable and total bacteria in drinking water. *J. Microbiol. Meth.* **37**, 77-86 (1999).
- Boyd, T. J. M.; Sanderson, J. J. *The physics of plasmas*. (Cambridge University press, Cambridge, 2003).
- Breeuwer, P.; Abee, T. Assessment of viability of microorganisms employing fluorescence techniques. *Int J. Food Microbiol.* **55**, 193-200 (2000).

- Bruch, C. W.; Bruch, M. K. Sterilization. In: Martin, E. W. (ed.) *Husa's pharmaceutical dispensing*. 592-693 (Mack Publishing, Easton, PA, 1971).
- Burgess, D. J.; Reich, R. R. Industrial ethylene oxide sterilization. In: *Sterilization Technology: A practical Guide for manufactures and users of health care products*. 152-195 (Morrisey, New York, 1993).
- Campanhã, M. T. N., Mamizuka, E. M., Carmona-Ribeiro, A. M., Interactions between cationic liposomes and bacteria: The physicalchemistry of the bactericidal action. *J. Lipid Res.*, 40 (8), 1495 (1999).
- Canal, C.; Gaboriau, F.; Ricard, A.; Mozetič, M.; Cvelbar, U.; Drenik, A. Density of O-atoms in an afterglow reactor during treatment of wool. *Plasma Chem. Plasma Process* **27**, 404-413 (2007).
- Canal, C.; Gaboriau, F., Villeger, S.; Cvelbar, U.; Ricard, A. Studies on antibacterial dressings obtained by fluorinated post-discharge plasma. *Int. J. Pharm.* **367**, 155-161 (2009).
- Carpenter, P. L. *Microbiology* (W. B. Saunders Co., Philadelphia, PA, 1972).
- Cartry, G. et al. Atomic oxygen recombination on fused silica: modelling and comparison to low-temperature experiments (300 K)*. *J. Phys. D: Appl. Phys.* **33**, 1303-1314 (2000).
- Cartry, G. et al. Atomic oxygen surface loss probability on silica in microwave plasmas studied by a pulsed induced fluorescence technique. *Plasma Sources Sci. Technol.* **15**, 79-488 (2006).
- Colins C. H.; Lyne P.M.; Grange, J. M. *Microbiological methods* (Butterworths, London, 1995).
- Cvelbar, U.; Mozetič, M.; Klanjšek Gunde, M. Selective oxygen plasma etching of coatings. *IEEE Trans. Plasma Sci.* **33**, 236-237 (2005).
- Cvelbar, U.; Mozetič, M.; Ricard, A. Characterization of oxygen plasma with a fiber optic catalytic probe and determination of recombination coefficients. *IEEE Trans. Plasma Sci.* **33**, 834-837 (2005).
- Cvelbar, U.; Vujošević, D.; Vratnica, Z.; Mozetič, M. The influence of substrate material on bacteria sterilization in an oxygen plasma glow discharge. *J. Phys. D: Appl. Phys.* **39**, 3487-3493 (2006).
- Cvelbar, U.; Mozetič, M.; Babič, D.; Poberaj, I.; Ricard, A. Influence of effective pumping speed on oxygen atom density in a plasma post-glow reactor. *Vacuum* **80**, 904-907 (2006).
- Cvelbar, U.; Krstulović, N.; Milošević, S.; Mozetič, M. Inductivity coupled RF oxygen plasma characterization by optical emission spectroscopy. *Vacuum* **82**, 224-227 (2007).
- Cvelbar, U.; Ostrikov, K.; Drenik, A.; Mozetič, M. Nanowire sensor response to reactive gas environment. *Appl. Phys. Lett.* **92**, 133505-1-133505-3 (2008).
- Dean, J. R. *Practical Inductively Coupled Spectroscopy* (Willey, West Sussex, England, 2007).
- Dorman, V. Sterilization processes and residuals. In: Braybrock, H. (ed.) *Biocompatibility Assessment of Medical Devices and Materials*. 101-118 (Wiley, Chichester, 1997).

- Drenik, A.; Cvelbar, U.; Vesel, A.; Mozetič, M. Weakly ionized oxygen plasma. *Info. Midem* **35**, 85-91 (2005).
- Drenik, A.; Cvebar, U.; Vesel, A.; Mozetič, M.; Vratnica, Z.; Vujošević, D. Meritve gostote atomov v šibkoionizirani kisikovi plazmi vzdolž zaprte cevi. *Vakuumist* **25**, 16-19 (2005).
- Drenik, A.; Cvelbar, U.; Vesel, A.; Mozetič, M. Detection of atoms in weakly ionised oxygen plasma along a closed tube. *Strojarstvo* **48**, 17-22 (2006).
- Duan, Y.; Huang, C.; Yu, Q. S. Low-temperature direct current glow discharges at atmospheric pressure. *IEEE Trans. Plasma Sci.* **33**, 328-329 (2005).
- Ehrenberg, L.; Hiesche, K. D.; Osterman, S.; Wenneberg, I. Evaluation of genetic risks of alkylating agents. *Mutat Res.* **24**, 83-103 (1974).
- Ernest, A. Why hospitals are adopting new sterilization technologies? *Adv. Steriliz.* **1**, 1-3 (1995).
- Favero, M. S. Patient infections: the relevance of sterility assurance levels. In: *Sterilization of medical products*. 156-163 (Polyscience Publications, Morin Heights, Canada, 1993).
- Favero, M. S. Developing indicators for sterilization. In: Rutala, W. (ed.) *Disinfection, sterilization and antisepsis in health care*. 119-132. (Association for Professionals in Infection Control and Epidemiology, Washington, DC, 1998).
- Favero, M. S.; Bond, W. W. Chemical Disinfection of Medical and Surgical Materials. In: Block, S. S. (ed.) *Disinfection, Sterilization, and Preservation*. 881-896 (Lippincott Williams & Wilkins, Philadelphia, 2001).
- Fraser, S. J.; Gillette, R. B.; Olson, R. L. Sterilizing process and apparatus utilizing gas plasma. *U. S. Patent* 948, 601 (1976).
- Goldman, M.; Priutt, L. Comparison of the effects of the gamma radiation and low temperature hydrogen peroxide gas plasma sterilization on the molecular structure, fatigue resistance, and wear behaviour of UHMWPE. *J. Biomed. Mat. Res.* **40**, 378-384 (1998).
- Goodhew, P. J. et al. *Electron Microscopy and Analyses* (Taylor and Francis, London, 2001).
- Goldstein, J. et al. *Scanning Electron Microscopy and X-Ray Microanalysis* (Springer, New York, 2003).
- Gombotz, W. R.; Hoffman, A. S. Gas-discharge techniques for biomaterial modification. *CRC Crit. Rev. Biocompat.* **4**, 1-42 (1987).
- Grill, A. (ed.) *Cold plasma in material fabrication: from fundamentals to applications*. 24-45 (IEEE, New York, 1994).
- Hacker, D. S.; Marshall, S. A.; Steinberg, M. Recombination of Atomic Oxygen on Surfaces. *J. Chem. Phys.* **35**, 1788 (1961).

- Haugland, R. P. *Handbook of Fluorescent Probes and Research Products* (Molecular Probes, Inc., Oregon, Eugene, 2002).
- Hury, S.; Vidal, D. R.; Desor, J.; Lagarde, T. A parametric study of the destruction efficiency of *Bacillus* spores in low pressure oxygen-based plasmas. *Lett. Appl. Microbiol.* **26**, 417-421 (1998).
- Helhel, S.; Oksuz, L.; Yousefi, A. R. Silicone catheter sterilization by microwave plasma; argon and nitrogen discharge. *Int. J. Inf. Milli.* **26**, 1613-1625 (2005).
- Herman, B. *Fluorescence Microscopy* (Springer, 1998).
- Herrmann, W.; Henins, I.; Park, I.; Selwyn, G. S. Decontamination of chemical and biological warfare (CBW) agents using an atmospheric pressure plasma jet (APPJ). *Phys. Plasmas* **6**, 2284-2289 (1999).
- Herrmann, H. W.; Henins, I.; Park, J. et al. Decontamination of chemical and biological warfare (CBW) agents using an atmospheric pressure plasma jet. *Phys. Plasmas* **6**, 2284-2289 (1999).
- Hippler, R.; Pfau, S.; Schmidt, M. *Low temperature plasma physics: fundamental aspects and applications*. (Wiley VCH, Berlin, 2001).
- Holyoak, G. R.; Wang, S.; Liu, Y.; Bunch, T. D. Toxic effects of ethylene oxide residues on bovine embryos in vitro. *Toxicology* **108**, 33-38 (1996).
- Isenberg, G. E. (ed.) *Clinical Microbiology Procedures Handbook* (American Society for microbiology, Washington, 1992).
- Jacobs, P.T.; Lin, S. M. Sterilization process utilizing low-temperature plasma. In: Block, S. S. (ed.) *Disinfection, Sterilization, and Preservation*. 747-763 (Lippincott Williams & Wilkins, Philadelphia, 2001).
- Kaiser, G. E. *Microbiology Laboratory Manual*.
<http://student.ccbcmd.edu/courses/bio141/labmanua/lab4/index.html> (July, 2005)
- Kanazawa, S.; Kogoma, M.; Moriwaki, S. et al. Glow plasma treatment at atmospheric pressure for surface modification and film depositon. *Nucl. Instr. & Meth.* **37-38**, 842-845 (1989).
- Klanjšek Gunde, M.; Kunaver, M.; Cvelbar, U.; Barle, N. Oxygen plasma etching of a two-component clear coating. *Vacuum* **80**, 189-192 (2005).
- Knomich, V.A.; Soloshenko, I. A.; Tsiolko, V. V.; Mikhno, I. L. Cold sterilization of medical devices and materials by plasma DC glow discharge. In: *Proceedings of the 12th International Conference on Gas Discharge and their Applications*. 740-744 (Greifswald, 1997).
- Knomich, V. A.; Soloshenko, I. A. Tsiolko, V. V.; Mikhno, I. L. Investigation of principal factors of the sterilization by plasma DC glow discharge. In: *Proceedings of the Int. Conf. on Plasma Physics*. 2745-2748 (Prague, 1998).
- Krebs, M. C.; Becasse, P. et al. Gas plasma sterilization: relative efficacy of the hydrogen peroxide phase compared with that of plasma phase. *Int. J. Pharm.* **160**, 75-81 (1998);.

- Krstulović, N.; Labazan, I.; Milošević, S.; Cvelbar, U.; Vesel, A.; Mozetič, M. Optical emission spectra of RF oxygen plasma. *Mater. tehnol.* **38**, 51-54 (2004).
- Krstulović, N.; Labazan, I.; Milošević, S.; Cvelbar, U.; Vesel, A.; Mozetič, M. Optical emission spectroscopy characterization of oxygen plasma during treatment of a PET foil. *J. Phys. D Appl. Phys.* **39**, 3799-3804 (2006).
- Kunhardt, E. E. Generation of large-volume, atmospheric-pressure, nonequilibrium plasmas. *IEEE Trans. Plasma Sci.* **28**, 189 (2000).
- Kuzmichev, A.I.; Soloshenko, I. A.; Tsiolko, V. V. Feature of sterilization by different type of atmospheric pressure discharge. In: *Proc. Int. Symp. High Pressure Low temperature Plasma Chemistry*. 402-406 (Greifswald, Germany, 2001).
- Kylian, O.; Rossi, F.; Sterilization and decontamination of medical instruments by low-pressure plasma discharges: application of Ar/O₂/N₂ ternary mixture. *J. Phys. D: Appl. Phys.* **48** (8), 085207 (2009)
- Laroussi, M. Nonthermal decontamination of biological media by atmospheric-pressure plasmas: review, analysis, and prospects. *IEEE Trans. Plasma Sci.* **30**, 1409-1415 (2002).
- Laroussi, M.; Mendis, D. A., Rosenberg, M., Plasma interaction with microbes. *New J. Phys.* **5**, 41.1-41.10 (2003).
- Laroussi, M.; Leipold, F. Evaluation of the roles of reactive species, heat, and UV radiation in the inactivation of bacterial cells by air plasmas at atmospheric pressure. *Int. J. Mass Spectrom.*, **233**, 81-86 (2004).
- Laroussi, M. Low temperature plasma-based sterilization: overview and state-of-the-art. *Plasmas Polym.* **2**, 391-400 (2005).
- Lawrence, C. A. Definition of terms. In: Lawrence C. A.; Block, S. S. (ed.) *Disinfection, sterilization and preservation*. 10-11 (Lea & Febiger, Philadelphia, 1968).
- Lerouge, S.; Wertheimer, M. R.; Marchand, R.; Tabrizian, M.; Yahia, L. H. Effect of gas composition on spore mortality during low-pressure plasma sterilization. *J. Biomed. Res.* **51**, 128-135 (2000).
- Lerouge, S., Fozza, A. C.; Wertheimer, M. R.; Marchand, R.; Yahia, L. H. Sterilization by low-pressure plasma: the role of vacuum-ultraviolet radiation. *Plasmas Polym.* **5**, 31-46 (2000).
- Lerouge, S.; Wertheimer, M. R.; Yahia, L. H. Plasma sterilization: a review of parameters, mechanisms, and limitations. *Plasmas Polym.* **6**, 175-188 (2001).
- Legrand, J. C.; Damiy, A. M. Atomic oxygen titration in a dioxygen microwave plasma. Part 1: recombination on silica walls. *New J. Chem.* **21**, 177-185 (1997).
- Lisovsky, V.A.; Yakovin, S. D.; Yegorenkov, V. D.; Terent'eva, A. G. Plasma sterilization in low-pressure RF discharges. *Probl. Atomic Sci. Technol.* **1**, 77-81 (2000).
- Macey, M. G. *Flow Cytometry: Clinical Applications* (Blackwell Scientific Publications, Oxford 1994).

- Mahon, C. R.; Manuselis, G. *Textbook of Diagnostic Microbiology* (W. B. Saunders Company, 2000).
- Menashi, W. P. Treatment of surfaces. *US Patent 3 383, 163* (1968).
- Mendis, D. A.; Rosenberg, M.; Azam, F. A note on the possible electrostatic disruption of bacteria. *IEEE Trans. Plasma Sci.* **28**, 1304-1306 (2000).
- MJCR/MBMB 403: Medical Microbiology. <http://www.cehs.siu.edu/fix/medmicro/genmicr.htm> (accessed June, 2008).
- Moisan, M.; Barbeau, J. et al. Low temperature sterilization using gas plasmas: a review of the experiment and an analysis of the inactivation mechanisms. *Int. J. Pharmacy* **226**, 1-21 (2001).
- Moisan, M.; Barbeau, J.; Crevier, M. C. et al. Plasma sterilization. Methods and mechanisms. *Pure Appl. Chem.* **74**, 349-358 (2002).
- Molecular Expressions Cell Biology and Microscopy.
<http://www.micro.magnet.fsu.edu/cells/bacteriacell.html> (accessed July, 2008).
- Monna, V.; Nguyen, C.; Kahil, M.; Ricard, A.; Sixou, M. Sterilization of dental bacteria in a flowing post-discharge reactor. *Du Vide.* **57**, 112 (2002).
- Montie, T. C.; Kelly-Wintenberg, K.; Roth, J. R. An overview of research using the one atmosphere uniform glow discharge plasma (OAUGDP) for sterilization of surfaces and materials. *IEEE Trans. Plasma Sci.* **28**, 41-55 (2000).
- Moreau, S.; Moisan, M.; Tabrizian, M. et al. Using the flowing afterglow of a plasma to inactivate *Bacillus subtilis* spores: influence of the operating conditions. *J. Appl. Phys.* **88**, 1166-1174 (2000).
- Morgan, J. E.; Ellias, L.; Schiff, H. I. Recombination of Oxygen Atoms in the Absence of O₂. *J. Chem. Phys.* **33**, 930 (1960).
- Mozetič, M. *Karakterizacija nizekpotlačne plazme z Langmuirjevimi sondami*. Magistrsko delo. (Tehniška fakulteta VTO Elektrotehnika, Maribor, 1992)
- Mozetič, M.; Ricard, A.; Babič, D.; Poberaj, I.; Levaton, J.; Monna, V.; Cvelbar, U. Comparison of NO titration and fiber optics catalytic probes for determination of neutral oxygen atom concentration in plasmas and postglows. *J. Vac. Sci. Technol., A, Vac. surf. Films* **21**, 369-374 (2003).
- Mozetič, M. *Thermodynamic gas phase* (DVTS, Ljubljana, 2003).
- Mozetič, M.; Zalar, A.; Cvelbar, U.; Babič, D. AES characterization of thin oxide films growing on Al foil during oxygen plasma treatment. *Surf. Interface Anal.* **36**, 986-988 (2004).
- Mozetič, M.; Cvelbar, U.; Vesel, A.; Ricard, A.; Babič, D.; Poberaj, I. A diagnostic method for real-time measurements of the density of nitrogen atoms in the postglow of an Ar-N₂ discharge using a catalytic probe. *J. Appl. Phys.* **97**, 103308-1-103308-7 (2005).

- Mozetič, M.; Vesel, A. Cvelbar, U.; Ricard, A. An iron catalytic probe for determination of the O-atom density in an Ar/O₂ afterglow. *Plasma Chem. Plasma Proc.* **26**,103-117 (2006).
- Molecular Probes Europe. LIVE/DEAD BacLight™ bacterial viability kit, product information sheet. (Molecular Probes Europe, Leiden, The Netherlands, 1996)
- Murphy, D. B. *Fundamentals of Light Microscopy and Electronic imaging* (Wiley-Liss, New York, 2001).
- Murray P. R. et al. *Manual of Clinical Microbiology* (American Society for Microbiology, Washinton, DC, 1999).
- Ormerod, M. G. *Flow Cytometry: A Practical Approach* (Oxford University Press, 2000).
- Paustian, T.; Roberts, G. *Through the Microscope* (Textbook Consortia, 2008).
- Philip, N.; Saoudi, B. et al. The respective role od UV photons and oxygen atoms in plasma sterilization at reduced gas pressure. The case of N-2-O-2 mixtures. *IEEE Trans. Plasma Sci.* **30**, 1429-1436 (2002).
- Rahman, M. *Introduction to Flow Cytometry* (Serotec, Kidlington, UK, 2005).
- Ratner, B.D.; Chilkoti, A.; Lopez, G. P. *Plasma Deposition, Treatment, and Etching of Polymers.* (Academic press, Boston, MA, 1990).
- Ricard, A. *Reactive plasmas.* (Societe Francaise du Vide, Paris, 1996).
- Ricard, A.; Jaoul, C.; Gaboriau, F.; Gherardi, N.; Villegier, S. Production of N, H, O, and C atoms in flowing microwave discharges. *Surf. Coat. Techno.* **188-189**, 287 (2004).
- Richardson, J. P.; Dyer, F. F.; Dobbs, F. C.; Alexeff, I.; Laroussi, M. On the use the resistive barrier discharge to kill bacteria: Recent results. *Proc. IEEE Int Conf. Plasma Science* **109**, (2000).
- Rutala, W. A.; Gergen, M. F.; Weber, D. J. Comparative evaluation of sporicidal activity of new low-temperature sterilization technologies; ethylene oxide, 2 plasma sterilization systems, and liquid peracetic acid. *Am. J. Infect. Control.*, **26**, 393-398 (1998).
- Rutala, W. A.; Webster; D. J. Infection control: the role of disinfection and sterilization. *J. Hosp. Infect.* **43**, S43-S55 (1999).
- Sampson, A. R. *Scanning Electron Microscopy* (Advanced Research Systems, 1996).
- Samuel, A. H.; Matthews, I. P. Microwave description: a combined sterilizer/aerator for the accelerated elimination of ethylene oxide residues from sterilized supplies. *Med. Instrum.* **22**, 39-44 (1998).
- Sharma, S. P.; Cruden, B.A.; Bolshakov, A. A. Analysis of emission data from O₂ plasmas used for microbe sterilization. *J. Appl. Phys.* **95**, 3324-3333 (2004).
- Seballos, R. J.; Walsh, A. L.; Mehta, A. C. Clinical evaluation of liquid chemical sterilization system for the flexible bronchoscope. *J Broncol.* **2**, 192-199 (1995).

- Shapiro, H. M. *Practical Flow Cytometry* (Wiley-Liss, Inc., New York, 2003).
- Shibata, M.; Nakano, N.; Makabe, T. Effect of O₂(a¹Δg) on plasma structures in oxygen radio frequency discharges. *J. Appl. Phys.* **80**, 6142 (1996).
- Shintani, H. The relative safety of gamma-ray. *Biomed. Instrum. Technol.* **29**, 513-519 (1995).
- Soloshenko, I. O.; Khomich, V. A.; Tsiolko, V. V.; Mikhno, I. L.; Shchedrin, A. I.; Ryabtsev, A. V. et al. Experimental and theoretical investigation of cold sterilization of medical instruments by plasma DC glow discharge. In: *Proceedings of the 14th Int. Sym. on Plasma Chemistry*. 2551 (Prague, 1999).
- Soloshenko, I. A., Tsiolko, V.; Khomich, V. A. et al. Sterilization of medical products in low-pressure glow discharges. *Plasma Phys. Rep.* **26**, 792-800 (2000).
- Schutze, A.; Jeong, J.Y.; Babayan, S.E.; Jaeyoung Park; Selwyn, G.S.; Hicks, R.F.; The atmospheric-pressure plasma jet: a review and comparison to other plasma sources. *IEEE Trans. Plasma Sci.* **26**, 1685 (1998).
- Stapelmann, K.; Kylian, O.; Denis, B.; Rossi, F.; On the application of inductively coupled plasma sustained in Ar/O₂/N₂ ternary mixtures for sterilization and decontamination of medical instruments. *J. Phys. D: Appl. Phys.* **41** (19), 192005 (2008).
- Stark, R. H.; Schoenbach, K. H. Direct current glow discharges in atmospheric air. *Appl. Phys. Lett.* **85**, 3770-3772 (1999).
- Stoffels, E., Sakiyama, Y., Graves, D.B., Cold atmospheric plasma: charged species and their interactions with cells and tissues. *IEEE Trans. Plasma Sci.* **36**, 1441 (2008).
- Swift, J. D.; Schwar, M. J. R. *Electrical probes for plasma diagnostics* (Iliffe Books Co., London 1969).
- Šorli, I.; Petasch, W.; Kegel, B. Plasma processes: Part I: Plasma basics, plasma generation. *Info. Midem* **26**, 35-45 (1996).
- Šorli, I.; Ročak, R. Determination of atomic oxygen density with a nickel catalytic probe *J. Vac. Sci. Technol.* **18**, 338-342 (March 2000).
- Taylor, L. A.; Barbeito, M. S.; Gremillion, G. G. Paraformaldehyde for surface sterilization and decontamination. *Appl. Microbiol.* **17**, 614-618 (1969).
- Veal, D. A. D.; Deere, B. et al. Fluorescence staining and flow cytometry for monitoring microbial cells. *J. Immunol. Methods* **243**, 191-200 (2000).
- Vickery, K.; Deva, A. K.; Zou, J. et al. Inactivation of duck hepatitis B virus by a hydrogen peroxide gas plasma sterilization system: laboratory 'in use' testing. *J. Hosp. Infect.* **41**, 317-322 (1999).
- Villeger, S.; Ricard, A.; Sixou, M. Sterilization of dental bacteria in N₂-O₂ microwaves post discharge, at low pressure influence of temperature. *Eur. Phys. J. – Appl. Phys.* **26**, 203-208 (2004).

- Villeger, S.; Sarrete, J. P.; Ricard, A. Synergy between N and O atom action and substrate surface temperature in sterilization process using flowing N-2-O-2 microwave post discharge. *Plasma Proces. Polym.* **2**, 709-714 (2005).
- Vratnica, Z.; Vujošević, D.; Bele, M.; Drenik, A.; Vesel, A.; Cvelbar, U.; Mozetič, M. Preiskave bakterij s sodobnim vrstičnim elektronskim mikroskopom. *Vakuumist* **25**, 20-23 (2005).
- Vratnica, Z.; Vujošević, Danijela, Cvelbar, U.; Mozetič, M. Degradation of bacteria by weakly ionized highly dissociated radio-frequency oxygen plasma. *IEEE Trans. Plasma Sci.* **36**, 1300-1301 (2008).
- Vujošević, D.; Vratnica, Z.; Bujko, M.; Cvelbar, U.; Mozetič, M. Sterilizacija plazmom - tehnologija budućnosti ili alternativa klasičnom postupku. *Med. zap.* **59**, 5-10 (2004).
- Vujošević, D.; Vratnica, Z.; Vesel, A.; Cvelbar, U.; Mozetič, M.; Drenik, A.; Mozetič, T.; Kljanšek Gunde, M.; Hauptman, N. Oxygen plasma sterilization of bacteria. *Mater. tehnol.* **40**, 227-232 (2006).
- Vujošević, D.; Mozetič, M.; Cvelbar, U.; Krestulović, N.; Milošević, S. Optical emission spectroscopy characterization of oxygen plasma during degradation of Escherichia coli. *J. Appl. Phys.* **101**, 103305-1-103305-7 (2007).
- Wertheimer, M. R.; Moisan, M. Comparison of microwave and lower frequency plasmas for thin film deposition and etching. *J. Vac. Sci. Technol.* **3**, 236-242 (1985).
- Wickramanayaka, S.; Hosokawa, N.; Hatanaka, Y. Variation of the Recombination Coefficient of Atomic Oxygen on Pyrex Glass with Applied RF Power. *Jpn. J. Appl. Phys.* **30**, 2897-2900 (1991).
- Wickramanayaka, S.; Meikle, S.; Kobayashi, T. Measurements of catalytic efficiency of surfaces for the removal of atomic oxygen using NO₂ continuum. *J. Vac. Sci. Technol.* **9**, 2999-3002 (1991).
- Xu, L.; Nonaka, H.; Zhou, H. Y. Et al. Characteristic of surface-wave plasma wit air-simulated N-2-O2 gas mixture for low-temparature sterilization. *J. Phys. D-Appl. Phys.* **40**, 803-808 (2007).
- Yamamoto, M.; Nishioka, M.; and Sadaka, M. Sterilization using a corona discharge with H₂O₂ droplets and examination of effective species. In: *Proc. 15th Int. Symp. Plasma Chemistry*. 743-751 (Orleans, France, 2001).

Index of Figures

Figure 1: <i>Spectrum of inactivation kinetic rates</i> . Comparative resistance of bacterial spores used as biological indicators and the naturally occurring bioburden exposed to a sterilization process (Favero, 1998).....	1
Figure 2: <i>Sterility assurance levels</i> . Determination of a sterility assurance level by using a specific biological indicator and constructing an inactivation curve (Favero, 1993).....	2
Figure 3: <i>Basic bacterial cell structure</i> . (http://www.micro.magnet.fsu.edu/cells/bacteriacell.html)	10
Figure 4: <i>Cell wall structure</i> . Gram positive and gram negative (bacteria) cell wall structure. (http://www.cehs.siu.edu/fix/medmicro/genmicr.htm)	11
Figure 5: <i>Schematic of the experimental system</i> . 1 - rotary pump, 2 - valve, 3 – trap with molecular sieves, 4 – air valve, 5 - vacuum gauge, 6 – optical emission spectroscopy / IR temperature measurements, 7 - catalytic probe, 8 – Langmuir probe, 9 - discharge chamber with RF coil, 10 - leak valves, 11 - oxygen flask.....	17
Figure 6: <i>Schematic of plasma reactors</i> . The schematic of plasma reactor vessels: a) glow setup and b) afterglow setup.	18
Figure 7: <i>Plasma density</i> . Plasma density or density of charged species versus pressure in the pressure range from 1 Pa to 200 Pa. (Mozetič, 1992; Vujošević et al. 2006)	19
Figure 8: <i>Density of neutral O atoms</i> . Density of neutral O atoms measured with FOCP vs. pressure in the range from 10 Pa to 160 Pa.....	19
Figure 9: <i>FACS results with gating protocol</i> . The presented FACS images show the gating process protocol for measured stained live (Syto 9) and dead (PI) bacteria with counted beads as well as the joint result.	24
Figure 10: <i>Substrate heating in plasma</i> . The temperature of Al substrate (upper curve) and the glass substrate (lower curve) in continuum mode exposed to oxygen plasma glow discharge.....	26
Figure 11: <i>Survival curve of Escherichia coli by PCT</i> . The graph represents CFUs of <i>Escherichia coli</i> vs. treatment time by oxygen plasma glow discharge at pressure of 75 Pa. The concentration of bacteria cells on glass substrate was 16×10^7	27
Figure 12: <i>Survival curves of Escherichia coli by PCT</i> . The graph represents CFUs of <i>Escherichia coli</i> vs. treatment time by oxygen plasma glow discharge at pressure of 75 Pa. The concentrations of bacteria cells on glass substrate were 16×10^7 and 8×10^7	28
Figure 13: <i>Survival curve of Bacillus stearothermophilus by PCT</i> . The graph represents CFUs of <i>Bacillus stearothermophilus</i> vs. treatment time by oxygen plasma glow discharge at pressure of 75 Pa. The concentration of bacteria cells on glass substrate was 1.8×10^7	29
Figure 14: <i>Survival curves of Bacillus stearothermophilus by PCT</i> . The graph represents CFUs of <i>Bacillus stearothermophilus</i> vs. treatment time by oxygen plasma glow discharge at pressure of 30 Pa and pressure of 150 Pa. The concentration of bacteria cells on glass substrate was 1×10^7	29
Figure 15: <i>Survival curve of Bacillus stearothermophilus by PCT</i> . The graph represents CFUs of <i>Bacillus stearothermophilus</i> vs. treatment time in oxygen plasma afterglow region of plasma reactor at pressure of 75 Pa. The concentration of bacteria cells on glass substrate was 1×10^7	30
Figure 16: <i>Survival curve of Staphylococcus aureus by PCT</i> . The graph represents CFUs of <i>Staphylococcus aureus</i> vs. treatment time by oxygen plasma glow discharge at pressure of 75 Pa. The concentration of bacteria cells on glass substrate was 1.7×10^8	31
Figure 17: <i>Survival curves of Staphylococcus aureus by PCT</i> . The graph represents CFUs of <i>Staphylococcus aureus</i> vs. treatment time by oxygen plasma glow discharge at pressure of 75 Pa obtained with two different concentrations. The concentrations of bacteria cells on glass substrate were 1.7×10^8 and 2.55×10^8	31

Figure 18: <i>Survival curves of Staphylococcus aureus by PCT.</i> The graph represents CFUs of <i>Staphylococcus aureus</i> vs. treatment time by oxygen plasma glow discharge at pressure of 30 Pa and pressure of 150 Pa. The concentration of bacteria cells on glass substrate was 7×10^8	32
Figure 19: <i>Survival curve of Staphylococcus aureus by PCT in plasma afterglow.</i> The graph represents CFUs of <i>Staphylococcus aureus</i> vs. treatment time in oxygen plasma afterglow region of plasma reactor at pressure of 75 Pa. The concentration of bacteria cells on glass substrate was 7×10^8	33
Figure 20: <i>SEM micrographs of bacteria Escherichia coli.</i> SEM images of <i>Escherichia coli</i> on Si substrate: (a) untreated; (b) treated with low-pressure highly dissociated oxygen plasma for 10 seconds; (c) 55 seconds; and (d) 240 seconds. Scale bar is 400 nm.....	34
Figure 21: <i>SEM micrographs of bacteria Bacillus stearothermophilus.</i> SEM images of <i>Bacillus stearothermophilus</i> on Si substrate: (a) untreated; (b) treated with low-pressure highly dissociated oxygen plasma for 10 seconds; (c) 55 seconds; and (d) 240 seconds. Scale bar is 400 nm.....	35
Figure 22: <i>SEM micrographs of bacteria Staphylococcus aureus.</i> SEM images of <i>Staphylococcus aureus</i> on Al substrate: (a) untreated; (b) treated with low-pressure highly dissociated oxygen plasma for 20 seconds; (c) 60 seconds; and (d) 240 seconds. Scale bar is 400 nm.....	36
Figure 23: <i>SEM micrographs of heat-treated bacteria.</i> SEM micrographs of heat-treated bacteria at 140 °C on Al substrate: (a) of <i>Bacillus stearothermophilus</i> for 20 seconds; (b) <i>Staphylococcus aureus</i> for 20 seconds; (c) <i>Bacillus stearothermophilus</i> for 10 minutes; <i>Staphylococcus aureus</i> for 10 minutes. Scale bar is 400 nm.	37
Figure 24: <i>SEM micrographs of vacuum-treated bacteria.</i> SEM micrographs of vacuum treated (a) <i>Bacillus stearothermophilus</i> ; (b) <i>Staphylococcus aureus</i> and (c) <i>Escherichia coli</i> . Scale bar is 400 nm.....	37
Figure 25: <i>Fluorescence microscopy images of bacteria Escherichia coli.</i> The bacteria <i>Escherichia coli</i> were labelled with DNA dyes SYTO 9 (green fluorescence in a, b and c) propidium iodide (red fluorescence in d, e and f). The images (a, d) show untreated bacteria, (b, e) bacteria treated with high-temperature dry heat for 10 minutes at 140 °C and (c, f) bacteria treated with oxygen plasma for 20 seconds. Untreated bacteria show strong SYTO 9 (a) staining (fluorescence), but weak propidium iodide (PI) staining (d). In high-temperature treated bacteria PI staining (red fluorescence) increased (e) compared to SYTO 9 (b). Plasma treated bacteria show poor or no SYTO 9 (c) or PI (f) fluorescence signal.	38
Figure 26: <i>Fluorescence microscopy images of bacteria Bacillus stearothermophilus.</i> The bacteria <i>Bacillus stearothermophilus</i> were labelled with DNA dyes: SYTO 9 (green fluorescence in a, b and c) and propidium iodide (red fluorescence in d, e and f). The images (a, d) show untreated bacteria, (b, e) bacteria treated with high-temperature dry heat for 10 minutes at 140 °C and (c, f) bacteria treated with oxygen plasma for 20 seconds. Untreated bacteria show strong SYTO 9 (a) staining (fluorescence) but weak propidium iodide (PI) staining (d). In high-temperature treated bacteria PI staining (red fluorescence) increased (e) compared to SYTO 9 (b). Plasma treated bacteria show poor or no SYTO 9 (c) or PI (f) fluorescence signal.	39
Figure 27: <i>Fluorescence microscopy images of bacteria Staphylococcus aureus.</i> The bacteria <i>Staphylococcus aureus</i> were labelled with DNA dyes SYTO 9 (green fluorescence in a, b and c) propidium iodide (red fluorescence in d, e and f). The images (a, d) show untreated bacteria, (b, e) bacteria treated with high-temperature dry heat for 10 minutes at 140 °C and (c, f) bacteria treated with oxygen plasma for 20 seconds. Un-treated bacteria show strong SYTO 9 (a) staining (green fluorescence). In untreated bacteria, a certain percentage of SYTO 9 negative cells also show propidium iodide (PI) staining (d). In high-temperatures treated bacteria PI (e) staining (red fluorescence) increased compared to SYTO 9 (b). Plasma treated bacteria show poor or no SYTO 9 (c) or PI (f) fluorescence signal.	40
Figure 28: <i>Flow cytometric plot analysis of Bacillus stearothermophilus and Staphylococcus aureus after dry heat treatment.</i> <i>Bacillus stearothermophilus</i> and <i>Staphylococcus aureus</i> were analysed by flow cytometry after staining with LIVE/DEAD BacLight™ Bacterial Viability Kit (L7012) untreated samples, and samples treated with dry heat at 140 °C for 20 s, 2 min and 10 min.....	41

- Figure 29: *Flow cytometric plot analysis of Escherichia coli after plasma treatment. Escherichia coli* was analysed by flow cytometry after staining with LIVE/DEAD BacLight™ Bacterial Viability Kit (L7012) initial bacterial suspension, dead cell control by 70% isopropyl alcohol, untreated samples, and oxygen plasma treated samples for 10 s, 50 s and 120 s.....42
- Figure 30: *Flow cytometric plot analysis of Bacillus stearothermophilus after plasma treatment. Bacillus stearothermophilus* was analysed by flow cytometry after staining with LIVE/DEAD BacLight™ Bacterial Viability Kit (L7012) initial bacterial suspension, dead cell control by 70% isopropyl alcohol, untreated samples, and oxygen plasma treated samples for 10 s, 50 s and 240 s.43
- Figure 31: *Flow cytometric plot analysis of Staphylococcus aureus after plasma treatment. Staphylococcus aureus* was analysed by flow cytometry after staining with LIVE/DEAD BacLight™ Bacterial Viability Kit (L7012) initial bacterial suspension, dead cell control by 70% isopropyl alcohol, untreated samples, and oxygen plasma treated samples for 10 s, 60 s and 240 s.43
- Figure 32: *Quantitative viability analysis of Escherichia coli after plasma treatment.* The number of live/dead *Escherichia coli* cells measured for various oxygen plasma treatment times at 75 Pa as well as in vacuum and 70 % isopropyl alcohol by flow cytometer. The concentration of bacteria cells per carrier was 16×10^744
- Figure 33: *Quantitative viability analysis of Escherichia coli after plasma treatment.* The number of live/dead *Escherichia coli* cells (with two-fold less initial concentration) measured for various oxygen plasma treatment times at 75 Pa, as well as in a vacuum and 70 % isopropyl alcohol by flow cytometers. The initial number of bacteria cells per carrier was 8×10^745
- Figure 34: *Quantitative viability analysis of Escherichia coli for 2 concentrations after plasma treatment.* The number of live/dead *Escherichia coli* cells with two different concentrations on sample glass carriers is plotted versus oxygen plasma treatment times at 75 Pa. The initial numbers of bacteria cells per carrier were 8×10^7 and 16×10^746
- Figure 35: *Quantitative viability analysis of Bacillus stearothermophilus after plasma treatment.* The number of live/dead *Bacillus stearothermophilus* cells (vegetative form with spores) measured for various oxygen plasma treatment times at 75 Pa as well as in vacuum and 70 % isopropyl alcohol by flow cytometer. The concentration of bacteria cells per carrier was 5×10^847
- Figure 36: *Quantitative viability analysis of Bacillus stearothermophilus after plasma treatment.* The number of live/dead *Bacillus stearothermophilus* cells (vegetative form with spores) measured for various oxygen plasma treatment times at 75 Pa as well as in vacuum and 70 % isopropyl alcohol by flow cytometer. The concentration of bacteria cells per carrier was 1.8×10^847
- Figure 37: *Quantitative viability analysis of Bacillus stearothermophilus after plasma treatment.* The number of live/dead *Bacillus stearothermophilus* cells (vegetative forms only) measured for various oxygen plasma treatment times at 75 Pa as well as in vacuum and 70 % isopropyl alcohol by flow cytometers. The concentration of bacteria cells per carrier was 5×10^848
- Figure 38: *Survival curve of Bacillus stearothermophilus for 2 concentrations.* The number of live *Bacillus stearothermophilus* cells (vegetative form with spores) with two different concentrations on sample glass carriers is plotted versus oxygen plasma treatment times at 75 Pa. The initial numbers of bacteria cells per carrier were 5×10^8 and 1.8×10^848
- Figure 39: *Survival curve of Bacillus stearothermophilus for 2 pressures of plasma treatment.* The number of live *Bacillus stearothermophilus* cells (in vegetative form) on sample glass carriers is plotted versus oxygen plasma treatment times at two pressures; 30 Pa and 150 Pa. The initial number of bacteria cells per carrier was 7×10^8 for 30 Pa and 150 Pa, and 5×10^8 for 75 Pa.49
- Figure 40: *Survival curve of Bacillus stearothermophilus for afterglow plasma treatment.* The number of live/dead *Bacillus stearothermophilus* cells on sample glass carriers is plotted versus oxygen plasma treatment times at 75 Pa in afterglow region of the reactor. The initial number of bacteria cells per carrier was 7×10^849
- Figure 41: *Quantitative viability analysis of Staphylococcus aureus after plasma treatment.* The number of live/dead *Staphylococcus aureus* cells measured for various oxygen plasma treatment times at 75 Pa, as well as in a vacuum and 70 % isopropyl alcohol by flow cytometer. The concentration of bacteria cells per carrier was 1.7×10^850

Figure 42: Quantitative viability analysis of <i>Staphylococcus aureus</i> after plasma treatment. The number of live/dead <i>Staphylococcus aureus</i> cells measured for various oxygen plasma treatment times at 75Pa as well as in a vacuum and 70 % isopropyl alcohol by flow cytometer. The concentration of bacteria cells per glass carrier was 2.55×10^8	51
Figure 43: <i>Survival curve of Staphylococcus aureus for 2 concentrations.</i> The number of live <i>Staphylococcus aureus</i> cells with two different concentrations on sample glass carriers is plotted versus oxygen plasma treatment times at 75 Pa. The initial numbers of bacteria cells per glass carrier were 1.7×10^8 and 2.55×10^8	51
Figure 44: <i>Survival curve of Staphylococcus aureus for 2 pressures of plasma treatment.</i> The number of live <i>Staphylococcus aureus</i> cells on sample glass carriers is plotted versus oxygen plasma treatment times at two pressures; 30 Pa and 150 Pa. The initial number of bacteria cells per carrier was 7×10^8	52
Figure 45: <i>Survival curve of Staphylococcus aureus for afterglow plasma treatment.</i> The number of live <i>Staphylococcus aureus</i> cells on sample glass carriers is plotted versus oxygen plasma treatment times at 75 Pa in plasma afterglow. The initial number of bacteria cells per carrier was 7×10^8	52
Figure 46: <i>Optical emission of molecular nitrogen from plasma and during the process.</i> Time evolution of N_2 peak during oxygen plasma treatment of 10^{10} cell/ml <i>Escherichia coli</i> at the pressure of 30 Pa and the corresponding background measured in an empty glow discharge chamber.....	53
Figure 47: <i>Optical emission of molecular nitrogen during the plasma treatment process.</i> Time evolution of N_2 C-B (0,0) peak during oxygen plasma treatment of <i>Escherichia coli</i> 10^{10} CFUs/ml at pressures of 30, 40, 50, and 75 Pa.....	54
Figure 48: <i>Optical emission of carbon dioxide during the plasma treatment process.</i> Time evolution of CO Angstrom band (0,0) peak during oxygen plasma treatment of <i>Escherichia coli</i> 10^{10} CFUs/ml at pressures of 30, 40, 50, 60, 75, 100, and 150 Pa.....	55
Figure 49: <i>Survival curve of Escherichia coli for received dose of O atoms (measured by PCT).</i> The number of surviving bacteria CFUs <i>Escherichia coli</i> in respect to received dose of neutral oxygen atoms. The two initial concentrations were used: 8×10^7 and 16×10^7 cells per carrier.	60
Figure 50: <i>Survival curve of Escherichia coli for received dose of O atoms (measured by FACS).</i> The number of surviving bacteria <i>Escherichia coli</i> cells in respect to received dose of neutral oxygen atoms. The two initial concentrations were used: 8×10^7 and 16×10^7 cells per carrier.	61
Figure 51: <i>Survival curve of Bacillus stearothermophilus for received dose of O atoms (measured by PCT).</i> The number of surviving bacteria (CFUs) <i>Bacillus stearothermophilus</i> (vegetative form only) in respect to received dose of neutral oxygen atoms at 3 different pressures. The two initial bacterial concentrations used were: 7×10^8 (at 30 Pa, 150 Pa) and 5×10^8 cells per carrier (at 75 Pa).....	63
Figure 52: <i>Survival curve of Bacillus stearothermophilus for received dose of O atoms (measured by PCT).</i> The number of surviving bacteria <i>Bacillus stearothermophilus</i> cells (vegetative form and vegetative plus spores) in respect to received dose of neutral oxygen atoms at 3 different pressures.....	64
Figure 53: <i>Survival curve of Bacillus stearothermophilus for received dose of O atoms in afterglow.</i> The number of surviving bacteria <i>Bacillus stearothermophilus</i> cells (vegetative form) in respect to received dose of neutral oxygen at 75 Pa. The graphs presents PCT and FACS results of inactivation.....	64
Figure 54: <i>Survival curve of Staphylococcus aureus for received dose of O atoms (measured by PCT).</i> The numbers of surviving bacteria (CFUs) <i>Staphylococcus aureus</i> in respect to received doses of neutral oxygen atoms at 3 different pressures. The two initial bacterial concentrations used were: 7×10^8 (at 30 Pa, 150 Pa) and 2.55×10^8 cells per carrier (at 75 Pa).....	66
Figure 55: <i>Survival curve of Staphylococcus aureus for received dose of O atoms (measured by FACS).</i> The number of surviving bacteria <i>Staphylococcus aureus</i> cells in respect to received dose of neutral oxygen atoms at 3 different pressures. The two initial bacterial concentrations used were: 7×10^8 (at 30 Pa, 150 Pa) and 2.55×10^8 cells per carrier (at 75 Pa).....	67
Figure 56: <i>Survival curve of Staphylococcus aureus for received dose of O atoms in afterglow.</i> The number of surviving bacteria <i>Staphylococcus aureus</i> cells in respect to received dose of neutral oxygen at 75 Pa. The graphs presents PCT and FACS results of inactivation.....	67

Index of Tables

Table 1: *Recombination of O atoms on material*. Recombination coefficients (γ) for different materials and calculated approximate plasma glow heating time to the temperature of 353 K (80°C). The presumption is that all materials have the same product of the mass and the specific heat, the n_0 is $1.5 \cdot 10^{22} \text{ m}^{-3}$ and ionic heating is negligible.26

Appendix - Bibliography

Papers

Vujošević, D. Sterilization effects of low-temperature highly dissociated oxygen plasma. *Med. zap.* **64**, 11-29 (2008).

Vratnica, Z.; **Vujošević, D.**; Cvelbar, U.; Mozetič, M. Degradation of bacteria by weakly ionized highly dissociated radio-frequency oxygen plasma. *IEEE Trans. Plasma Sci.* **36**, 1300 (2008).

Vujošević, D.; Mozetič, M.; Cvelbar, Uroš.; Krstulovič, N.; Milošević, S. Optical emission spectroscopy characterization of oxygen plasma during degradation of Escherichia coli. *J. Appl. Phys.* **101**, 103305-1-103305-7 (2007).

Cvelbar, U.; **Vujošević, D.**; Vratnica, Z.; Mozetič, M. The influence of substrate material on bacteria sterilization in an oxygen plasma glow discharge. *J. Phys., D, Appl. Phys.* **39**, 3487-3493 (2006).

Vujošević, D.; Vratnica, Z.; Vesel, A.; Cvelbar, U.; Mozetič, M.; Drenik, Aleksander, Mozetič, T.; Kljanšek Gunde, M.; Haumtman, N. Oxygen plasma sterilization of bacteria. *Mater. tehnol.* **40**, 227-232 (2006).

Drenik, A.; Cvelbar, U.; Vesel, A.; Mozetič, Miran.; Vratnica, Z.; **Vujošević, D.** Meritve gostote atomov v šibkoionizirani kisikovi plazmi vzdolž zaprte cevi. *Vakuumist* **25**, 16-19 (2005).

Vratnica, Z.; **Vujošević, D.**; Bele, M.; Drenik, A.; Vesel, A.; Cvelbar, U.; Mozetič, M. Preiskave bakterij s sodobnim vrstičnim elektronskim mikroskopom. *Vakuumist* **1-2**, 20-23 (2005).

Vujošević, D.; Vratnica, Z.; Bujko, M.; Cvelbar, U.; Mozetič, M. Sterilizacija plazmom - tehnologija budućnosti ili alternativa klasičnom postupku. *Med. zap.* **59**, 5-10 (2004).

Vujošević, D. Gene therapy for HIV. *Med. zap.* **57**, 71-75 (2003).

Conference contributions

Vujošević, D.; Cvelbar, U.; Mozetič, M. Sterilization of organic materials by cold oxygen plasma. V: Amon, S. (ur.), Mozetič, M. (ur.), Šorli, I. (ur.). 44th International Conference on Microelectronics, Devices and Materials and the Workshop on Advanced Plasma Technologies, September 17. - September 19. 2008, Fiesa, Slovenia. Proceedings. Ljubljana: MIDEM - Society for Microelectronics, Electronic Components and Materials, pp. 227-229 (2008).

- Mijović, G.; Drašković, N.; **Vujošević, D.**; Dupanović, B.; Terzić, D. Praćenje “*Viral load*“ kod HIV pozitivnih osoba u Crnoj Gori. V: VI kongres medicinske mikrobiologije sa međunarodnim učešćem MICROMED 2008. Zbornik sažetaka radova. Beograd, pp. 238. (2008).
- Eleršič, K.; Vratnica, Z.; **Vujošević, D.**; Junkar, I.; Kovač, J.; Mozetič, M.; Cvelbar, U. Surface analysis of damages on *Escherichia coli* caused by oxygen plasma radicals. V: ICOPS 2008, The 35th IEEE International Conference on Plasma Science, June 15-19, 2008, Karlsruhe, Germany. IEEE Conference records - abstracts. Danvers: Institute of Electrical and Electronics Engineers, 293 (2008).
- Vujošević, D.**; Junkar, I.; Krstulović, N.; Milošević, S.; Mozetič, M.; Cvelbar, U. Characterization of oxygen plasma during degradation of *Escherichia coli* by optical emission spectroscopy. V: ŠETINA, Janez (ur.), KOVAČ, Janez (ur.). 14. mednarodni znanstveni sastanak Vakuumska znanost in tehnika, Bled, 1. junij 2007. Zbornik povzetkov. Ljubljana: Društvo za vakuumsko tehniko Slovenije; Zagreb: Hrvatsko vakuumsko društvo, 12 (2007).
- Zeković, Ž.; **Vujošević, D.**; Ivanović, Lj. The Quality of water supplying in some municipalities in Montenegro, from 2001 to 2005, in the aspect of Microbiology. Quality of water and water supplying. Book section, Budva (2007).
- Vujošević, D.**; Zeković, Ž.; Seme, K.; Poljak, M.; Babič, D. Hepatitis C virus core antigen enzym immunoassay for detection and quantification of hepatitis C viremia. V: 5th Balkan Congress for Microbiology, 24-27 October 2007, Budva, Montenegro. [Programme, abstract book]. Podgorica: Balkan Society for Microbiology: Montenegrin Society for Microbiology, pp. 59 (2007).
- Cvelbar, U.; **Vujošević, D.**; Mozetič, M.; Vratnica Z.; Krstulović, N.; Milošević, S.; Repnik, U. Monitoring plasma sterilization efficiency. V: 5th Balkan Congress for Microbiology, 24-27 October 2007, Budva, Montenegro. [Programme, abstract book]. Podgorica: Balkan Society for Microbiology: Montenegrin Society for Microbiology, 2007, pp. 63.
- Vujošević, D.**; Cvelbar, U.; Mozetič, M. Plasma reactor for sterilization of implants. V: Radić, N. (ur.). 13. Međunarodni sastanak Vakuumska znanost i tehnika, Koprivnica, 13. lipnja 2006, Koprivnica. Zbornik sažetaka. [Zagreb]: Hrvatsko vakuumsko društvo, 15 (2006).
- Cvelbar, U.; **Vujošević, D.**; Vratnica, Z.; Mozetič, M. Treatment of bacteria with inductively coupled oxygen plasma : [invited talk]. V: JVC 11, 11th Joint Vacuum Conference, September 24 - 28, 2006, Prague, Czech Republic. Programme and book of abstracts. [S.l.: s.n.], 38 (2006).
- Vratnica, Z, **Vujošević, D.**; Bujko, M.; Cvelbar, U.; Mozetič, M. SEM investigation of bacteria deposited on aluminium foil. V: MOZETIČ, Miran (ur.), Šetina, J. (ur.), Kovač, J. (ur.). 10. združena vakuumska konferenca [tudi] 11. srečanje slovenskih in hrvaških vakuumistov [in] 24. slovenski vakuumski simpozij, 28. september - 2. oktober 2004, Portorož, Slovenija = 10th Joint Vacuum Conference [being also] 11th Meeting of Slovenian and Croatian Vacuum Scientists [and] 24th Slovenian Vacuum Symposium, September 28-October 2, 2004, Portorož, Slovenia. Program in knjiga povzetkov. Ljubljana: Društvo za vakuumsko tehniko Slovenije, 94 (2004).

Optical emission spectroscopy characterization of oxygen plasma during degradation of *Escherichia coli*

D. Vujošević, M. Mozetič, and U. Cvelbar^{a)}

Plasma Laboratory F4, Jožef Stefan Institute, Jamova 39, 1000 Ljubljana, Slovenia (EU)

N. Krstulović and S. Milošević

Institute of Physics, Bijenička 46, 10000 Zagreb, Croatia

(Received 17 January 2007; accepted 13 March 2007; published online 31 May 2007)

Optical emission spectroscopy was applied for plasma characterization during sterilization of substrates contaminated with bacteria. The amount of 10^{10} /ml cells of *Escherichia coli* was carefully applied to glass substrates and exposed to oxygen plasma glow discharge at different pressures between 30 and 200 Pa. Plasma was created in a glass discharge tube by an inductively coupled rf generator at the frequency of 27.12 MHz and output power of about 250 W. The electron temperature and plasma density were estimated with a double Langmuir probe. They were between 3 and 5 eV and 2 and $35 \times 10^{15} \text{ m}^{-3}$. Density of neutral oxygen atoms was measured with a catalytic probe, and was between 2 and $6 \times 10^{21} \text{ m}^{-3}$. Optical emission spectroscopy was performed with a low resolution spectrometer. The emission from carbon monoxide and nitrogen molecules was used to monitor the evolution of bacteria degradation. Both signals expressed a well defined maximum corresponding to peak erosion of bacteria by plasma radicals. As the sterilization was accomplished, both CO and N₂ lines fell below the detection limit of the spectrometer. The bacteria degradation was also monitored by scanning electron microscope (SEM) and culturing. The SEM images corresponded well with the evolution of CO and N₂ lines so the optical emission spectroscopy found a reliable tool for monitoring the sterilization process. © 2007 American Institute of Physics. [DOI: 10.1063/1.2732693]

I. INTRODUCTION

In the past decade, oxygen plasma has been successfully applied to technologies such as cold plasma ashing, discharge cleaning, selective plasma etching, nanofabrication, and plasma sterilization.^{1–10} All the technologies are based on controlled oxidation of organic compounds. In contrary to standard oxidation that is carried on close to the thermodynamic equilibrium, the oxidation in low pressure oxygen plasma is a well nonequilibrium process.¹¹ The main advantage of the nonequilibrium oxidation is the capability of controlling the oxidation rate independently from the sample temperature.^{12,13} This is possible due to a low potential barrier for oxidation with reactive particles from oxygen plasma. Low temperature oxidation is particularly suitable for sterilization of biocompatible materials, where the substrate temperature should be always kept low in order to prevent degradation of the substrate itself.^{14,15} Oxygen plasma is a source of different reactive particles including excited molecules and atoms, positive and negative molecular and atomic ions, and ozone and neutral oxygen atoms.^{16–18} The concentration of these particles depends largely on discharge parameters (i.e., type of discharge, discharge power and frequency, magnetic field, size and shape of discharge vessel, type of material facing plasma, pressure and gas mixture, etc.).^{17,18} Interaction of plasma radicals with solid materials is both physical and chemical. Physical interaction is usually performed with charged radicals that can be

accelerated by biasing samples,^{19,20} while neutral radicals usually do not have substantial kinetic energy so the interaction is purely potential and therefore very selective.^{12,21}

Plasma sterilization is a promising technology which may be applied not only in medicine but also in biology and food industry.^{22,23} A drawback is definitely a lack of reliable methods for monitoring the sterilization efficiency. Sterilization efficiency is traditionally detected only after the process is performed. The samples that are supposed to be sterile are immersed in a suitable nutrient medium where the bacteria grow and multiply under controlled conditions.^{24,25} This is a time consuming process that may also sometimes fail.

In the present paper, we present the results of plasma characterization by optical emission spectroscopy (OES), which proves that this method is very suitable to monitor the bacteria degradation during sample treatment with oxygen radicals in a plasma glow discharge.

II. EXPERIMENTAL DETAILS

A. Experimental setup

Experiments were performed in a discharge vessel shown in Fig. 1. The samples were inserted into the glow discharge region, and were on floating potential to prevent any additional acceleration of ions and heating of the sample surface. The discharge vessel was a 50 cm long glass tube with the inner diameter of 36 mm. It was made from borosilicate glass that has a very low recombination coefficient for the heterogeneous surface recombination of oxygen atoms.^{11,26,27} The discharge chamber was pumped with a two

^{a)}Electronic mail: uros.cvelbar@guest.arnes.si

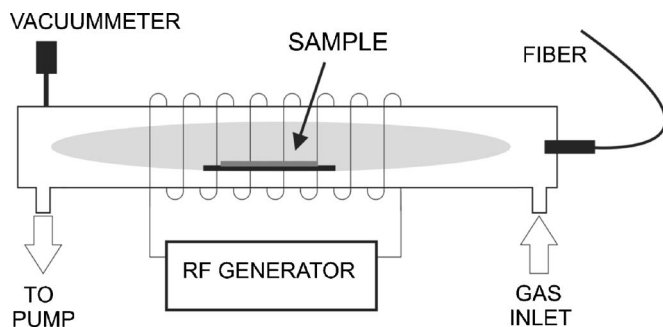


FIG. 1. Schematic of the discharge vessel.

stage rotary pump with the pumping speed of $16 \text{ m}^3/\text{h}$, while on the other side, commercially available oxygen is leaked through a precise leak valve. Pressure was measured with a calibrated Pirani gauge. Plasma glow discharge was created by inductively coupled rf generator with the frequency of 27.12 MHz and output power of about 250 W. The plasma density and the electron temperature were estimated with a simple double Langmuir probe mounted in the center of the discharge chamber prior to sterilization experiments.²⁸ The electron temperature slowly decreases with increasing pressure: at 20 Pa, it is about 5 eV, while at 100 Pa, it is about 3 eV. The plasma density depended largely on pressure and is plotted in Fig. 2. The density of neutral oxygen atoms was also measured prior to sterilization experiments with a catalytic probe mounted at the side of the discharge chamber, where no glow was detected. This was done to assure proper reading of the O-atom density.^{29,30} The O-atom density versus pressure is plotted in Fig. 3.

Optical emission spectroscopy was performed with the HR2000CG-UV-NIR spectrometer (OceanOptics), spectral resolution 1 nm, and spectral range of 200–1100 nm. A quartz window is mounted perpendicularly to the discharge tube, and an optical fiber is fixed on the axis, as shown in Fig. 1. The fiber (600 μm diameter, solar resistant) therefore collects radiation from the entire length of the discharge tube. Typically spectra were recorded with integration time of 300 ms with the rate of three spectra per second.

B. Sample preparation

Bacteria were deposited onto smooth glass substrates. The substrates were well activated before bacteria deposition in order to avoid their agglomeration on the substrate. The

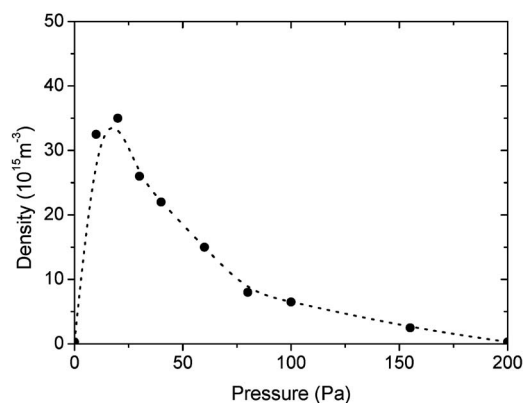


FIG. 2. Plasma density versus pressure.

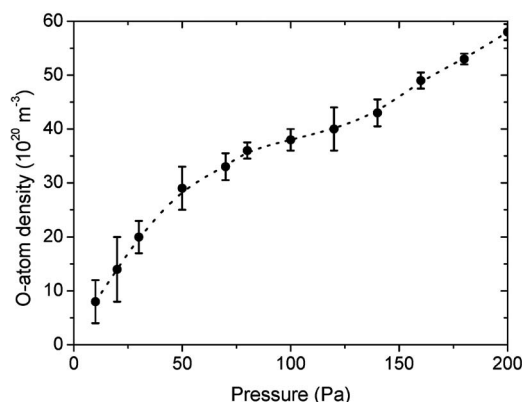


FIG. 3. Density of neutral O atoms vs pressure.

bacteria *Escherichia coli* (ATCC 11775) were obtained from *Microbiologics* (St. Cloud, MN). They were cultivated on Columbia agar plate (Merck KGaA, Darmstadt) for 24 h at 37 °C. Cells were harvested, washed by centrifugation in sterile water, and resuspended in water. The sample was then diluted in a water to obtain the desired bacterial density. Cell numbers were adjusted to approximately $10^{10}/\text{ml}$ ($\text{OD}_{550} \approx 7.20$) by spectrophotometry. The quantity of bacteria to obtain good light emission signal on wide pressure range of plasma was always 10^{10} cfu (colony forming units), which was controlled by reculturing on Columbia agar plates, and counted after 24 h.

C. Results

Optical emission spectroscopy was performed at different conditions. First, it was performed in the empty discharge tube to recognize spectral features. As the plasma is ignited, several impurities are detected due to desorption from the walls. After few seconds, the emission becomes constant. Figure 4 is a plot of spectra measured in empty discharge chamber at different pressures (30, 50, 60 and 100 Pa). The spectral features are marked only in the spectrum measured at 30 Pa. In the spectrum measured at 100 Pa, the spectral response of the spectrometer is plotted as well. As usual for this kind of spectrometers, the response is the highest at about 500 nm, while it is pretty low in UV and IR parts of the spectrum. Strongest oxygen atomic lines at 777.2 and 844.6 nm and H_{α} at 656.5 nm (for 30 and 50 Pa) are in saturation in Fig. 4.

Samples were treated in oxygen plasma at different pressures. All samples were exposed for 250 s, and the evolution of different spectral features was measured during plasma treatment. The survey spectra measured with bacteria in plasma were not remarkably different from the corresponding spectra measured in the empty discharge vessel. The difference was only observed after systematic and detail examination of the time evolution of spectra. Namely, a detailed study of the spectra revealed spectral features not observed in the spectra obtained in bacteria-free discharge. A comparison of a spectral feature for an empty and loaded discharge vessel is plotted in Fig. 5. Therefore, for all experiments with plasma degradation of bacteria, the background was also measured in order to eliminate the effects of the gas desorp-

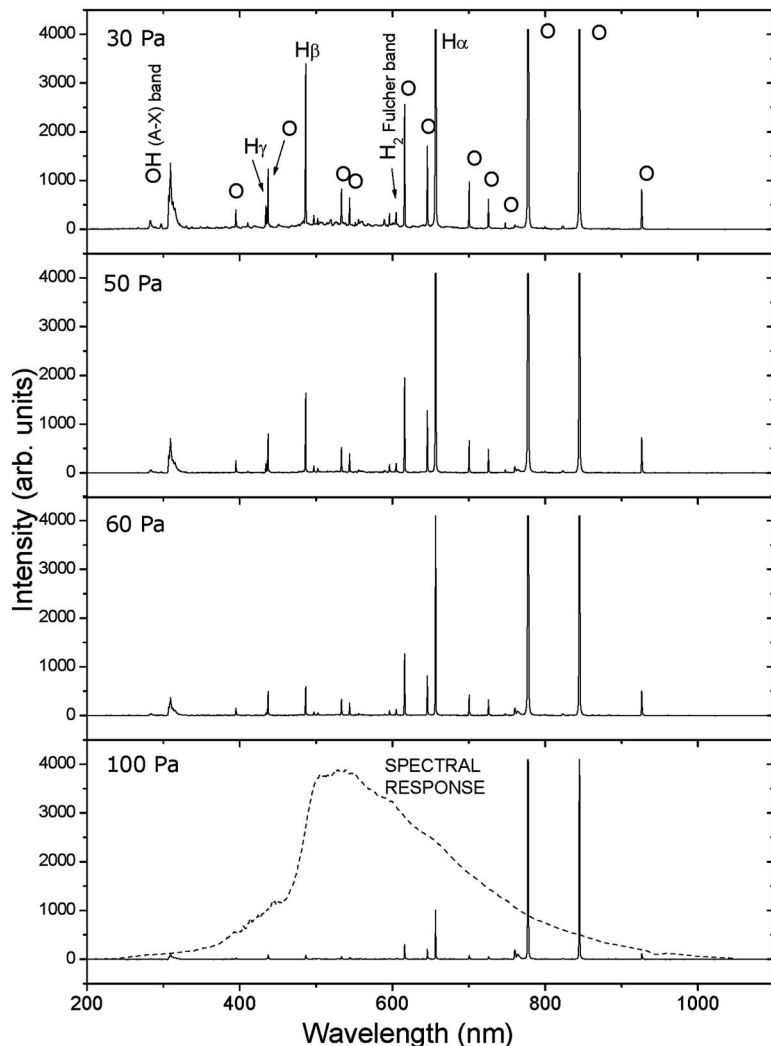


FIG. 4. Survey emission spectra from oxygen plasma created at pressures 30, 50, 60, and 100 Pa.

tion and possible leakage of the system. However, the sensitivity of this method was limited to the discharge vessel loaded with less than 10^5 cfu of bacteria.

Organic materials, especially bacteria, usually contain hydrogen, carbon, oxygen, and nitrogen atoms. During plasma treatment, they react with oxygen radicals forming different compounds. Obviously, only those compounds with spectral features in the spectrometer range are suitable for monitoring reactions between the radicals and bacteria. In our case, we are showing results for nitrogen molecules and carbon monoxide. Hydrogen and OH molecules may also be useful for monitoring the bacteria degradation, but since the residual atmosphere in our vacuum system is largely water vapor, the results of H and OH monitoring might be doubtful. The appearance of nitrogen is monitored by measuring intensity of the peak corresponding to the second positive band $C^3\Pi_u - B^3\Pi_g(0,0)$ at 337.29 nm. The time evolution of this peak during plasma sterilization is plotted in Fig. 6.

Carbon monoxide is a reaction product of carbon oxidation. It emits both in UV (third positive band) and visible ranges (Angstrom band). Due to spectral response of the spectrometer, we chose the peak in the Angstrom band. The transition between vibrational levels ($0 \rightarrow 2$) of the upper and

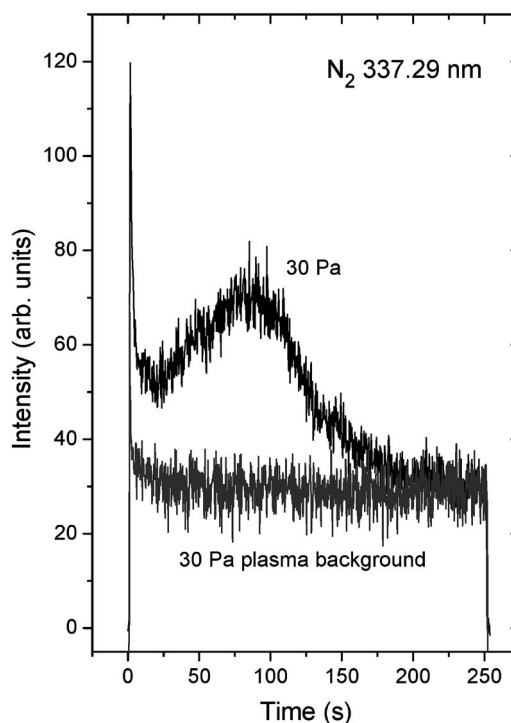


FIG. 5. Time evolution of N_2 C-B (0,0) peak during oxygen plasma treatment of *E. coli* 10^{10} cfu at the pressure of 30 Pa and the corresponding background measured in empty glow discharge chamber.

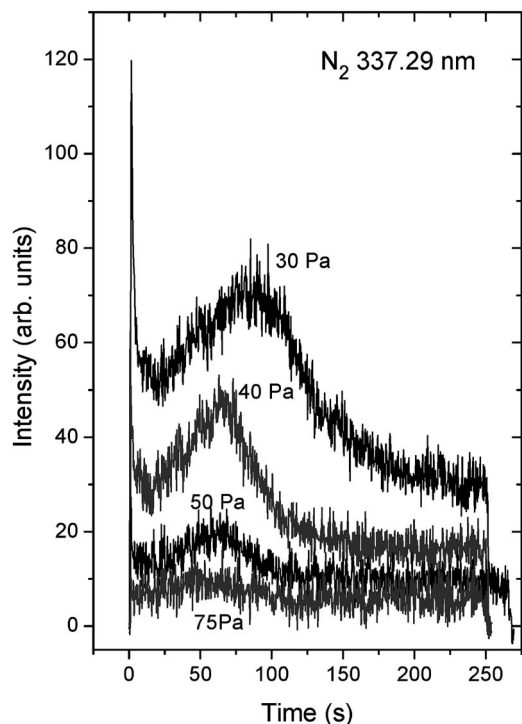


FIG. 6. Time evolution of N₂ C-B (0,0) peak during oxygen plasma treatment of *E. coli* 10¹⁰ cfu at pressures of 30, 40, 50, and 75 Pa.

lower electron states appears at about 519 nm, where the spectrometer response is the highest. The evolution of the CO peak is plotted in Fig. 7.

The samples with bacteria were also investigated by SEM. The SEM images were taken after different treatment times in order to monitor visible modifications of bacteria on

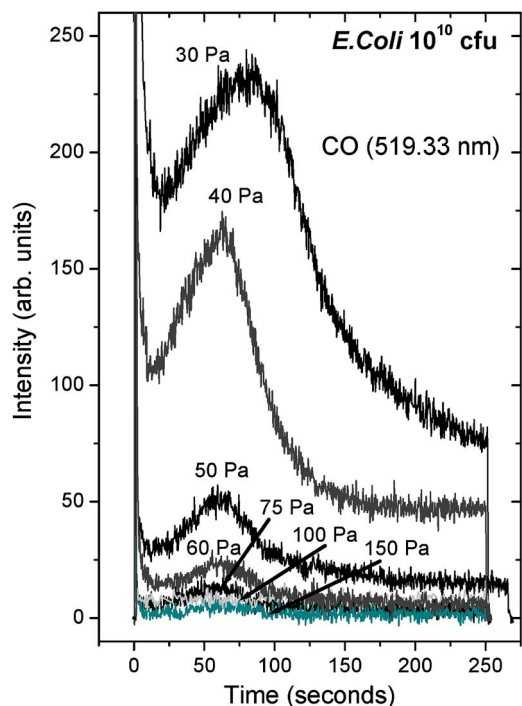


FIG. 7. Time evolution of CO Angstrom band (0,0) peak during oxygen plasma treatment of *E. coli* 10¹⁰ cfu at pressures of 30, 40, 50, 60, 75, 100, and 150 Pa.

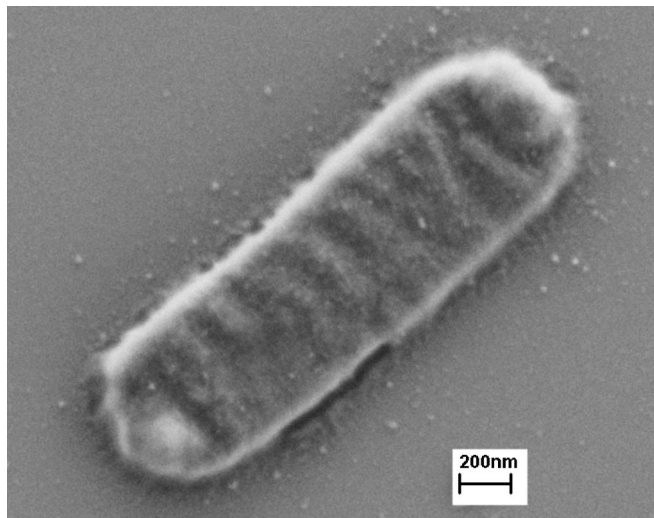


FIG. 8. SEM image of untreated *E. coli*.

substrates. Figure 8 represents a SEM image of untreated bacteria. Although the exposure of bacteria to vacuum causes some damage, the majority was still vital after exposure to vacuum. This was checked by positive control growth after bacteria exposure to vacuum overnight. The bacteria exposed to plasma for 55 s are shown in Fig. 9, while those treated for 120 s are shown in Fig. 10.

III. DISCUSSION

A. Characteristics of oxygen plasma

Inductively coupled rf discharges are known to produce plasma with a low neutral gas temperature, low ion temperature, and moderate electron temperature.³¹ In our case, the electron temperature is between 3 and 5 eV, while their density is of the order of 10¹⁵ m⁻³. The density decreases with increasing pressure, which is due to the increasing collision frequency between electrons and neutral molecules or atoms at higher pressure. Namely, the electron acceleration in induced electric field within the rf coil is optimal when the

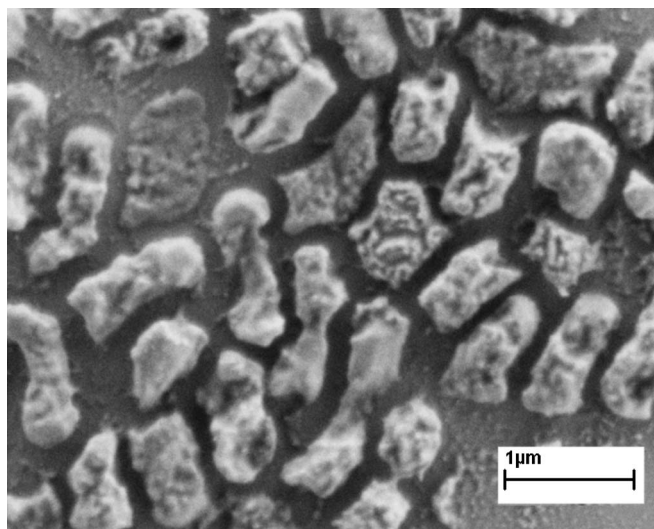


FIG. 9. SEM image of bacteria *E. coli* treated for 55 s at the pressure of 75 Pa.

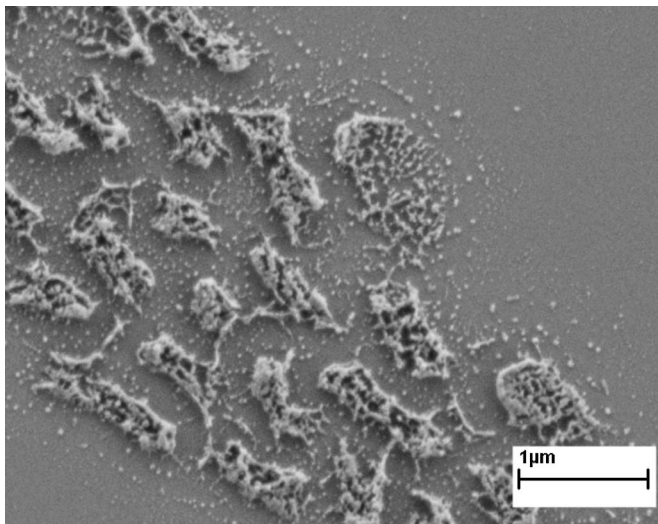


FIG. 10. SEM image of bacteria *E. coli* treated for 120 s at the pressure of 75 Pa.

oscillation amplitude is close to its mean free path. At the field of 10 V/cm, the oscillation amplitude is 6 mm. The electron mean free path of 6 mm is obtained at the pressure of about 1 Pa. A higher pressure therefore causes poorer acceleration which reflects in both lower electron temperature and lower ionization probability. On the other hand, the surface loss of charged particles increases with decreasing pressure due to the increasing mobility. At low pressure, say, below 20 Pa, the surface loss of charged particles becomes dominant. The result of the two opposite effects is a maximum in the electron density, as noticeable from Fig. 2.

Fast electrons in plasma are causing not only ionization but also dissociation of oxygen molecules. Since the dissociation energy is at 5.2 eV much lower than the ionization energy (which is about 12 eV), the dissociation is obviously more probable event at the electron temperature of few eV. The higher probability for dissociation, however, cannot explain the huge difference between the dissociation and the ionization fraction. Comparison of Figs. 2 and 3 clearly shows that the dissociation fraction is at least five orders of magnitude higher than the ionization fraction. This observation is explained by surface effects. The probability for surface neutralization of slow oxygen ions is always high, close to 1. The probability for surface recombination of atoms, however, depends largely on the properties of the plasma facing materials. For many glasses including our borosilicate glass, the recombination coefficient is often below 0.001. Low surface loss of neutral oxygen atoms therefore assures a high atom density, as observed in Fig. 3. Here, it is worth mentioning that oxygen atoms are perfectly stable in the gas phase. The conservation of momentum and energy at collisions between two oxygen atoms in the gas phase prevents their recombination. The recombination in the gas phase is possible only by three-body collisions, which are unlikely to occur at low pressure (say, below few 100 Pa).

Figure 4 represents some OES spectra obtained in empty discharge vessel. The spectrum is rich at low pressure, but as the pressure is increased, many spectral features decreased and eventually disappear below the detection limit of the

spectrometer. At the pressure of 100 Pa, only the oxygen lines originating from the two lowest oxygen atom excited states are observed, and H_{α} is clearly distinguished, too. The evolution of the spectral lines versus pressure is explained by the following effects: partial pressure of impurities (mainly water vapor), electron density, and electron temperature. The base pressure in our system is about 7 Pa. The residual atmosphere is mainly water vapor. At 30 Pa the oxygen partial pressure is only few times larger than the base pressure, so the concentration of water vapor is relatively high. Water molecules are not stable in plasma. They are almost fully dissociated to OH and H. Both OH and H are excited at inelastic collisions with electrons, and radiation is observed at relaxation of excited states. As expected, the H_{α} is dominant since the excitation energy of this state is the lowest (here, we cannot consider relaxations from the first excited state to the ground state, which should appear in the far UV range, undetectable by our spectrometer). As pressure is increased, the ratio between the H_{α} and H_{β} increases and H_{γ} vanishes. This effect is explained by lower electron temperature at higher pressure. Namely, the excitation energy of H_{β} and H_{γ} is higher than for H_{α} , so slower electrons are not capable to excite these states at the same extent as at low pressure.

The same applies for oxygen lines. At low pressure, fast electrons are capable of exciting a variety of highly excited states, while at higher pressure only lines originating from the two lowest radiative excited states remain.

B. OES during bacteria treatment

The majority of experiments with optical emission spectroscopy were performed during bacteria treatment. Optical emission spectra were measured simultaneously as the sterilization was in progress. For each pressure, the background was measured as well to prove that particular spectral features are really due to bacteria degradation, and not to any other effect. For example, comparison of the nitrogen emission between the loaded and empty discharge vessels is plotted in Fig. 5.

The evolution of the nitrogen peak during treatment of bacteria is shown in Fig. 6. The intensity of the C–B (0,0) transition was measured at different pressures. As expected, the nitrogen peak is the highest at 30 Pa, where both electron temperature and density are high. At the origin, the peak is very high—probably due to desorption of nitrogen molecules from the walls facing plasma. In the next few seconds, a minimum is observed. As the treatment proceeds, the peak increases and reaches a rather broad maximum. The position of the maximum depends on pressure: at low pressure it is shifted to longer times. At 30 Pa the maximum nitrogen radiation is observed for about 85 s of treatment time, and at 40 Pa it is at about 70 s, while at 50 Pa it is at about 60 s. The shift in the maximum radiation is explained by different etching rates. At low pressure, the density of neutral oxygen atoms (that are major reactants in plasma) is rather low (Fig. 3), so the time needed for bacteria destruction is rather high. As the pressure is increased, the etching rate is increased, too. The increased etching rate causes a shift of the nitrogen

emission, as observed from Fig. 6. At higher pressure, the peak would be probably shifted even to lower time, but the emission becomes too weak. As mentioned before, the electron density and temperature at high pressure are too low to provide enough molecular excitation.

Similar observation is found for the case of CO emission (Fig. 7). The CO line is more intense than the nitrogen so the peak in this line is detectable up to the pressure of about 75 Pa. The time evolution of the CO peak corresponds to the evolution of the nitrogen peak: the maximum is after about 85 s of plasma treatment for the pressure of 30 Pa, 65 s for 40 Pa, 60 s for 50 Pa, and it remains at this position for higher pressure.

The SEM images just confirm that the appearance of the nitrogen and CO peaks originates from bacteria oxidation. Figure 7 represents the SEM image of bacteria after 55 s of plasma treatment at 75 Pa. The bacteria are already badly damaged: the cell wall still persists, but it is so badly damaged that the cytoplasm has already escaped. The cytoplasm consists of water mainly (80%), and the rest are proteins, lipids, polysaccharides, and minerals. There is no distinguished nucleus in the bacterial cytoplasm, but the proteins are rather dispersed in water. These materials are easily evaporated in vacuum, and they enter the plasma when the cell wall is damaged enough to become permeable. As this occurs, a sharp peak should be observed in Figs. 6 and 7. The peak is, however, not all that sharp. This is explained by slight differences of cell wall erosion for particular bacteria: some bacteria are eroded before others resulting in the peak broadening, as shown in Figs. 6 and 7.

Both nitrogen and CO peaks are pretty low in the initial stage of plasma treatment. Since the concentration of oxygen radical practically does not depend on time, a poor etching rate in first, say, 30 s of plasma treatment cannot be explained by low radical density. Other effects should be predominant. There are two possible explanations for poor N₂ and CO peaks during initial 30 s of plasma treatment: (i) bacteria temperature and (ii) structure of the bacteria cell wall. While it is fairly impossible to measure the temperature of the bacteria during plasma treatment, we measured the temperature of the substrates and they were only slightly heated during plasma treatment. So, in the first approximation, one can neglect temperature effects. The peaks in spectral features are rather explained by different etching probabilities as the process is on its way. The construction of bacterial wall is very complex and detailed study of the material erosion is beyond the scope of this paper. Still, it is worth mentioning that gram-negative bacteria such as *Escherichia coli* are normally covered with outer membrane. Lipoproteins and the associated polysaccharides together form the structure of outer membrane which is definitely the most resistant part of bacteria. This outer membrane is only slowly etched by plasma radicals, resulting in a minimum of N₂ and CO emission in the first 30 s of treatment time. When the outer membrane is well damaged, the next structure is uncovered. The next structure consists of peptidoglycan layer, which is not so resistant, and is etched at much higher rate than the outer membrane.

The bacteria shown in Fig. 9 have rich surface morphology. It is well known that ion etching always causes enrichment of surface morphology. In our case, however, kinetic effects are easily neglected for two reasons: first, the plasma potential is low, and second, the mean free path of oxygen ions at 75 Pa is much lower than the Debye length resulting in poor kinetic energy of ions reaching the surface. The rich morphology is therefore due to chemical etching: some parts of the outer membrane are thinner than others. As the membrane is etched away, then other structures, not so resistant to oxidation, are revealed. This is resulted in removal of inner material. This effect probably causes shrinkage of bacteria as well as rich surface morphology.

When inner parts of bacteria have been removed, there are still the remains of the cell wall to be etched by oxygen radicals. As stated above, the etching rate is poor and that is probably the reason for long exponential-like tails observed in Figs. 6 and 7. Again, it is worth mentioning that not all bacteria are degraded at the same rate and this effect certainly contributes to the long tail. In any case, there some remains to be oxidized even after 120 s of plasma treatment at 75 Pa, as shown in Fig. 10. The bacteria themselves, however, have been devitalized well before. Figure 9 proves that most bacteria are already dead after 55 s of plasma treatment at 75 Pa. This was also proven by culturing bacteria from treated samples, where most samples proved to be negative. So, it can be concluded that the bacteria are enough damaged as soon as the peak intensity of the N₂ and CO peaks is reached.

IV. CONCLUSIONS

Several techniques for plasma characterization during degradation of bacteria *E. coli* were applied: Langmuir probe, catalytic probe, and optical emission spectroscopies. While the electron temperature, the plasma density, and the density of the neutral oxygen atoms were not affected by the presence of bacteria in the discharge chamber, optical emission spectroscopy proved useful for monitoring the bacteria degradation process. The time evolution of the nitrogen and carbon monoxide peaks supplied reliable data that allowed for monitoring the bacteria degradation process. As the sterilization process starts, there is rather poor emission from these molecules. As soon as the bacteria are being devitalized, both peaks increase and reach a maximum value, when the bacteria are dead. Further treatment of bacteria by oxygen radicals results in slow etching of the remained cell walls. Since the bacteria are already dead at the peak intensity of both N₂ and CO emissions, the optical emission spectroscopy can be considered an excellent tool for monitoring the sterilization process.

ACKNOWLEDGMENT

The research was supported by Slovenian Ministry of Science, Croatian Ministry of Science, Education and Sports, and Montenegro Government, Grant Nos. 33.BI-SLO-HR07-08, and 1.BI-SLO-CG07-08.

- ¹D. J. Wilson, N. P. Rhodes, and R. L. Williams, *Biomaterials* **24**, 5069 (2003).
- ²M. K. Gunde and M. Kunaver, *Appl. Spectrosc.* **57**, 1266 (2003).
- ³M. Mozetic, U. Cvelbar, M. K. Sunkara, and S. Vaddiraju, *Adv. Mater. (Weinheim, Ger.)* **17**, 2138 (2005).
- ⁴K. Ostrikov, *Rev. Mod. Phys.* **77**, 489 (2005).
- ⁵A. Vesel, M. Mozetic, A. Drenik, S. Milosevic, N. Krstulovic, M. Balat-Pichelin, I. Poberaj, and D. Babic, *Plasma Chem. Plasma Process.* **26**, 577 (2006).
- ⁶Z. Y. Wu, N. Xanthopoulos, F. Reymond, J. S. Rossier, and H. H. Girault, *Electrophoresis* **23**, 782 (2002).
- ⁷A. G. Whittaker *et al.*, *J. Hosp. Infect.* **56**, 37 (2004).
- ⁸M. Nagatsu, F. Terashita, and Y. Koide, *Jpn. J. Appl. Phys., Part 2* **42**, L856 (2003).
- ⁹S. Villegier, S. Cousty, A. Ricard, and M. Sixou, *J. Phys. D* **36**, L60 (2003).
- ¹⁰S. Moreau, M. Moisan, M. Tabrizian, J. Barbeau, J. Pelletier, A. Ricard, and L. H. Yahia, *J. Appl. Phys.* **88**, 1166 (2004).
- ¹¹S. Gomez, P. G. Steen, and W. G. Graham, *Appl. Phys. Lett.* **81**, 19 (2002).
- ¹²M. Mozetic, *Vacuum* **71**, 237 (2003).
- ¹³U. Cvelbar, S. Pejovnik, M. Mozetic, and A. Zalar, *Appl. Surf. Sci.* **210**, 255 (2002).
- ¹⁴U. Cvelbar, D. Vujosevic, Z. Vratnica, and M. Mozetic, *J. Phys. D* **39**, 3487 (2006).
- ¹⁵M. Klanjsek-Gunde, M. Kunaver, M. Mozetic, and M. Horvat, *Powder Technol.* **148**, 64 (2004).
- ¹⁶G. Cartry, X. Duten, and A. Rousseau, *Plasma Sources Sci. Technol.* **15**, 476 (2006).
- ¹⁷K. N. Ostrikov, S. Xu, and A. B. M. S. Azam, *J. Vac. Sci. Technol. A* **20**, 251 (2002).
- ¹⁸U. Cvelbar, N. Krstulovic, S. Milosevic, and M. Mozetic, *Vacuum* **81** (in press).
- ¹⁹K. N. Ostrikov, M. Y. Yu, and H. Sugai, *J. Appl. Phys.* **86**, 2425 (1999).
- ²⁰K. N. Ostrikov and M. Y. Yu, *IEEE Trans. Plasma Sci.* **26**, 100 (1998).
- ²¹U. Cvelbar, M. Klanjsek-Gunde, and M. Mozetic, *IEEE Trans. Plasma Sci.* **33**, 236 (2005).
- ²²M. Moisan, J. Barbeau, M. C. Cervier, J. Pelletier, N. Philip, and B. Saoudi, *Pure Appl. Chem.* **74**, 349 (2002).
- ²³M. Blank and R. Goodman, *IEEE Trans. Plasma Sci.* **30**, 1497 (2002).
- ²⁴R. E. J. Sladek and E. Stoffels, *J. Phys. D* **38**, 1716 (2005).
- ²⁵W. A. Rutala, M. F. Gergen, and D. J. Weber, *Infect. Control Hosp. Epidemiol.* **26**, 393 (1998).
- ²⁶A. Drenik, U. Cvelbar, A. Vesel, and M. Mozetic, *Inf. MIDEM, J. Microelectron. Compon. Mat.*, **35**, 85 (2005).
- ²⁷L. Lefevre, T. Belmonte, and H. Michel, *J. Appl. Phys.* **87**, 7497 (2000).
- ²⁸H. Singh, J. W. Coburn, and D. B. Graves, *J. Appl. Phys.* **88**, 3748 (2000).
- ²⁹U. Cvelbar, M. Mozetic, and A. Ricard, *IEEE Trans. Plasma Sci.* **33**, 834 (2005).
- ³⁰M. Mozetič, A. Vesel, U. Cvelbar, and A. Ricard, *Plasma Chem. Plasma Process.* **26**, 103 (2006).
- ³¹Z. L. Tsakadze, K. Ostrikov, J. D. Long, and S. Xu, *Diamond Relat. Mater.* **13**, 1923 (2004).

The influence of substrate material on bacteria sterilization in an oxygen plasma glow discharge

U Cvelbar^{1,2,3}, D Vujošević², Z Vratnica² and M Mozetič¹

¹ Plasma Laboratory, Jozef Stefan Institute, Jamova 39, 1000 Ljubljana, Slovenia (EU)

² Institute for Public Health, Ljubljanska bb, 81000 Podgorica, Montenegro

E-mail: uros.cvelbar@ijs.si

Received 14 March 2006, in final form 15 March 2006

Published 4 August 2006

Online at stacks.iop.org/JPhysD/39/3487

Abstract

A critical approach to plasma sterilization is presented with the aim of sterilizing biocompatible materials such as TiO₂ and polymer implants. Oxygen plasma was applied to sterilize glass and aluminium samples containing *Bacillus subtilis* spores. Sterilization was performed with a low pressure weakly ionized oxygen plasma created with a RF generator with an output power of 300 W and frequency 27.12 MHz. The density of charged particles, density of neutral oxygen atoms and the electron temperature were about $1 \times 10^{16} \text{ m}^{-3}$, $1.5 \times 10^{22} \text{ m}^{-3}$ and 5 eV, respectively. The sterilization effects were observed by SEM and by bacterial cultivation. It was found that the surface recombination of O-atoms plays an important role, since it causes temperature changes in the substrate. The sterilization efficiency increased with increasing plasma exposure time. The results showed that the sterilization efficiency is not necessarily just the effect of oxygen plasma radical interactions, but also of the sample heating due to radical interaction with the substrate. Plasma sterilization should be done differently according to the substrate material used for sterilization.

(Some figures in this article are in colour only in the electronic version)

1. Introduction

Surface treatment of different materials with oxygen plasma has become a technique widely used on experimental and also industrial scale [1–4]. Oxygen plasma is used in the electronic industry, the automobile industry, chemistry, biology, medicine and nanotechnology. The technologies based on the application of oxygen plasma include non-isotropic plasma etching, selective etching, low-temperature ashing, degreasing, surface activation and plasma sterilization [5–7].

Plasmas for such treatments are often created in high frequency discharges at a pressure between 1 and 100 Pa. Characteristics of plasmas (i.e. neutral gas temperature, electron temperature or electron energy distribution function, density of positive ions, negative

ions, neutral atoms in the ground state, metastable excited molecules, rotational–vibrational molecular temperature) used in different technologies depend on the nature of the material treated.

Many applications require plasma with a high degree of ionisation, while some prove better if weakly ionised plasma is used. Modern reactors for cold plasma ashing, for instance, use post-glow for sample treatment rather than plasmas themselves.

A modern technique that is based on application of low temperature plasma is the plasma sterilization of different materials [8,9]. Such plasma is often a source of UV irradiation and oxygen atoms. They both interact with microorganisms. The rather high-energy UV photons produce strong cidal effects because their energy corresponds to a maximum of absorption by deoxyribonucleic acid (DNA) and other nucleic acids [10]. The typical depth of photo-chemical reaction is restricted to about one micrometre, so deactivation is

³ Author to whom any correspondence should be addressed.

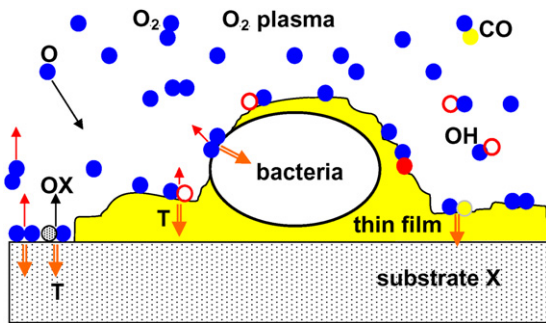


Figure 1. Schematic of the surface process where the recombination of neutral O-atoms takes place on the material surface with the bacteria in the thin film. After the recombination on the surface, the molecule is desorbed from the surface and the redundant energy is transformed into heat.

rather restricted to thin layer surface modifications and will, therefore, be more efficacious when dealing with smaller non-sporulated bacteria. In glow discharge plasma there are also other excited species including charged particles, particularly ions. These species mostly execute the function of material bond breaking. On the other hand, oxygen atoms mainly interact with bacteria by oxidizing them, creating material and distortion of DNA material, followed by the deactivation process of bacteria.

There are two main mechanisms of bacteria deactivation glow discharge. The first one is erosion of the microorganism, atom by atom, through intrinsic photodesorption. Energetic particle induced desorption results from UV photons and ions breaking chemical bonds in the microorganism material and leading to the formation of volatile compounds from atoms intrinsic to the microorganism. The volatile by-products of this non-equilibrium chemistry are small molecules (eg. CO, OH and CH_x should be possible).

The second main mechanism is erosion of the microorganism, atom by atom, through etching. Etching results from the adsorption of reactive species from the plasma on the microorganism, with which they subsequently undergo chemical reactions to form volatile compounds (spontaneous etching). The reactive species can be atomic or molecular radicals, for example O or OH, respectively, and excited molecules, for example, the $^1\text{O}_2$ singlet state. This chemistry, under thermodynamic equilibrium conditions after recombination in the gas or on the chamber walls, yields small molecules (e.g. CO_2 , H_2O), which are the final products of the oxidation process (figures 1 and 2). In certain cases, the etching mechanism is enhanced by UV photons acting synergistically with the reactive species, thereby accelerating the elimination rate of microorganisms. This UV-induced chemistry under non-equilibrium conditions can result in desorption of radicals and molecules, at both the intermediate and final stages of oxidation [8].

During these processes the reactive species do not interact with just the microorganism, but also with the microorganism holders or material being sterilized. There are no data on plasma effects, such as heating from neutral atom recombination on material, reported in published papers. In any case, an important parameter is the surface recombination coefficient of material used for sterilization. Due to the relaxation and recombination of neutral atoms

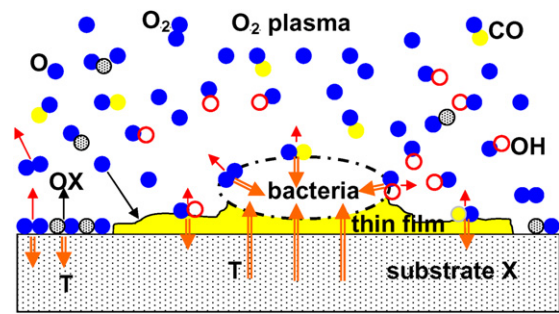


Figure 2. Schematic of the sterilization surface process in oxygen plasma after a short period of time (approximately 40 s).

in highly dissociated weakly ionized plasma, we can obtain extensive energy release causing local heating of material and its distortion including microorganism deactivation through unwanted heat (figures 1 and 2). This correlation will be shown in this paper.

2. Experimental

2.1. Sample preparation

We used standard strains of *Bacillus subtilis* from producer *Microbiologics* (MN, USA) to prepare specimens. Standard strains were vitalized in the proper manner. Bacteria were subcultivated on Columbia agar plates and from colonies. The agar base per litre of demineralized water consisted of 2.0 g heart muscle and infusion from solids, 13.0 g pancreatic digest of casein, 5.0 g yeast extract, 5.0 g sodium chloride and 15 g agar. The cell suspension was prepared with the sterilized water comprising 6% (w v^{-1}) agar base with 10^6 cfu ml^{-1} (colony forming units per ml) bacteria and 94% (w v^{-1}) water. Holders from glass and Al-foil, cut into 1×3 cm rectangular platelets were used as holders. In the first step, each of them was cleaned with ethanol and distillate water. After wet chemical cleaning, the holders were activated and plasma cleaned in a glow discharge reactor with oxygen plasma, so that 1 ml of cell suspension uniformly covered the surface of the holders. Due to an oxygen surface treatment the oxide layer of Al_2O_3 grew on aluminium foil [11], but there were no changes of structure on the glass substrate. Prepared holders were dried slowly, to allow spore forming. There were approximately 10^6 cfu on each holder. Due to the presence of agar base in the suspension, the coating from proteins and solids is formed on the sample surface covering some bacteria spores. Holders prepared in the manner described above were placed in and treated in a plasma reactor. For each treatment time, 14 samples were used to prove positive ($\text{cfu ml}^{-1} \geq 1$) or negative colony forming units ($\text{cfu ml}^{-1} = 0$). The absence of a colony forming unit was therefore called sterilization.

2.2. Plasma sterilization system

Samples were mounted in a discharge vessel of a vacuum system. The discharge vessel was a cylindrical tube with a diameter of 40 mm and length 600 mm. The tube was made of a borosilicate glass (Shott 8250) with a recombination coefficient for oxygen atoms at room temperature of 1.9×10^{-4} [12]. On one side, the tube was

connected to a vacuum pump. The system was pumped with a two-stage oil rotary pump with a pumping speed of 2.21 s^{-1} and a base pressure of 0.1 Pa. All connections between the pump and discharge vessel are made of components with a conductance of approximately two orders of magnitude higher than the pumping speed of the pump, so that the effective pumping speed in the discharge vessel is nearly as high as that of the pump. The pressure in the system was measured with an absolute gauge and was set to 75 Pa. The discharge vessel was placed in a coil connected to a RF generator with a frequency of 27.12 MHz and an output power of approximately 300 W. The other side of the discharge vessel was connected to a gas inlet system. Commercially available oxygen was leaked into the system through a leak valve. The discharge vessel was forced-air cooled.

The plasma parameters in the discharge vessel were measured with a double Langmuir probe [13], a standard nickel catalytic probe [14] and an optical spectrometer [15]. Measurements of plasma parameters were performed prior to experiments with composite samples in order to assure a proper reading of the O-atom density [16]. The density of charged particles was about $1 \times 10^{16} \text{ m}^{-3}$ and the electron temperature was about 5 eV. The density of neutral oxygen atoms was $1.5 \times 10^{22} \text{ m}^{-3}$. The floating potential, as calculated from T_e and n_e was about 10 V. The sample material temperature was measured with fibre optic probes [17] physically connected to treated material. The lower detection limit for the probe was a temperature of 355 K. Samples were exposed to plasma separately for different periods of time in continuum (for example 1, 5, 10, 30, 60, 120 or 300 s) or pulse mode (for example 5 s for 5 times or $5 \times 5 \text{ s}$, then $10 \times 5 \text{ s}$, $30 \times 5 \text{ s}$ and $50 \times 5 \text{ s}$ with 25 s cooling period breaks) to prevent extensive sample heating.

2.3. Sample analysis

After treatment, holders with *B. subtilis* were immersed in Tryptic glucose yeast broth and incubated at 35°C for 14 days and monitored daily. When turbidity occurred in any container, we subcultivated it on Columbia agar plates and searched for nominated (or any other) bacteria.

For identification, we used a API 50CH + API 20E identification system from the producer *bioMerieux*, France. After 14 days, the contents of all containers were subcultivated on Columbia agar plates to prove absence of growth. The results were monitored also with a scanning electron microscope (SEM) to observe the plasma destruction process of bacteria on the sample surface.

3. Results and discussion

3.1. The plasma–surface interaction

The oxygen plasma used for plasma sterilization was created in a glow discharge with high dissociation and low ionisation degree. A typical emission from the plasma is presented in figure 3. The neutral O-atoms peaks at 777 and 844.6 nm dominate at 75 Pa pressure. The main lines are O transition $3s^5S^0-3p^5P$ at 777.2 nm, O $3s^3S^0-3p^3P$ at 844.6 nm and O $3p^5P-4d^5D^0$ at 615 nm. A weak O_2 molecular band can be observed at 760.5 nm and thereafter, showing the existence

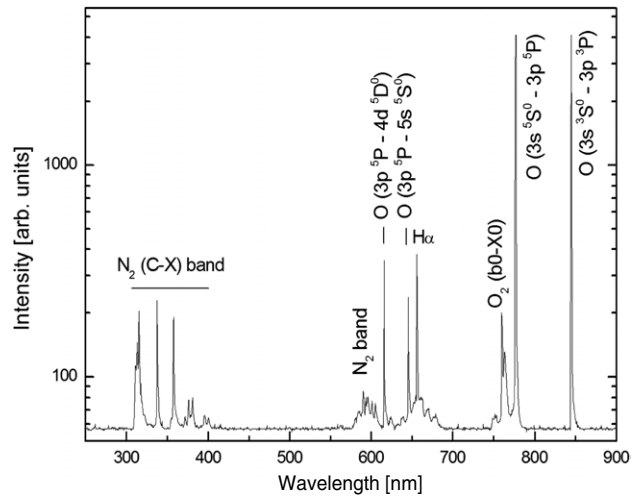


Figure 3. The optical emission from the oxygen plasma glow at the sample holder position, created in inductively coupled RF (27.12 MHz) discharge of oxygen at pressure 75 Pa and discharge power 300 W.

of some non-dissociated oxygen. There is also a small peak of charged O_2^+ vibrational transition (1,0) at 558.7 nm, characterizing weakly ionized plasma. Some impurities can also be observed, such as the nitrogen band of $\text{N}_2(\text{C-X})$ at 337.29 nm and hydrogen as the H_α peak. There is practically no emission in the UV range, and ionic bands are weak. The role of UV photons and ions can therefore be negligible. Most of the reaction with bacteria is therefore done atom by atom, through etching. On the other hand, some ions can help the atoms heating the sample holders.

During the etching of bacteria spores, predominantly oxygen atoms interact with the sample holder and relax on the surface. This surface recombination of oxygen atoms is described by two models; the Langmuir–Hinshelwood and the Eley–Rideal model [18]. The Langmuir–Hinshelwood model predicts the recombination of two surface adatoms (that are rather well accommodated on the surface), while the Eley–Rideal model predicts a direct interaction of an O atom from the gas phase with a surface adatom. In the first case, the molecules leaving the surface are reasonably well accommodated and the resultant energy of a desorbing molecule is rather low—the kinetic energy is well below 1 eV, while the rotational–vibrational temperature of the molecule is not too far from the surface temperature. On the other hand, the molecules following the Eley–Rideal model are often rather fast and found in high vibrational excited states. According to upper considerations, the released energy of the recombination can be several electron volts. In both cases, the probability of recombination is often expressed in terms of the recombination coefficient (γ), which is defined as the ratio between the flux of recombined O_2 leaving the surface and the O-atom flux onto the surface. The γ value for a flat oxidized Al foil is 0.02 [19]. The excessive energy is always transferred to the solid material, causing its heating. The rate of local heating depends on the recombination coefficient of treated material. The substrate material is heated [13] according to

$$\frac{dT}{dt} = \gamma \frac{v n_o S W_D}{8 m c_p}, \quad (1)$$

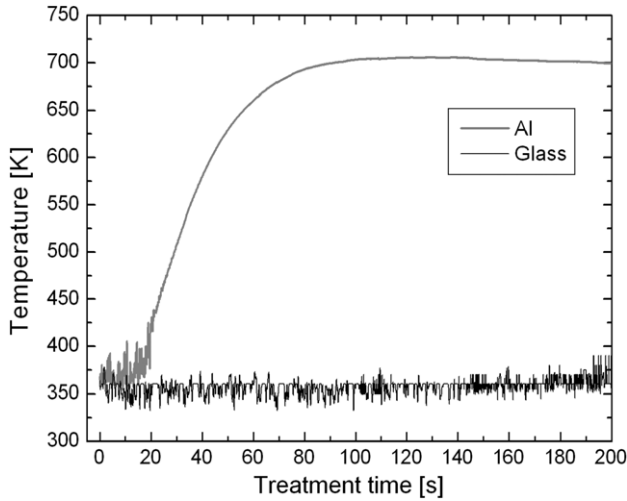


Figure 4. The sample temperature of the Al substrate (upper curve) and the glass substrate (lower curve) in continuum mode.

were n_0 is the O-atom density in the vicinity of the material, v the average thermal velocity of O-atoms, W_D (5.2 eV) the dissociation energy of an oxygen molecule, S the catalyst area, m the mass of the treated material, c_p its specific heat capacity and γ the recombination coefficient for O-atoms.

An additional heating can occur due to weak ion bombardment of the sample holders by positive ions from oxygen plasma. Taking into account that the sample is on floating potential and assuming a thin sheath approximation, as well as full recombination of ions on the surface (recombination probability is 1), the energy released on the surface in unit time due to ion interaction with ions is $P = j_i \cdot W_E$. Here, the estimated maximal kinetic and potential energy of oxygen ions is W_E (in our case 20 eV), the flux of ions onto the surface is $j_i = \frac{1}{4}n_i v_i$, where n_i is the ion density and v_i the average thermal velocity of ions in the plasma. The acceleration of ions in the high frequency (RF) electric field is always neglected, so the velocity is close to the velocity of neutral molecules, which is 630 m s^{-1} . Taking into account numerical values, the energy dissipated on the surface of the sample is therefore approximately a few $\text{W m}^{-2} \text{ s}^{-1}$.

On the other hand, the energy dissipated due to recombination of neutral oxygen atoms on the sample surface with $\gamma = 0.01$ is approximately $1000 \text{ W m}^{-2} \text{ s}^{-1}$. Heating by atom recombination is orders of magnitude bigger than heating by ions as long as the sample is kept at floating potential and therefore neglectable.

3.2. The sterilization process

The heating of material in a sterilizing plasma due to recombination has tremendous influence on the process of material sterilization. The material overheating can cause sterilization. In order to understand this mechanism, particularly for biocompatible materials such as different polymers, the recombination coefficient has to be known. The effect of surface recombination and heating of the material can be seen in figure 4, where we measured the temperature of two different substrates during continuous oxygen plasma exposure in the glow discharge.

Table 1. Recombination coefficients for different materials and calculated approximate plasma heating time to a temperature of 353 K (80 °C). The presumption is that all materials have the same product of mass and specific heat, n_0 is $1.5 \times 10^{22} \text{ m}^{-3}$ and ionic heating is negligible.

Material	Recombination coefficient γ	Time (s)	γ reference
Glass bacteria holder	10^{-3}	145	
Pyrex, quartz, soda, glass, etc	5×10^{-3} – 1×10^{-5}	29–14500	[31–33]
Al oxide (Al_2O_3)	0.02	7	[19]
Ti oxide (TiO_2)	0.03	5	[34]
Teflon	7.3×10^{-5}	1986	[35]
Polypropylene	0.35	0.4	[28]
Copper (Cu)	0.3	0.5	[36]
Nickel (Ni)	0.27	0.5	[13]

Here we present temperature measurements with an inert fibre optic catalytic probe immersed in sample holders for the case of aluminium and glass material. The material of the sample holders is heated differently. The aluminium holder is heated to approximately 620 K in the first 40 s of continuous plasma treatment. Here, the heating rate near the origin is 8 K per second. The temperature is stabilized after a minute of plasma treatment, because heating equals cooling by the gas in its reached equilibrium. On the other hand, the glass substrate is heated very slowly and is for a long while below the detection limit of the probe. The probe detection temperature of 370 K is reached after approximately 200 s. The plasma heating of the glass substrate is therefore at least 20 times slower than for aluminium. This difference is due to recombination coefficients (table 1), where the difference between the two is about 20. The calculation with the given parameters from equation (1) also gives the same result, e.g. 18.5 times faster heating of the aluminium sample holder than the glass holder.

There could also be some discrepancies due to the coating material on the sample holders from suspensions with bacteria spores, but in our case we generally neglect this effect. If the coating is made of material with high oxidation probability (high recombination coefficient), the sterilization is faster since the oxygen radicals readily interact with the coating oxidizing it, and thus cause additional heating of the substrate. On the other hand, some oxidation resistant coatings can protect the bacteria from direct interaction with plasma radicals. This effect is particularly important for the case of oxygen plasma sterilization since oxygen plasma is a poor emitter of UV radiation and the only mechanism of sterilization (apart from thermal effects) is chemical degradation.

The heating definitely influences the sterilization of an aluminium sample contaminated with *B. subtilis* spores, as shown in figure 5. In continuous mode, when the sample is treated non-stop for 30 s with plasma (as seen in figure 4) and has reached a temperature of 510 K, half the samples become non-active. This temperature is supposed to be deadly for *B. subtilis* spores, but some obviously still survive quick heating by plasma radicals. This can also be the result of the thin film protection covering the bacteria spores. After a 60 s treatment when the sample temperature reaches 660 K, there are no more survivors. This sterilization is probably due to the high temperature. To prevent such heating, a pulse mode with 25 s cooling periods was introduced. In this case, some atom

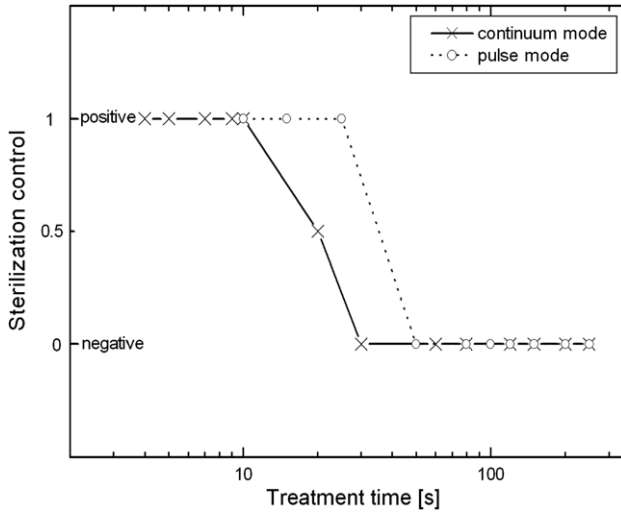


Figure 5. The sterilization of *B. subtilis* spores on the aluminium sample holder in continuum and pulse mode.

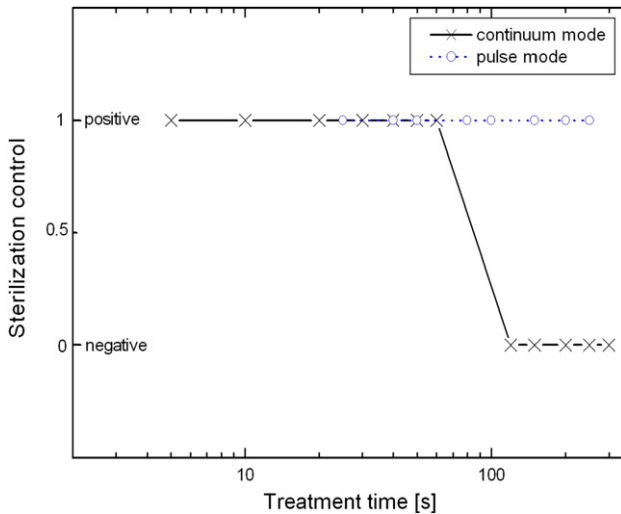


Figure 6. The sterilization of *B. subtilis* spores on the glass sample holder in continuum and pulse mode.

etching effect can be observed from the curve in figure 5. It is obvious that heating is at least partially eliminated, because at 25 s (5 × 5 s with 25 s cooling period) of total treatment all samples are still positive with the colony forming units. However, after the 10 × 5 s with a 25 s cooling period treatment time the aluminium foil is sterilized already, due to the predominant effect of the atom by atom etching at increased temperature of around 343 K (70 °C). Samples heated just to this temperature are all positive with cfu, since the temperature is lower than the temperature needed for *B. subtilis* spore deactivation [20]. To confirm this theory some SEM images were taken of the sporulated bacteria within the dried cultivated material before and after the treatment. This atom etching can be seen in figures 7 and 8, where we observe non-treated bacteria spores (covered by a thin film of cultivating agar material) and bacteria treated for 50 s on the aluminium foil sample. It can be seen how the O-atom disintegrated the spore envelope, etching the material away. After 60 s of total treatment time almost all bacteria are deactivated either by temperature

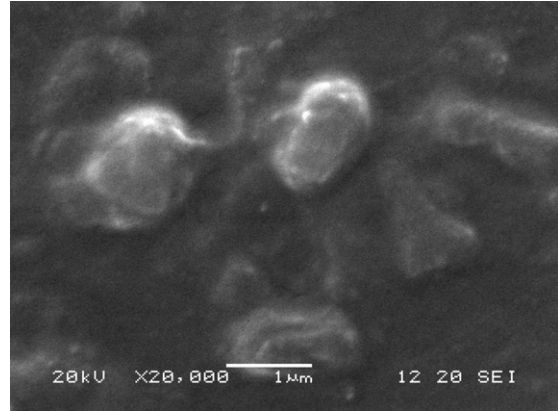


Figure 7. The SEM image of non-treated bacteria *B. subtilis* spores on the aluminium substrate holder covered with thin film of cultivating material.

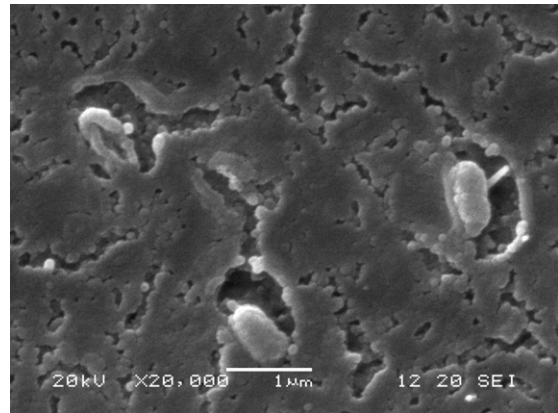


Figure 8. The SEM image of bacteria spores on the aluminium substrate treated by oxygen plasma glow from inductively coupled RF discharge at pressure 75 Pa and 300 W. The sample was treated in continuous mode for 50 s.

or the combined effect of temperature and atom by atom etching.

The situation with the glass sample holder with bacteria is somehow different, because the temperatures are much lower than with the aluminium sample. As seen in figure 4, the combined sterilization effect can be observed in the case of Al. The glass sample is heated 20 times slower than aluminium, due to neutral atom surface recombination. The limiting temperature for destruction of bacteria *B. subtilis* spores is between 400 and 450 K, depending on environmental conditions [20]. On the glass sample, the sterilization with no cfu occurs at 120 s of continuous plasma treatment (figure 6) when the temperature increases to approximately 320 K. On the other hand, when the pulse treatment is introduced, the sample is kept at virtually room temperature, 300 K; there are no sterilizing effects. The sterilization in this case would happen after much longer exposure to O-atom radicals. These observations confirm that increased sample temperature helps O-atom radicals to sterilize material more effectively. The combination of temperature heating as a consequence of the surface O-atom recombination and etching atom by atom are therefore the most desirable mechanisms for effective oxygen plasma sterilization.

3.3. The sterilization-heating model for material treatment

The problem gets more complicated when we work with biocompatible materials or a combination of more than one material, being sterilized for implantation into the human body [21]. On the one hand we have to sterilize the material, and at the same time we have to be careful so as to not corrupt and destroy the material. These seem to be small problems with the use of TiO₂ [22,23] for bone implants, because it behaves similarly to our aluminium substrate. The recombination coefficient is fairly the same, as seen in table 1, and the heating with sterilization effect follows the same pattern. More problems are to be expected with sensitive materials such as blood implants [24, 25], tissue [26] or ophthalmic materials [27] made from polymers (PET, PMMA, PHEMA, PHPTFE, etc.) The recombination coefficient for these materials is sometimes fairly high, from 0.1 to 0.9 [28], and this means that the heating of the material is fairly quick. The heating rate actually depends also on the material mass and its specific heat capacity. From equation (1), one can write the heating rate as

$$\frac{dT}{dt} = \frac{\gamma}{mc_p} \xi, \quad (2)$$

where the constant part, which keeps constant at the same plasma parameters, is

$$\xi = \frac{1}{8} v n_o S W_D. \quad (3)$$

The heating rate of any material exposed to plasma therefore depends on the recombination coefficient (γ), the substrate mass (m) and its specific heat capacity (c_p). Equation (2) can be used for estimation of the plasma exposure time to prevent the sample from overheating. If the temperature gradient of a known material is denoted as $(dT/dt)_1$ and the gradient of the other material is $(dT/dt)_X$, then

$$dT_X = dT_1, \quad (4)$$

and

$$dt_X = \frac{\gamma_1 m_X c_{pX}}{\gamma_X m_1 c_{p1}} dt_1, \quad (5)$$

where γ_1 is in our case the recombination coefficient for a material of known treatment time and γ_X the recombination coefficient of the material that is to be treated. If we also know the mass and specific heat capacity for both materials, then we can calculate the right heating time for the material to reach a designated temperature. To give some idea of the heating time-rates for different materials presented in table 1, we took into account that the product of mass and specific heat capacity are equal for all materials. One can see that for the polymer with approximately the same mass as our measured samples it is less than a second. The same applies for metal samples such as copper and nickel. Materials for implants such as titanium dioxide or oxidized titanium have rates of the order of a couple of seconds; on the other hand, materials such as glass and ceramics have a time of tens of seconds. The most resistant material to oxygen plasma allowed treatment is Teflon, a polymer that can withstand a much longer treatment than all other polymer materials. The same applies for some other resistant polymers including polyethersulfon (PES).

The allowed treatment time is increased with the mass of implant material that is to be treated in the oxygen glow discharge plasma. But one has to keep in mind that not all materials are sterilized equally. Treatment has to be adapted according to the material, defining the treatment period, cooling time and the repetition rate of a cycle until all bacteria on the surface are deactivated.

For the sterilization of an item made from different materials, one can encounter the restriction of oxygen plasma sterilization, if materials do not have approximately the same recombination coefficients or thermal conductance is low. This problem arises with the treatment, for example, of a metal plate incorporated into a surrounding polymer [29, 30] or an endoscope combination of polymer hosing and metal tip. The same problem arises when dealing with implants combining implant material and its coating, like collagen. To solve this problem, however, there is always the possibility of adopting the treatment cycle to the material with the highest recombination coefficient and reduced treatment time.

4. Conclusions

A critical study of plasma sterilization of materials was presented. The influence of substrate heating due to oxygen atom recombination for different materials to be sterilized is presented. It was observed that temperature accelerates sterilization and it helps O-atoms to etch bacteria atom by atom. On the other hand, it limits the allowed treatment time in oxygen glow discharge plasma, because of the extensive heating that comes from the energy released due to recombination of the same atoms on the substrate surface. The problem is more complicated with biocompatible materials or combinations of more than one material being sterilized for implantation. Some polymers and metals have high recombination coefficients, so their heating-rate is very short. The model for heating was presented, giving some idea about the orders of magnitudes for heating different materials. It was demonstrated that in many cases a pulsed plasma treatment is needed in order to avoid overheating of substrates before sterilization is completed.

Acknowledgments

The authors would like to thank Dr S Milošević from the Institute of Physics, Zagreb, for the spectroscopy and Dr M Klanjšek-Gunde from the National Institute of Chemistry, Ljubljana, for the SEM analysis.

References

- [1] Boenig H V 1982 *Plasma Science and Technology* (Ithaca, NY: Cornell University Press)
- [2] Ricard A 1996 *Reactive Plasmas* (Paris: Société Française du Vide)
- [3] Wertheimer M R, Marinu L and Liston E M 1998 *Handbook of Thin Film Process Technology—Plasma Sources For Polymer Surface Treatment* (Bristol: Institute of Physics Publishing)
- [4] Šorli I, Petasch W, Kegel B, Schmidt H and Leibel G 1996 *Inf. Midem* **26** 35

- [5] Moreau S *et al* 1999 Optimum operation conditions leading to complete sterilization at low temperatures in a plasma afterglow *Proc. 12th Int. Colloq. on Plasma Processes (Antibes, France)* ed A Ricard (Paris: Société Française du Vide) pp 46–51
- [6] Holy C E, Cheng C, Davies J E and Shoichet M S 2001 *Biomaterials* **22** 25
- [7] Montes-Moran M A, Martinez-Alonso A, Tascon J M D and Young R J 2001 *Composites A* **S 32** 361
- [8] Moisan M, Barbeau J, Moreau S, Pelletier J, Tabbrizan M and Yahia L H 2001 *Int. J. Pharm.* **226** 1
- [9] Villeger S, Cousty S, Ricard A and Sixou M 2003 *J. Phys. D* **36** L60
- [10] Boucher G R M 1985 *Med. Device Diagn. Ind.* **7** 51
- [11] Mozetic M, Zalar A, Cvelbar U and Babic D 2004 *Surf. Interface Anal.* **36** 986
- [12] Van Hest M F A M, Haartsen J R, Van Weert M H M, Schram D C and Van de Sanden M C M 2003 *Plasma Sources Sci. Technol.* **12** 539
- [13] Šorli I and Ročak R 2000 *J. Vac. Sci. Technol. A* **18** 338
- [14] Poberaj I, Babič D and Mozetič M 2001 *J. Vac. Sci. Technol. A* **20** 189
- [15] Mozetič M, Ricard A, Babič D, Poberaj I, Levaton J, Monna V and Cvelbar U 2003 *J. Vac. Sci. Technol. A* **21** 369
- [16] Vesel A and Mozetič M 2001 *Vacuum* **61** 373
- [17] Babič D, Poberaj I and Mozetič M 2001 *Rev. Sci. Instrum.* **72** 4110
- [18] Santrio J A B, Glatzer H J and Doraiswamy L K 2000 *Chem. Eng. Sci.* **55** 5013
- [19] Mozetič M 2003 *Thermodynamic Gas Phase* (Ljubljana: DVTS)
- [20] Pflug I J, Holcomb R G and Gómez M 2001 Principles of the thermal destruction of microorganisms *Disinfection, Sterilisation and Preservation* (Philadelphia, PA: Lippincott Williams Wilkins)
- [21] Chu P K, Chen J Y, Wang L P and Huang N 2002 *J. Mater. Sci. Eng. R* **36** 146
- [22] Hanawa T 1999 *Mater. Sci. Eng. A* **267** 260
- [23] Serro A P and Saramago B 2003 *Biomaterials* **24** 4749
- [24] Montanari L *et al* 1998 *J. Control Rel.* **56** 219
- [25] Favia P and D'Agostino R 1998 *Surf. Coat. Technol.* **98** 1102
- [26] Holy C E, Cheng C, Davies J E and Scoichet M S 2001 *Biomaterials* **22** 25
- [27] Lloyd A W, Faragher R G A and Denyer S P 2001 *Biomaterials* **22** 769
- [28] Gomez S, Steen P G and Graham W G 2002 *Appl. Phys. Lett.* **81** 19
- [29] Charnley J and Halley D K 1975 *Clin. Orthop. Relat. R* **112** 180
- [30] Lombardi A V, Malloy T H, Vaughn B K and Drouillard P 1989 *J. Bone Joint Surg. A* **71** 1337
- [31] Wickramanayaka S, Hosokawa N and Hatanaka Y 1991 *Japan. J. Appl. Phys.* **30** 2897
- [32] Hacker D S, Marshall S A and Steinberg M 1961 *J. Chem. Phys.* **35** 1788
- [33] Morgan J E, Ellias L and Schiff H I 1960 *J. Chem. Phys.* **33** 930
- [34] Legrand J C and Diamo A M 1997 *New J. Chem.* **21** 1047
- [35] Wickramanayaka S *et al* 1991 *J. Vac. Sci. Technol. A* **9** 2999
- [36] Shibata M, Nakano N and Makabe T 1996 *J. Appl. Phys.* **80** 6142